Integrated Ocean Drilling Program Expedition 323 Scientific Prospectus

Pliocene–Pleistocene paleoceanography and climate history of the Bering Sea

Kozo Takahashi
Co-Chief Scientist
Department of Earth and Planetary Sciences
Graduate School of Sciences
Kyushu University
Hakozaki 6-10-1, Higashi-ku
Fukuoka 812-8581
Japan

Ana Christina Ravelo
Co-Chief Scientist
Ocean Sciences Department
University of California
Santa Cruz CA 95064
USA

Carlos A. Alvarez Zarikian
Staff Scientist/Expedition Project Manager
Integrated Ocean Drilling Program
Texas A&M University
1000 Discovery Drive
College Station TX 77845
USA

Published by
Integrated Ocean Drilling Program Management International, Inc.,
for the Integrated Ocean Drilling Program

Publisher's notes

Citation:
Takahashi, K., Ravelo, A.C., and Alvarez Zarikian, C.A., 2009. Pliocene–Pleistocene paleoceanography and climate history of the Bering Sea. *IODP Sci. Prosp.,* 323. doi:10.2204/iodp.sp.323.2009

Distribution:
Electronic copies of this series may be obtained from the Integrated Ocean Drilling Program (IODP) Scientific Publications homepage on the World Wide Web at **www.iodp.org/scientific-publications/.**

This publication was prepared by the Integrated Ocean Drilling Program U.S. Implementing Organization (IODP-USIO): Consortium for Ocean Leadership, Lamont-Doherty Earth Observatory of Columbia University, and Texas A&M University, as an account of work performed under the international Integrated Ocean Drilling Program, which is managed by IODP Management International (IODP-MI), Inc. Funding for the program is provided by the following agencies:

National Science Foundation (NSF), United States

Ministry of Education, Culture, Sports, Science and Technology (MEXT), Japan

European Consortium for Ocean Research Drilling (ECORD)

Ministry of Science and Technology (MOST), People's Republic of China

Korea Institute of Geoscience and Mineral Resources (KIGAM)

Australian Research Council (ARC) and New Zealand Institute for Geological and Nuclear Sciences (GNS), Australian/New Zealand Consortium

Ministry of Earth Sciences (MoES), India

Disclaimer

May 2009

Abstract

Over the last 5 m.y., global climate has evolved from being warm with only small Northern Hemisphere glaciers to being cold with major Northern Hemisphere glaciations every 100–40 k.y. The ultimate reasons for this major transition are unknown. Over the last hundreds of thousands of years, Milankovitch- and millennial-scale climate oscillations have occurred; although processes responsible for these oscillations are known in some regions, the global nature of these oscillations are due to unknown mechanisms. Possible mechanisms responsible for both the long-term evolution of global climate as well as the generation of high-frequency climate oscillations involve intermediate water ventilation of the North Pacific. However, the paucity of data in critical regions of the Pacific, such as the Bering Sea, has prevented an evaluation of the role of North Pacific processes in global climate change. The Bering Sea is a marginal sea in the North Pacific that has experienced major climate changes. Because North Pacific Intermediate Water (NPIW) is known to form in the Bering Sea, the basin does not only record, but it is potentially critically involved in causing major climate changes. Thus, drilling in the Bering Sea can help to answer questions not only about the global extent of climate trends and oscillations but also about the mechanisms that produce them.

We plan to core sediments to study the Pliocene–Pleistocene evolution of millennial- to Milankovitch-scale climatic oscillations in the Bering Sea. Biological, chemical, and physical oceanography, as well as the adjacent continental climate of the Bering Sea, are highly sensitive to global climate conditions and are recorded by variations in the sedimentary composition of diatoms and other microfossil groups, as well as many other paleoclimatic indicators. Intermediate water formation in these regions can be tracked using paleoceanographic proxies of subsurface water that can be related to open Pacific records. Sediments can not only be used to produce records of climate and intermediate water ventilation in these critical marginal seas but can also be applied to testing the effect of changes in the Bering Strait Gateway and its influence (via the Arctic) on heat and nutrient partitioning between the Atlantic and Pacific. Planned coring will provide continuous and high-resolution paleoenvironmental records from these critical marginal seas for the first time. These new records can then be used to understand the processes that influence intermediate water ventilation and its role in global climate change over the last 5 m.y.

Major objectives of planned drilling in the Bering Sea are as follows:

1. To elucidate a detailed evolutionary history of climate and surface ocean conditions since the earliest Pliocene in the Bering Sea where amplified high-resolution changes of climatic signals are recorded;
2. To shed light on temporal changes in the origin and intensity of NPIW and possibly deeper water mass formation in the Bering Sea;
3. To characterize the history of continental glaciation, river discharges, and sea ice formation, in order to investigate the link between continental and oceanic conditions of the Bering Sea and adjacent land areas; and
4. To investigate linkages, through comparison to pelagic records, between ocean/climate processes that occur in the more sensitive marginal sea environment and processes that occur in the North Pacific and/or globally. This objective includes an evaluation of how the history of ocean/climate of the Bering Strait gateway region may have had an effect on North Pacific and global conditions.

All of these scientific objectives will focus on the long-term ocean and climate trends, as well as the evolution of higher frequency glacial–interglacial to millennial-scale oscillations through the Pliocene–Pleistocene.

Schedule for Expedition 323

Integrated Ocean Drilling Program (IODP) Expedition 323 is based on IODP drilling proposal number 477-Full4 (available at **iodp.tamu.edu/scienceops/expeditions/bering_sea.html**). Following ranking by the IODP Scientific Advisory Structure, the expedition was scheduled for the research vessel *JOIDES Resolution,* operating under contract with the U.S. Implementing Organization (USIO). The expedition is scheduled to start in Victoria, Canada, on 5 July 2009 and to end in Yokohama, Japan, on 4 September 2009. A total of 56 days will be available for the drilling, coring, and downhole measurements described in this report (for the current detailed schedule, see **iodp.tamu.edu/scienceops/.** Further details about the facilities aboard the *JOIDES Resolution* and the USIO can be found at **www.iodp-usio.org/.** Supporting site survey data for Expedition 323 are archived at the IODP-MI Site Survey Data Bank (**ssdb.iodp.org**).

Introduction

Over the last 5 m.y., global climate has evolved from being warm with only small Northern Hemisphere glaciers and ice sheets (~5–3 Ma) to being cold with major Northern Hemisphere glaciations every 100 to 40 k.y. The reasons for this major transition are unknown. Although there are data to show that the Pacific experienced oceanographic reorganizations that were just as dramatic as those in the Atlantic, the scarcity of data in critical regions of the Pacific (the largest ocean with arguably the largest potential to influence global climate) has prevented a comprehensive evaluation of the role of North Pacific processes in global climate evolution.

Over the last hundreds of thousands of years, glacial–interglacial and millennial-scale climate oscillations have also occurred because of mechanisms that are unknown, although several studies from the North Pacific subtropical and mid-latitude regions indicate that the generation and/or transmission of climate oscillations around the globe might involve intermediate water ventilation of the North Pacific. Drilling in the Bering Sea to recover comprehensive records of environmental conditions during periods of time with different climate boundary conditions can help answer questions about the global extent of climate oscillations and the mechanisms that produce them.

This expedition will obtain sedimentary sequences to study the Pliocene–Pleistocene evolution of millennial- to Milankovitch-scale climatic oscillations in the Bering Sea, the marginal sea connecting the Pacific and Arctic Oceans. Paleoclimatic indicators will be used to generate complete and detailed records of changes in the biological, chemical, and physical oceanographic conditions in the Bering Sea, as well as those of the adjacent continental climate. In addition to being sensitive to regional and potentially global climate change, the Bering Sea is one of the source regions of North Pacific Intermediate Water (NPIW). Because the production of NPIW is thought to be tied to global climate change and to Pacific Ocean circulation and nutrient distributions, investigating the evolution of conditions in regions of NPIW formation is critical for understanding Pacific paleoceanography.

Drilling in the Bering Sea will also document the effect of changes in the Bering Strait Gateway region. The Bering Strait is the main gateway through which communication (flux of heat, salt, and nutrients) between the Atlantic and Pacific, via the Arctic Ocean, occurs today. Investigating the evolution of the Bering Strait is critical to an understanding of transitions in global ocean heat and nutrient budgets.

Detailed high-resolution paleoenvironmental reconstructions from the Bering Sea have not been achieved in the past, although there was some reconnaissance work during Deep Sea Drilling Project (DSDP) Leg 19 (Scholl and Creager, 1973), as well as shallow-penetration piston core work that focused on generating paleoceanographic records from the latest Pleistocene (e.g., Cook et al., 2005; Takahashi et al., 2005). Planned drilling (Fig. **F1;** Table **T1**), including triple coring with the advanced piston corer (APC) at all sites, will provide the first continuous sedimentary records that can be used to reconstruct the history of this important marginal sea and its role in global climate and oceanographic changes over the past 5 m.y.

Background

Geological and physical setting

With an area of 2.29×10^6 km^2 and a volume of 3.75×10^6 km^3, the Bering Sea is the third largest marginal sea in the world, surpassed only by the Mediterranean and South China seas (Hood, 1983). Approximately one-half of the Bering Sea is a shallow (0–200 m) neritic environment, with the majority of the continental shelf spanning the eastern side of the basin off Alaska, from Bristol Bay to the Bering Strait (Fig. **F1**). The northern continental shelf is seasonally ice covered, but little ice forms over the deep southwest areas. In addition to the shelf regions, two significant topographic highs have better $CaCO_3$ preservation than the deep basins: the Shirshov Ridge, which extends south of the Koryak Range in Eastern Siberia along 170°E and separates the southwestern part of the Bering Sea into two basins: Komandorski (western part) and Aleutian (eastern part); and the Bowers Ridge, which extends 300 km north from the Aleutian Island arc (Figs. **F1**, **F2**). The Aleutian Basin is a vast plain 3800–3900 m deep with occasional gradually sloping depressions as deep as 4151 m (Hood, 1983).

Three major rivers flow into the Bering Sea: the Kuskokwim and Yukon drain central Alaska and the Anadyr drains eastern Siberia (Fig. **F1**). The Yukon is the longest of the three rivers and supplies the largest discharge into the Bering Sea. Its discharge peaks in August because of meltwater and is about equal to the Mississippi. It has a mean annual flow of 5×10^3 m^3/s, about two-thirds the annual flow of the Columbia River (Hood, 1983).

A substantial amount of water is transported in and out of the Bering Sea across the Aleutian Island arc and the Bering Strait today, through passes illustrated in Figure **F1** and by a bathymetric cross section in Figure **F3**. The water mass exchange with the

Pacific through Aleutian Island passes such as the Kamchatka Strait is significant, which links Bering Sea conditions to the Pacific climate. The Alaskan Stream, an extension of the Alaskan Current, flows westward along the Aleutian Islands and enters the Bering Sea mainly through the Amchitka Strait and to some extent through the Near Strait west of Attu Island in the eastern Aleutian Islands (Fig. **F1**). A part of the Subarctic Current also joins the Alaskan Stream, resulting in a combined volume transport of 11 Sv (Ohtani, 1965). Much of the Pacific water entering the Bering Sea is matched by outflow through the Aleutian Islands. The most significant outflow is through the Kamchatka Strait, which has a maximum depth of 4420 m (Fig. **F3**). If some component of NPIW or deep water formed in the Bering Sea in past times, particularly when sea level was lower, it would have flowed out through the Kamchatka Strait or a secondary outlet near the Commander-Near Strait at 2000 m (Fig. **F3**).

Furthermore, the unidirectional northerly transport of water mass (0.8 Sv) from the Bering Sea through the Bering Strait to the Arctic Ocean contributes to the biogeochemical contrast between the Pacific and the Atlantic. The Bering Strait region is one of the most highly biologically productive regions in the world, 324 g $C/m^2/y$ over a wide area (2.12×10^4 km^2; Sambrotto et al., 1984). Much of the biologically produced organic matter and associated nutrients flow into the Arctic Ocean because of the northward current direction. This may profoundly influence the present dominance of carbonate production in the Atlantic versus opal production in the Pacific, as described by models of basin-to-basin fractionation (Berger, 1970) and of the "carbonate ocean vs. silica ocean" (Honjo, 1990). Flow through the Bering Strait, which is ~50 m deep today, was certainly different at times with a lower sea level or enhanced perennial sea ice cover. Closing of this gateway and accompanying changes in ocean and river flow through time could have caused changes in global patterns of circulation or in nutrient and salinity distributions (Takahashi, 1998, 1999).

Relationship to previous drilling in the Bering Sea, the sub-Arctic North Pacific, and the Arctic Ocean

During DSDP Leg 19 in 1971, six sites were drilled in the Bering Sea and four just south of the Aleutian Islands, in order to generally characterize the sedimentary units and tectonic and structural evolution of the Bering Sea (Scholl and Creager, 1973). Although much of the sediment section was washed away and not cored, DSDP Leg 19 provided basic information on the types and ages of sediments in two of the regions (Umnak Plateau and Bowers Ridge) that are targeted by the planned IODP Bering Sea expedition. The current drilling plan will provide the first deployment of APC technology in the region and thus the first continuous high-resolution records of the past 5 m.y. or longer from the Bering Sea. Specifically, drilling of DSDP Sites 184 and 185 on the Umnak Plateau revealed a Pleistocene to upper Miocene clay-rich diatomaceous ooze (Unit A) above clayey siltstone with sparse fossils (Unit B). At DSDP Site 188 on the Bowers Ridge, sedimentary units similar in lithology and age to those found at the Umnak Plateau sites were found. Although Sites 190 and 191 were drilled close to the Shirshov Ridge and the Kamchatka Strait, they are located in the deep basins around the Shirshov Ridge (water deeper than 3800 m), and sediments recovered were mainly turbidite sequences with reworked microfossils, making paleoceanographic interpretations difficult. This IODP expedition to the Bering Sea will not include drilling in the deep basins; rather, it targets topographic highs above the basin floors where deposition of reworked sediments will be minimal.

In 1992, several important sites adjacent to the Bering Sea were explored during ODP Leg 145: Sites 881, 882, 883, and 884 (Rea et al., 1995; Rea, Basov, Janecek, Palmer-Julson, et al., 1993; Rea, Basov, Scholl, Allen, et al., 1995). Maslin et al. (1996) observed a dramatic increase in IRD, a decrease in sea-surface temperature (>7.5°C) and opal mass accumulation rates (MARs) (five fold decrease), and a decrease in both total organic carbon and $CaCO_3$ MARs at Site 882 (50°22′N, 167°36′E; 3244 m) at 2.75 Ma, which is coeval with the IRD change found in the Norwegian Sea and suggests that the Arctic and northeast Asia were significantly glaciated from 2.75 Ma onward. Furthermore, they suggested that the onset of Eurasian Arctic and northeast Asia glaciation occurred ~100 k.y. before the Alaskan glaciation and 200 k.y. before the glaciation of Greenland and the northeast American continent. Both McKelvey et al. (1995) and Krissek (1995) suggest that the provenance of IRD in the northwest Pacific Ocean and the Gulf of Alaska is the Bering Sea off the Kamchatka Peninsula and southeastern Alaska, respectively. By studying the Bering Sea in relation to other regions, we should be able to uncover details of the inception of glaciation in the Arctic and North Pacific regions at ~2.75 Ma. Furthermore, the reasons for differences in the timing of glaciation can be investigated in detail using the much higher resolution sections, relative to those available in the pelagic realm, that we anticipate.

IODP Expedition 302 (Arctic Coring Expedition [ACEX]) to the Lomonosov Ridge in the central Arctic Ocean took place in 2004, and the scientific community anticipated the acquisition of new information regarding the age and effects of the Bering Strait Gateway to the Arctic. However, despite the expedition's success in terms of the acquisition of sediments spanning from the Holocene to the Cretaceous (Backman, Moran, McInroy, Mayer, et al., 2006; Moran et al., 2006), it has been difficult to advance the understanding of the significance of the Bering Strait Gateway on global or regional climate change without being able to compare new Arctic records to those on the Pacific side of the Bering Strait. Thus, the present plan for drilling in the Bering Sea is essential to deciphering the history of the Bering Strait Gateway and its potential impact on global and regional climatic and oceanic processes. The role of the exchange of heat and chemical constituents through the Bering Strait on Arctic and North Pacific environments, as well as the influence of changes in this exchange on Northern Hemisphere glaciation and higher frequency climate oscillations, can only be assessed by comparing results from Bering Sea drilling together with the results from Expedition 302.

Millennial-scale climate changes

The Bering Sea contains sediments with high accumulation rates appropriate for the reconstruction of surface and deepwater conditions and for the validation of climate/ocean hypotheses that call on these regions as a variable source of open Pacific intermediate and deep water. In addition, climate change records from the Bering Basin tend to be extremely sensitive to high-frequency changes due to the semi-isolated nature of the marginal sea. Sea level drop, for example, may produce a profound effect on water mass circulation, sea ice formation, salinity, and biological productivity in the basin (e.g., Takahashi, 1999). The pelagic signals of the open Pacific do not adequately provide the high-frequency climatic history of the northwest Pacific Rim.

Changes in ventilation of subsurface water in the North Pacific may also influence climate downstream and be tied to North Atlantic climate changes on millennial timescales. Interestingly, millennial cycles in climate proxy records are apparently correlative across the North Pacific, such as those in the Bering Sea (Cook et al., 2005), the Okhotsk Sea (Sakamoto et al., 2005; Ono et al., 2005), the California margin (e.g., Behl and Kennett, 1996), and the Japan Sea (e.g., Tada et al., 1999). Although the mechanisms for strong teleconnections between different sides of the North Pacific are not known, it has been proposed that changes in the Okhotsk (Ono et al., 2005) or Bering Sea source(s) of NPIW could reach the California margin and influence the depth or strength of the oxygen minimum zone (OMZ) (Cannariato and Kennett, 1999; Zheng et al., 2000), thereby connecting climate/ocean changes across the Pacific Ocean. The fact that millennial-scale records from the Pacific margins also appear to correlate with changes in North Atlantic climate (e.g., Behl and Kennett, 1996; Tada et al., 1999) indicates that processes linking Atlantic and Pacific climates could play an important role in global climate change.

There are a number of possible theories that explain paleoceanographic data from the North Pacific marginal seas by implicating changes in NPIW formation (e.g., like that used by Behl and Kennett [1996] to explain observations in the Santa Barbara Basin), changes in flow through the Bering Strait (Hasumi, 2002; De Boer and Nof, 2004; Shaffer and Bendtsen, 1994), and teleconnections from the tropics (Niebauer and Day, 1989; Alexander et al., 2002; Niebauer, 1998; Zhao et al., 2004; Gloersen, 1995). Tests of these theories would greatly benefit from documentation of surface and deep water conditions from the North Pacific marginal seas. Only drilling will allow for the reconstruction of the climate cycles and for the evaluation of whether patterns observed in the last glacial cycle are characteristic of all glacial–interglacial cycles. Only recovery of continuous Pliocene–Pleistocene sediments will allow us to evaluate if the mean state of the climate system (warm versus cold) determines the higher frequency sensitivity, behavior, and climatic impact of these marginal seas. Finally, comparing millennial climate oscillations in the Bering Sea in the Pleistocene when there were large Northern Hemisphere ice sheets to those in the Pliocene warm period when there were only small Northern Hemisphere ice sheets will provide insight into whether the generation of these oscillations is related to NPIW ventilation and/or to ice sheet size and dynamics.

Glacial–interglacial climate change

There was enhanced dense water formation in the last glacial cycle, probably from the Okhotsk and the Bering Seas (e.g., Zahn et al., 1991; Gorbarenko, 1996). In fact, the degree of ventilation of deep and intermediate Pacific waters appears to have been fluctuating during the cold and warm periods, implying changes in the configuration of Pacific Ocean circulation (Keigwin, 1995; Matsumoto et al., 2002). However, there are some contradictory results depending on the nutrient proxy used ($\delta^{13}C$ versus Cd/Ca in benthic foraminifers). Furthermore, the limited spatial coverage of sites in the open Pacific prevents detailed identification of the exact source of intermediate and deep water as well as the exact circulation path of subsurface water masses. Observations have been made in glacial records from the Bering Sea and just outside the Bering Sea on the Detroit Seamount in the North Pacific, suggesting a source of ventilated intermediate water coming from the Bering Sea and/or Detroit Seamount region (Gorbarenko, 1996).

Two examples of prospective reconstructions of Bering Sea paleoceanography made possible by Bering drilling can be viewed from recent studies performed on piston cores collected during the 1999 R/V *Hakuhou-Maru* site survey cruise (Takahashi et al., 2005). Sea ice distribution during the glacial period was modulated by the surface water circulation partially governed by the topography resulting from the sea level drop (Fig. **F4**). It is noteworthy that the distribution of sea ice and water masses is significantly different in the two basins west and east of the Bowers Ridge, depending on water circulation. Past sources of NPIW formation during four different time slices have been reconstructed based on the intermediate water–dwelling radiolarian species *Cycladophora davisiana* (Fig. **F5**). The role of the Bering Sea in NPIW formation is visible during the cold intervals.

Despite evidence that Pacific circulation was different during the last glacial cycle, little is known about what caused circulation to change or what role the Pacific played in determining extreme climate conditions. From extensive studies of the North Atlantic, it is clear that ice sheet dynamics and changes in thermohaline circulation in the Atlantic can readily influence climate, yet there is no widely accepted paradigm that explains how the North Pacific participates in and possibly dominates global climate change. Construction of long records of glacial–interglacial changes by drilling, especially under a range of boundary conditions over the Pliocene–Pleistocene will contribute critical information needed to formulate a new North Pacific climate change paradigm.

Pliocene–Pleistocene trends

In the warm Pliocene (~4.5–3.0 Ma) there is compelling evidence that North Pacific mid-depth water (~2500 m) had much lower nutrient concentrations than today, indicating that it was more strongly ventilated (Kwiek and Ravelo, 1999; Ravelo and Andreasen, 2000). Although increased subsurface ventilation in the cold Last Glacial Maximum (LGM) and the warm Pliocene could be interpreted in a number of different ways and are likely not explained by the same processes, only data that directly reflect conditions in the Bering Sea (and the Okhotsk Sea) can help to constrain interpretations.

The end of the early Pliocene warm period is characterized by the development of modern density stratification in the surface and deep North Pacific. Records of ice-rafted debris (IRD), benthic foraminiferal $\delta^{18}O$ and $\delta^{13}C$, and other paleoceanographic proxies from DSDP and ODP sites indicated that the increased water mass stratification coincided with more extensive glaciation (Haug et al., 1999; Kwiek and Ravelo, 1999; Ravelo and Andreasen, 2000; Rea and Schrader, 1985). Furthermore, more ice-rafted debris is found along the Aleutian Islands (DSDP Site 192) than farther north in the Bering Sea (Sites 186 and 191) because of more extensive ice cover in the north compared to more seasonal ice cover at the Aleutian site (McKelvey et al., 1995; Krissek, 1995). The fact that this North Pacific climate reorganization occurred synchronously with the onset of significant Northern Hemisphere glaciation as recorded in the Atlantic Ocean highlights the importance of studying North Pacific climate evolution as part of a comprehensive investigation of the regional expression of global climate trends.

The emergence of the Bering land bridge (Beringia) prior to the Neogene is not well understood. However, Pliocene climate change, perhaps the onset of Northern Hemisphere glaciation specifically, could have been affected by changes in the marine gateway connection through the Bering Strait region. The connection may have developed in the late Miocene or the early Pliocene, based on occurrences of Atlantic-type mollusks in Hokkaido, Kamchatka, and the Alaska Peninsula in the late Miocene and early Pliocene. The oldest ages for these occurrences range from 6.3–5.1 to 2.2 Ma (e.g., Uozumi et al., 1986), but a recent study documented that the age of first occurrence was 5.5–5.4 Ma (Gladenkov, 2006). One aim of this planned drilling is to recover better records of the oceanographic evolution related to the Miocene/Pliocene gateway history.

Pacific to Arctic flow through the Bering Strait (~0.8 Sv) (Coachman and Aagaard, 1981) significantly influences the Pacific/Atlantic partitioning of physical and nutrient properties in the modern ocean and was possibly quite sensitive to past changes in sea level because of its shallow sill of ~50 m (see Takahashi [2005] for an illustration of the cross section). During glacial intervals, Atlantic Ocean biogenic sedimentation and preservation became more “Pacific-like” and vice-versa and there were major changes in nutrient distributions. Drilling near the Bering Strait will help to resolve whether major changes in Pacific/Atlantic partitioning of oceanographic properties were related to changes in flow through the Bering Sea. Recent findings of *Neodenticula seminae,* a dominant extant subarctic Pacific diatom, in Atlantic waters may be in response to global warming, with the Arctic Ocean providing a passage for this species from the Pacific to the Atlantic. This species has been extinct in the Atlantic since 0.8 Ma (Baldauf, 1986); thus, the recent reemergence in the Atlantic appears to be a significant indication that climate change in the Arctic influenced the distribution of this species.

Seismic studies and site survey data

Seismic and acoustic profiles of the sediments to be drilled at the Bering/Arctic Gateway (GAT), Bowers Ridge (BOW), and Umnak Plateau (UMK) sites were primarily surveyed during the *Hakuhou-Maru* cruise (Seattle–Tokyo) in August 1999, and their details are incorporated in this *Scientific Prospectus*. Together with the geophysical survey effort, piston coring was performed during the same cruise in order to verify that promising paleoceanographic studies can be accomplished in the Bering Sea (Takahashi et al., 2005). In addition to the *Hakuhou-Maru* site survey, seismic profiles obtained by U.S. expeditions—U.S. Naval Service *Bartlett* Cruise 02 (1970) and U.S. Geological Survey *Lee* Cruise L6-80-BS (1980)—were utilized to facilitate drilling approval at the Umnak Plateau, Shirshov Ridge (SHR), and Kamchatka Strait (KST) sites and also have been incorporated here (Fig. **F6**). Crossing seismic lines that were used to target alternate Site NAV-1B include *Farnella*-2-86 SCS Line 4A and *Discoverer* 4-80 Line 18. Supporting site survey data for this expedition are archived at the IODP-MI Site Survey Data Bank (**ssdb.iodp.org**).

Scientific objectives

Study of sedimentary records from the Bering Sea will provide an understanding of

1. The evolution of Pliocene–Pleistocene surface water conditions, paleoproductivity, and sea ice coverage, including millennial- to Milankovitch-scale oscillations;
2. The history of past production of Pacific intermediate and/or deep water masses within the marginal sea and its link to surface water processes;
3. Interactions between marginal sea conditions and continental climate.;
4. Linkages between processes in the marginal sea (e.g., variations in deep water formation or water mass exchange through gateways) and changes in the pelagic Pacific; and
5. Possible effects of the history of ocean/climate of the Bering Strait Gateway region on the North Pacific and global conditions.

These scientific objectives will focus on both long-term ocean and climate trends and the evolution of higher frequency glacial–interglacial to millennial-scale oscillations through the Pliocene–Pleistocene.

Expedition 323 will also target the scientific objectives of IODP Ancillary Program Letter #739, “Microbial respiration, biomass, and community composition in subseafloor sediment of the very high-productivity Bering Sea.” APL #739 aims at constraining global models of organic-fueled subseafloor respiration, subseafloor biomass, and the impact of subseafloor microbes on global biogeochemical fluxes in an extremely high productivity region. APL #739 is available in the “Precruise Information” section at **iodp.tamu.edu/scienceops/expeditions/bering_sea.html.**

Coring and drilling strategy

The coring program prioritizes seven sites (Plan A) (Table **T2**), along with four alternate sites (Table **T4**), in the Bering Sea (Figs. **F1, F2**). However, the final operations plan and number of sites to be cored is contingent upon changes to the *JOIDES Resolution* operations schedule, operational risks (see below), and the outcome of a request for permission to occupy three sites in Russian territorial waters (Sites SHR-1B, SHR-3B, and KST-1B). In the event that such approval is not forthcoming, a back-up plan (Plan B) (Table **T3**) has been devised that substitutes Sites SHR-3B and KST-1B for high-priority Site GAT-3C (and/or Site NAV-1B).

The drilling strategy will consist of advance piston coring in three holes at each site to refusal, with the possible exception of proposed Site BOW-15A, which has shallower depth objectives. An additional hole will be cored to a depth of 25 mbsf at most sites. The sedimentary material recovered from these additional holes will be dedicated to microbiological sampling to satisfy the requirements for achieving the scientific objectives of IODP APL #739. The “drillover” technique will be employed to maximize APC penetration where desirable. For planning purposes, the APC refusal depth for most sites is estimated at 200 meters below seafloor (mbsf). The depth objective for Site BOW-15A is 165 mbsf. Triple-coring at each site will ensure continuity and undisturbed recovery of the stratigraphic section, but additional short APC holes may be drilled as required to achieve complete stratigraphic coverage (i.e., to eliminate all coring gaps and disturbed intervals in a composite section) in the APC interval. In accordance with routine drilling procedures, downhole temperature measurements will be obtained with the advanced piston corer temperature (APCT-3) tool and, where warranted, with the Davis-Villinger Temperature Probe (DVTP). Temperature measurements will allow reconstruction of the thermal gradient at each site. This information will help constrain the history of burial diagenesis of the sediments encountered.

The target depth at three proposed sites (BOW-12B, BOW-14B, and GAT-4C) is greater than the APC refusal depth; the deeper sections will be advanced with the extended core barrel (XCB) and may be cored with the rotary core barrel (RCB) to the final depth objective of 700 mbsf for Sites BOW-12B and GAT-4C and 555 mbsf for Site BOW-14B. XCB drilling will allow penetration through a significant portion of the Pliocene and possibly into the upper Miocene. Time estimates assume that the rotary system will be deployed in the two deeper sites. Should the drilling and coring of the Russian sites not be approved, Site GAT-3C will be cored with the APC to refusal and then with the XCB to 400 mbsf. Site NAV-1B will be cored with the APC system to 150 mbsf.

Wireline logging with the triple combination (triple combo) and Formation MicroScanner (FMS)-sonic tool strings is planned for four sites (UMK-4D, BOW-12B, GAT-4C and SHR-3B) and for four sites in the back-up plan (UMK-4D, BOW-12B, GAT-4C and GAT-3C). Logging will be used for correlating the sediment column to the sediment physical properties and the seismic reflection profiles (see **"Wireline logging"**).

Operational risks

Weather and the nature of the sediments in the Bering Sea may present operational risks that could negatively impact drilling/coring operations, core recovery, core quality, and rate of penetration. Expedition 323 has been scheduled to take place during the summer, the optimum weather season; however, severe weather and fog may still occur and could adversely impact operational efficiency and transit speed. Additionally, the possible presence of ice rafted debris, chert layers, and glacial deposits could lead to bent core barrels and damaged APC shoes and XCB bits.

Drill sites

Age estimates of targeted drilling holes

Our age estimates of the deepest sediments at the bottom of each hole (Table **T1**) are mostly based on the thickness of Holocene sections in nearby locations and the ages of sediments recovered during DSDP Leg 19 based on biostratigraphic data. However, given the known variations in sedimentation rates in the region, actual sedimentation rates, particularly during cold periods and in the older part of the geologic record, could be quite variable. Using a range of possible sedimentation rates, we expect that the proposed triple-APC drilling will penetrate through a significant part of the Pleistocene at least, and that deeper drilling will penetrate into the Pliocene and hopefully at least to the lower Pliocene and/or the upper Miocene at the Bowers Ridge (BOW-12B and BOW-14B) and Bering/Arctic Gateway sites (GAT-4C and GAT-3C).

Umnak Plateau (primary Site UMK-4D and alternate Site UMK-3B)

The first drill site will be UMK-4D on the Umnak Plateau, located off Bristol Bay (Figs. **F1, F2**). Parts of the Alaskan Stream flow into the Bering Sea through Unimak Pass and Amukta Pass today; thus the sediments on the Umnak Plateau can be studied to monitor the exchange of Pacific and Bering Sea waters. These passes are fairly shallow (~50 m and 430 m) so that no intermediate or deep water flows out to the Pacific in this region. According to Scholl and Creager (1973), there are Pleistocene diatomaceous sediments with ash layers in the uppermost 120 m at DSDP Sites 184 and 185, followed by Pliocene diatomaceous sediments below. Sedimentation rates are ~67 m/m.y. They also indicated that the diatomaceous sediments have neritic components, probably influenced from the Bristol Bay region. Thus, we anticipate encountering Pleistocene and Pliocene diatomaceous sediments in the 200 m of APC cores to be drilled here. Sediment samples from these sites will be used to monitor the surface water exchange from the Pacific into the Bering Sea, as well as surface conditions in the easternmost part of the Bering Sea. Site UMK-3B is an alternate.

Bowers Ridge (primary Sites BOW-12B, BOW-14B, and BOW-15A)

Three high-priority drilling locations are located on the Bowers Ridge, which is topographically linked and perpendicular to the Aleutian Island arc, extending northward from the Aleutian Island arc with the top of the ridge generally shallower than 1000 m (Figs. **F1, F2**). The three primary sites are BOW-15A (near the top of the ridge, 837 m water depth), BOW-12B (1313 m), and BOW-14B (on the western slope of the Bowers Ridge at 2166 m), where we expect to encounter foraminiferal preservation as good as that found at DSDP Site 188 (Echols, 1973), based on piston core data. Based on results from DSDP Leg 19, we anticipate that drilling at one site (BOW-15A) to 165 m and at two sites (BOW-12B and BOW-14B) to APC refusal will allow for the recovery of diatomaceous sediments from the entire Pleistocene and into the middle Pliocene; extending penetration deeper using the RCB (at Sites BOW-12B and BOW-14B) will allow for recovery of lower Pliocene diatomaceous sediments and upper Miocene mudstones (Scholl and Creager, 1973).

Samples from these sites will provide records from the shallowest part of our vertical depth transect to a slightly deeper depth at 2166 m and will be used to evaluate vertical water mass gradients when compared to other sites. They will also be used to represent surface water and climate conditions in the southernmost part of the Bering Sea when compared to other drilling sites.

Bering/Arctic Gateway (primary Site GAT-4C and alternate Sites GAT-3C and NAV-1B)

This northern Aleutian Basin region represents a gateway to the Arctic Ocean through the Bering Strait. High-priority Site GAT-4C (1975 m water depth) and alternate Site GAT-3C (3209 m) are located in areas that are topographically protected from possible turbidites (Figs. **F1, F2**). The upper Miocene/Pliocene boundary was placed at ~400 mbsf at DSDP Site 190 (water depth = 3875 m) in the Aleutian Basin (Koizumi, 1973), and the bottom age of the hole at 627 mbsf was in the middle Miocene. Thus, we can be reasonably certain that by drilling to 700 mbsf we will at least have the entire Pliocene–Pleistocene–Holocene sequence, if not the upper Miocene, at this site. Because of the scanty nature of the previous DSDP coring effort, we do not know whether hiatuses existed at Site 190, although it is probable that we have a continuous section here. Based on our 1999 *Hakuhou-Maru* site survey Cruise KH99-3, we have prioritized a relatively shallow site (GAT-4C) to optimize the chances of good carbonate preservation and the nearby alternate site (GAT-3C) at deeper depths for comparison.

Alternate Site NAV-1B is situated near the location of piston core HLY-02-02-3JPC (60°07.6738′N, 179°26.5078′W) at 1132 m water depth. Core 3JPC yielded high sedimentation rates (0.14 m/k.y. during the Holocene, 2.42 m/k.y. during the deglaciation, and 0.91 m/k.y. during the Last Glacial Maximum) and intermittently laminated sediments (Cook et al., 2005). This site is well situated to record changes in surface ocean conditions and NPIW at a resolution that may allow comparison with other high-resolution sites such as the Santa Barbara and Cariaco Basins and the GISP2 record.

Influx of sediments from the Bering/Arctic Gateway region can be readily captured here to reconstruct the gateway's evolution. Change in $CaCO_3$ and opal contents in sedimentary records may tell us Pacific–Atlantic water mass exchange history. Pollen analysis may play an important role here to decipher the temporal variability of the continental environments to the west and east. Ice-rafted pebbles as well as ice algae analyses will tell us the history of glaciation and sea ice formation. Sediment trap data close to these sites will provide groundtruthing for paleoceanographic reconstruction of surface water conditions near the Bering Strait based on diatoms and coccolithophores (e.g., *Coccolithus pelagicus,* a cold-water taxon that occurs in high abundances at the trap stations, and its ancestors).

Shirshov Ridge (primary Site SHR-3B and alternate Site SHR-1B)

The Shirshov Ridge extends south from Siberia, forming a shallow topographic ridge that separates the Aleutian and Komandorski Basins (Figs. **F1, F2**). Samples from the highest priority Site SHR-3B (2232 m water depth) will be used to monitor deep water mass flowing out of the Bering Sea to the Pacific and surface conditions in the eastern Bering Sea. Alternate Site SHR-1B (963 m) could expand the vertical extent of the reconstruction of subsurface water mass conditions. Based on known sedimentation rates in this region, drilling to 200 mbsf will penetrate through the Pleistocene and possibly into the upper Pliocene.

Kamchatka Strait (primary Site KST-1B)

Proposed primary Site KST-1B is inside of the Kamchatka Strait (sometimes called the Komandorski Strait) and located at 3435 m water depth. This represents a strategic location for a deep water mass exiting from the Kamchatka Basin (sill depth through Kamchatka Strait is >4000 m) (Figs. **F1, F3**). Mammerick (1985) discussed a possibility of a bottom thermohaline circulation as a cause of the Meiji sediment tongue (Ewing et al., 1968), which has features similar to the North Atlantic drifts, especially in the general shape, length, and thickness of the various sediment bodies (Scholl et al., 1977, 2003). Drilling here will help to test the Mammerick hypothesis of the thermohaline circulation. Sediments in the Meiji sediment tongue may be supplied from the Bering Sea through the Kamchatka Strait (Scholl et al., 2003). This site represents one of the deepest sites of our vertical depth transect and is the site closest to the outflow of water from the Bering Sea into the North Pacific Ocean.

Logging/downhole measurements strategy

Wireline logging

We plan to acquire wireline logs from four of the seven sites proposed in the primary operations plan. The logging plan for the remaining site (with the shallowest penetration depths) is dependent on assessment, subsequent to coring operations, of the scientific value of acquiring logging data versus the available time. The two standard IODP tool string configurations will be deployed in all holes where logging operations are planned. These are the triple combo and Formation MicroScanner (FMS)-sonic tool strings. In the deeper holes two high-resolution Lamont-Doherty Earth Observatory Borehole Research Group (LDEO-BRG) tools used to acquire spectral gamma rays and magnetic susceptibility (currently under development) are planned to be added to the standard triple combo tool string. Deployment of these high-resolution tools in shallower holes will be determined on a site-to-site basis, taking into consideration the scientific value of these data, final coring depths, hole conditions, and available time.

In addition to the standard logging tools, the Versatile Seismic Imager (VSI) tool will be available for check shot surveys at the deeper drill sites (>200 m). Check shot surveys may help to integrate seismic reflection and velocity profiles with drilling and core data for crosshole and site correlation. Additional operational and planning time may be necessary to respond to air gun deployment and marine mammal policy issues, respectively.

The tool string configurations that are planned to be deployed are as follows:

- Triple combo (potentially with additional high-resolution tools)
    - High-resolution spectral gamma ray (in deeper holes)
    - Spectral gamma ray
    - Neutron porosity
    - Bulk density
    - Hole diameter
    - Resistivity
- FMS-sonic
    - Natural gamma radiation
    - Sonic velocities
    - Resistivity images

The triple combo tool string acquires basic petrophysical parameters of the borehole and provides in situ measurements that can be used to recognize lithologic variations and can be correlated with analogous measurements on recovered core. Density measurements in combination with sonic velocities will be used to compute synthetic seismograms, linking borehole data with seismic lines. FMS images provide high-resolution (~1 cm) azimuthally oriented 360° resistivity images of the borehole walls that are valuable for interpreting sedimentary and structural features and comparing these features to the recovered core. The LDEO-BRG Multi-Sensor Spectral Gamma Ray Tool (MGT) will provide high-resolution continuous records of spectral gamma radiation. This should enable spectral analysis of climatic cycles and recognition of lithologic variations, as well as improved core-log integration. The integration of log and core data will provide a robust stratigraphic framework for each site.

Hole depth can affect the effectiveness of the deployed logging tool string and may determine the importance of allocating time to acquire logging data versus core acquisition. For example, logging shallow holes may be less effective because the drill pipe must remain securely in the hole during logging operations, resulting in loss of logging data in the uppermost section of the hole. Also, tools nearer the top of a tool string are not able to acquire data at the base of the hole. Therefore, in shallower holes, data unattainable from both top and bottom of the hole represent a more significant proportion of the total than in deeper holes where the length of the tool string presents less concern. Because near 100% recovery of the sedimentary sequence is anticipated for the shallow holes, logging will be of a lower priority for this expedition at the shallowest penetration site (e.g., BOW-15A). In contrast, the importance of logging increases in deeper holes and at sites where recovery levels are lower.

In the primary operations plan (Table **T2**), logging operations are proposed for four of the seven sites. Two sites are planned to be cored to a depth of ~700 mbsf (Sites BOW-12B and GAT-4C). For these sites the LDEO-BRG high-resolution spectral gamma tool (MST) is proposed to be run on the standard triple combo tool string. A checkshot survey is also proposed to be done at these two sites. For Sites UMK-4D and SHR-3B, where coring and drilling operations target ~200 mbsf, deployment of the two standard tool strings is proposed. Sites where the coring targets are shallower than 200 mbsf are omitted from the logging program. Final logging operations in these holes will be determined during the expedition, taking into consideration completeness of core recovery, hole condition, and final penetration depth. If time allows, one or both of the higher resolution LDEO-BRG tools may be deployed. A potential tool string that may alternatively be deployed in shallow holes (e.g., if final coring depth is less than ~200 mbsf) comprises a modified tool string with the high-resolution LDEO-BRG tools run in combination with the standard high-resolution lithodensity tool. This represents a shorter length of tool string suited for acquiring high-resolution data in a shallow hole. Logging operations for the back-up operations plan (Plan B, Table **T3**) are similar to the primary plan with the exception of downhole logging at Site GAT-3C (~400 mbsf) (see Table **T3**). Total logging time is comparable for both primary and back-up operations plans.

Further details on logging tools and their applications can be found on the LDEO-BRG Web site (**www.ldeo.columbia.edu/BRG**).

Research plan proposals (samples and data sharing)

Shipboard and shore-based researchers should refer to the IODP Sample, Data, and Obligations Policy (**www.iodp.org/program-policies**). Every member of the scientific party is obligated to carry out scientific research for the expedition and publish it. For this purpose each scientist must submit a detailed research plan and a sample and/or data request prior to the expedition, using the Sample/Data Request form available at **smcs.iodp.org**. A sample/data request is also required for individuals not requesting samples but working on cruise data only. The sampling plan should be limited to samples needed to fulfill the expedition scientific objectives within 36 months postexpedition. All sample and data requests must be submitted 3 months prior to the expedition to ensure the coordinated preparation of an integrated sampling plan.

Based on research (sample and data) requests submitted, the Sample Allocation Committee (SAC; composed of the Co-Chief Scientists, the Staff Scientist, and the IODP-USIO Curator) will work with the scientific party to formulate a formal sampling and data-sharing plan for shipboard and postcruise activities.

The sampling strategy will be subject to modification depending upon the actual material/data recovered and collaborations that may evolve between scientists before and during the expedition. Substantial collaboration and cooperation are highly encouraged. Modifications to the sampling plan and access to samples and data during the expedition and the 1 year postexpedition moratorium period require SAC approval. All sample frequencies and sizes must be justified on a scientific basis and will depend on core recovery, the full spectrum of other requests, and the expedition objectives. Success will require collaboration, integration of complementary data sets, and consistent methods of analysis.

We anticipate having a shore-based sampling party roughly 3–5 months after the expedition for the bulk of everyone's personal research. All sampling to acquire ephemeral data types or to achieve essential sample preservation will be conducted during the expedition. Other shipboard sampling generally will be restricted to low-resolution sampling (e.g., biostratigraphic sampling and toothpick-sized samples for bulk carbonate isotopes), mainly so that we can rapidly produce age model data critical for the overall objectives of the expedition and for planning for higher resolution sampling postcruise. Small intervals (e.g., one core) of high-resolution sampling may be sampled at sea with SAC approval to provide initial material for study prior to the postcruise sampling party. Cores will be delivered to the IODP Core Repository at the

Kochi Core Center in Kochi, Japan, where the main postcruise sampling effort will occur. Deferring most sampling to a shore-based sampling party means that the 1 year moratorium period will not begin until after the postcruise sampling party ends. Therefore, expedition scientists will not experience a reduced moratorium period because of deferred shore-based sampling.

Critical intervals may require special handling, a higher sampling density, reduced sample size, or continuous core sampling for a set of particular high-priority research objectives. The SAC may require an additional formal sampling plan before critical intervals are sampled.

Acknowledgments

The idea for Bering Sea drilling was conceived as part of a two-basin international drilling plan initially submitted as Proposal 477Full in June 1995 during the Ocean Drilling Program era and successively revised several times since then, entitled “The Okhotsk and Bering Seas: High resolution Plio-Pleistocene Evolution of the Glacial/Interglacial Changes in the Marginal Seas.” The proponents involved in the series of proposals include K. Takahashi, I. Koizumi, H. Okada, T. Oba, A. Taira, S. Svarichevsky, S.A. Gorbarenko, R. Tiedemann, D.W. Scholl, M. Okada, A.C. Ravelo, T. Sakamoto, M. Ikehara, H. Tokuyama, K. Iijima, Y. Kido, V. Bezverkhny, K. Katsuki, A. Rezanov, U. Suzuki, T. Tsuru, and F. Yamamoto.

References

Alexander, M.A., Bladé, I., Newman, M., Lanzante, J.R., Lau, N.-C., and Scott, J.D., 2002. The atmospheric bridge: the influence of ENSO teleconnections on air-sea interaction over the global oceans. *J. Clim.,* 15(16):2205–2231. **doi:10.1175/1520-0442(2002)015<2205:TABTIO>2.0.CO;2**

Backman, J., Moran, K., McInroy, D.B., Mayer, L.A., and the Expedition 302 Scientists, 2006. *Proc. IODP,* 302: Edinburgh (Integrated Ocean Drilling Program Management International, Inc.). **doi:10.2204/iodp.proc.302.2006**

Baldauf, J.G., 1987. Diatom biostratigraphy of the middle- and high-latitude North Atlantic Ocean, Deep-Sea Drilling Project Leg 94. *In* Ruddiman, W.F., Kidd, R.B., Thomas, E., et al., *Init. Repts. DSDP,* 94: Washington, DC (U.S. Govt. Printing Office), 729–762. **doi:10.2973/dsdp.proc.94.115.1987**

Behl, R.J., and Kennett, J.P., 1996. Brief interstadial events in the Santa Barbara Basin, NE Pacific, during the last 60 kyr. *Nature (London, U. K.),* 379(6562):243–246. **doi:10.1038/379243a0**

Berger, W.H., 1970. Biogenous deep-sea sediments: fractionation by deep-sea circulation. *Geol. Soc. Am. Bull.,* 81:1385–1401.

Cannariato, K.G., and Kennett, J.P., 1999. Climatically related millennial-scale fluctuations in strength of California margin oxygen-minimum zone during the past 60 k.y. *Geology,* 27(11):975–978. **doi:10.1130/0091-7613(1999)027<0975:CRMSFI>2.3.CO;2**

Coachman, L.K., and Aagaard, K., 1981. Re-evaluation of water transports in the vicinity of Bering Strait. *In* Hood, D.W., and Calder, J.A. (Eds.), *The Eastern Bering Sea Shelf: Oceanography and Resources:* Seattle (Univ. Washington Press), 95–110.

Cook, M.S., Keigwin, L.D., and Sancetta, C.A., 2005. The deglacial history of surface and intermediate water of the Bering Sea. *Deep-Sea Res., Part II,* 52:2163–2173. **doi:10.1016/j.dsr2.2005.07.004**

De Boer, A.M., and Nof, D., 2004. The Bering Strait's grip on Northern Hemisphere climate. *Deep-Sea Res., Part I,* 51(6):1347–1366. **doi:10.1016/j.dsr.2004.05.003**

Echols, R.J., 1973. Foraminifera, Leg 19, Deep Sea Drilling Project. *In* Creager, J.S., Scholl, D.W., et al., *Init. Repts. DSDP,* 19: Washington (U.S. Govt. Printing Office), 721–735. **doi:10.2973/dsdp.proc.19.123.1973**

Ewing, J., Ewing, M., Aitken, T., and Ludwig, W.J., 1968. North Pacific sediment layers measured by seismic profiling. *In* Knopoff, L., Drake, C.L., and Hart, P.J. (Eds.), *The Crust and Upper Mantle of the Pacific Area.* Geophys. Monogr., 12:147–173.

Gladenkov, A.Y., 2006. Neogene diatoms from the Sandy Ridge section, Alaska Peninsula: significance for stratigraphic and paleogeographic reconstructions. *Stratigr. Geol. Correl.,* 14(1):73–90. **doi:10.1134/S0869593806010059**

Gloersen, P., 1995. Modulation of hemispheric sea-ice cover by ENSO events. *Nature (London, U. K.),* 373:503–506. **doi:10.1038/373503a0**

Gorbarenko, S.A., 1996. Stable isotope and lithological evidence of late glacial and Holocene oceanography of the northwestern Pacific and its marginal seas. *Quat. Res.,* 46(3):230–250. **doi:10.1006/qres.1996.0063**

Gorbarenko, S.A., Basov, I.A., Chekhovskayac, M.P., Southon, J., Khusid, T.A., and Artemova, A.V., 2005. Orbital and millennium scale environmental changes in the southern Bering Sea during the last glacial–Holocene: geochemical and paleontological evidence. *Deep-Sea Res., Part II,* 52(16–18):2174–2185. **doi:10.1016/j.dsr2.2005.08.005**

Hasumi, H., 2002. Sensitivity of the global thermohaline circulation to interbasin freshwater transport by the atmosphere and the Bering Sea throughflow. *J. Clim.,* 15(17):2516–2526. **doi:10.1175/1520-0442(2002)015<2516:SOTGTC>2.0.CO;2**

Haug, G.H., Sigman, D.M., Tiedemann, R., Pedersen, T.F., and Sarnthein, M., 1999. Onset of permanent stratification in the subarctic Pacific Ocean. *Nature (London, U. K.),* 401(6755):779–782. **doi:10.1038/44550**

Honjo, S., 1990. Particle fluxes and modern sedimentation in the polar oceans. *In* Smith, W.O., Jr. (Ed.), *Polar Oceanography* (Pt. B): *Chemistry, Biology, and Geology:* New York (Academic), 687–739.

Hood, D.W., 1983. The Bering Sea. *In* Ketchum, B.H. (Ed.), *Estuaries and Enclosed Seas:* The Netherlands (Elsevier), 337–373.

Katsuki, K., and Takahashi, K., 2005. Diatoms as paleoenvironmental proxies for seasonal productivity, sea-ice and surface circulation in the Bering Sea during the late Quaternary. *Deep-Sea Res., Part II,* 52(16–18):2110–2130. **doi:10.1016/j.dsr2.2005.07.001**

Keigwin, L.D., 1995. Northwest Pacific paleohydrography. *In* Tsunogai, S., Iseki, K., Koike, I., and Oba, T. (Eds.), *Global Fluxes of Carbon and Its Related Substances in the Coastal Sea-Ocean-Atmosphere System: Proceedings of the 1994 Sapporo IGBP Symposium:* Yokohama (M and J Int.), 473–478.

Koizumi, I., 1973. The late Cenozoic diatoms of Sites 183–193, Leg 19 Deep Sea Drilling Project. *In* Creager, J.S., Scholl, D.W., et al., *Init. Repts. DSDP,* 19: Washington (U.S. Govt. Printing Office), 805–855. **doi:10.2973/dsdp.proc.19.130.1973**

Krissek, L.A., 1995. Late Cenozoic ice-rafting records from Leg 145 sites in the North Pacific: late Miocene onset, late Pliocene intensification, and Pliocene–Pleistocene events. *In* Rea, D.K., Basov, I.A., Scholl, D.W., and Allan, J.F. (Eds.), *Proc. ODP, Sci. Results,* 145: College Station, TX (Ocean Drilling Program), 179–194. **doi:10.2973/odp.proc.sr.145.118.1995**

Kwiek, P.B., and Ravelo, A.C., 1999. Pacific Ocean intermediate and deep water circulation during the Pliocene. *Palaeogeogr., Palaeoclimatol., Palaeocol.,* 154(3):191–217. **doi:10.1016/S0031-0182(99)00111-X**

Mammerickx, J., 1985. A deep-sea thermohaline flow path in the northwest Pacific. *Mar. Geol.,* 65(1–2):1–19. **doi:10.1016/0025-3227(85)90043-X**

Maslin, M.A., Haug, G.H., Sarnthein, M., and Tiedemann, R., 1995. The progressive intensification of the Northern Hemisphere glaciation as seen from the North Pacific. *Geol. Rundsch.,* 85:452–465.

Matsumoto, K., Oba, T., Lynch-Stieglitz, J., and Yamamoto, H., 2002. Interior hydrography and circulation of the glacial Pacific Ocean. *Quat. Sci. Rev.,* 21(14–15):1693–1704. **doi:10.1016/S0277-3791(01)00142-1**

McKelvey, B.C., Chen, W., and Arculus, R.J., 1995. Provenance of Pliocene–Pleistocene ice-rafted debris, Leg 145, northern Pacific Ocean. *In* Rea, D.K., Basov, I.A., Scholl, D.W., and Allan, J.F. (Eds.), *Proc. ODP, Sci. Results,* 145: College Station, TX (Ocean Drilling Program), 195–204. **doi:10.2973/odp.proc.sr.145.120.1995**

Moran, K., Backman, J., Brinkhuis, H., Clemens, S.C., Cronin, T., Dickens, G.R., Eynaud, F., Gattacceca, J., Jakobsson, M., Jordan, R.W., Makinski, M., King, J., Koc, N., Krylov, A., Martinez, N., Matthiessen, J., McInroy, D., Moore, T.C., Onodera, J., O'Regan, M., Pälike, H., Rea, B., Rio, D., Sakamoto, T., Smith, D.C., Stein, R., St. John, K., Suto, I., Suzuki, N., Takahashi, K., Watanabe, M., Yamamoto, M., Farrell, J., Frank, M., Kubik, P., Jokat, W., and Kristoffersen, Y., 2006. The Cenozoic palaeoenvironment of the Arctic Ocean. *Nature (London, U. K.),* 441(7093):601–605. **doi:10.1038/nature04800**

Niebauer, H.J., 1998. Variability in Bering Sea ice cover as affected by a regime shift in the North Pacific in the period 1947–1996. *J. Geophys. Res.,* 103(C12):27717–27737. **doi:10.1029/98JC02499**

Niebauer, H.J., and Day, R.H., 1989. Causes of interannual variability in the sea ice cover of the eastern Bering Sea. *GeoJournal,* 18(1):45–59. **doi:10.1007/BF00722385**

Ohtani, K., 1965. On the Alaskan Stream in summer. *Bull. Fac. Fish., Hokkaido Univ.,* 15:260–273. (In Japanese).

Okazaki, Y., Takahashi, K., Asahi, H., Katsuki, K., Hori, J., Yasuda, H., Sagawa, Y., and Tokuyama, H., 2005. Productivity changes in the Bering Sea during the late Quaternary. *Deep-Sea Res., Part II,* 52(16–18):2150–2162. **doi:10.1016/j.dsr2.2005.07.003**

Ono, A., Takahashi, K., Katsuki, K., Okazaki, Y., and Sakamoto, T., 2005. The Dansgaard–Oeschger cycles discovered in the upstream source region of the North Pacific Intermediate Water formation. *Geophys. Res. Lett.,* 32(11):L11607. **doi:10.1029/2004GL022260**

Ravelo, A.C., and Andreasen, D.H., 2000. Enhanced circulation during a warm period. *Geophys. Res. Lett.,* 27(7):1001–1004. **doi:10.1029/1999GL007000**

Rea, D.K., Basov, I.A., Janecek, T.R., Palmer-Julson, A., et al., 1993. *Proc. ODP, Init. Repts.,* 145: College Station, TX (Ocean Drilling Program). **doi:10.2973/odp.proc.ir.145.1993**

Rea, D.K., Basov, I.A., Krissek, L.A., and the Leg 145 Scientific Party, 1995. Scientific results of drilling the North Pacific transect. *In* Rea, D.K., Basov, I.A., Scholl, D.W., and Allan, J.F. (Eds.), *Proc. ODP, Sci. Results,* 145: College Station, TX (Ocean Drilling Program), 577–596. **doi:10.2973/odp.proc.sr.145.146.1995**

Rea, D.K., Basov, I.A., Scholl, D.W., and Allan, J.F. (Eds.), 1995. *Proc. ODP, Sci. Results,* 145: College Station, TX (Ocean Drilling Program). **doi:10.2973/odp.proc.sr.145.1995**

Rea, D.K., and Schrader, H., 1985. Late Pliocene onset of glaciation: ice-rafting and diatom stratigraphy of North Pacific DSDP cores. *Palaeogeogr., Palaeoclimatol., Palaeoecol.,* 49(3–4):313–325. **doi:10.1016/0031-0182(85)90059-8**

Sakamoto, T., Ikehara, M., Aoki, K., Iijima, K., Kimura, N., Nakatsuka, T., and Wakatsuchi, M., 2005. Ice-rafted debris (IRD)-based sea-ice expansion events during the past 100 kyrs in the Okhotsk Sea. *Deep Sea Res., Part II,* 52(16–18):2275–2301. **doi:10.1016/j.dsr2.2005.08.007**

Sambrotto, R.N., Goering, J.J., and McRoy, C.P., 1984. Large yearly production of phytoplankton in the western Bering Strait. *Science,* 225(4667):1147–1150. **doi:10.1126/science.225.4667.1147**

Scholl, D.W., and Creager, J.S., 1973. Geologic synthesis of Leg 19 (DSDP) results; far North Pacific and Aleutian Ridge, and Bering Sea. *In* Creager, J.S., Scholl, D.W., et al., *Init. Repts. DSDP,* 19: Washington, D.C. (U.S. Govt. Printing Office), 897–913. **doi:10.2973/dsdp.proc.19.137.1973**

Scholl, D.W., Hein, J.R., Marlow, M., and Buffington, E.C., 1977. Meiji sediment tongue: North Pacific evidence for limited movement between the Pacific and North American plates. *Geol. Soc. Am. Bull.,* 88 (11):1567–1576. **doi:10.1130/0016-7606(1977)88<1567:MSTNPE>2.0.CO;2**

Scholl, D.W., Stevenson, A.J., Noble, M.A., and Rea, D.K., 2003. The Meiji drift body of the northwestern Pacific—modern and paleoceanographic implications. *In* Prothero, D. (Ed.), *From Greenhouse to Icehouse: The Marine Eocene–Oligocene Transition:* New York (Columbia Univ. Press).

Shaffer, G., and Bendtsen., J., 1994. Role of the Bering Strait in controlling North Atlantic ocean circulation and climate. *Nature (London, U. K.),* 367(6461):354–357. **doi:10.1038/367354a0**

Tada, R., Irino, T., and Koizumi, I., 1999. Land-ocean linkages over orbital and millennial time-scales recorded in late Quaternary sediments of the Japan Sea. *Paleoceanography,* 14(2):236–247. **doi:10.1029/1998PA900016**

Takahashi, K., 1998. The Bering and Okhotsk Seas: modern and past paleoceanographic changes and gateway impact. *J. Asian Earth Sci.,* 16(1):49–58. **doi:10.1016/S0743-9547(97)00048-2**

Takahashi, K., 1999. Paleoceanographic changes and present environment of the Bering Sea. *In* Loughlin, T.R., and Ohtani, K. (Eds.), *Dynamics of the Bering Sea:* Fairbanks (Univ. Alaska Sea Grant), 365–385.

Takahashi, K., 2005. The Bering Sea and paleoceanography. *Deep-Sea Res., Part II,* 52(16–18):2080–2091. **doi:10.1016/j.dsr2.2005.08.003**

Takahashi, K., Jordan, R.W., and Boltovskoy, D. (Eds.), 2005. Paleoceanography of the Bering Sea and adjacent regions—preface. *Deep-Sea Res., Part II,* 52(16–18):2079–2364. **doi:10.1016/j.dsr2.2005.08.002**

Tanaka, S., and Takahashi, K., 2005. Late Quaternary paleoceanographic changes in the Bering Sea and the western subarctic Pacific based on radiolarian assemblages. *Deep-Sea Res., Part II,* 52(16–18):2131–2149. **doi:10.1016/j.dsr2.2005.07.002**

Uozumi, S., Akamatsu, M., and Takagi, T., 1986. Takikawa-Honbetsu and Tatsunokuchi faunas (*Fortipecten takahashii*-bearing Pliocene faunas). *Spec. Pap.—Palaeontol. Soc. Japan,* 29:211–226.

Zahn, R., Rushdi, A., Pisias, N.G., Bornhold, B.D., Blaise, B., and Karlin, R., 1991. Carbonate deposition and benthic $\delta^{13}C$ in the subarctic Pacific: implications for changes of the oceanic carbonate system during the past 750,000 years. *Earth Planet. Sci. Lett.,* 103(1–4):116–132.

Zhao, P., Zhang, X., Zhou, X., Ikeda, M., and Yin, Y., 2004. The sea ice extent anomaly in the North Pacific and its impacts on the east Asian summer monsoon rainfall. *J. Clim.,* 17(17):3434–3447. **doi:10.1175/1520-0442(2004)017<3434:TSIEAI>2.0.CO;2**

Zheng, Y., van Geen, A., Anderson, R.F., Gardner, J.V., and Dean, W.E., 2000. Intensification of the northeast Pacific oxygen minimum zone during the Bolling-Allerod warm period. *Paleoceanography,* 15(5):528–536. **doi:10.1029/1999PA000473**

Table T1. Planned drill site details.

Site	Location (latitude, longitude)	Water depth (m)	Penetration (mbsf)		Expected sediment type	Estimated bottom age	Site-specific objectives
			Planned	Approved			
Bowers Ridge							
BOW-12B	53°24.0′N, 179°31.3′W	1313	745	745	Hemipelagic silty clay with siliceous and calcareous microfossils	late Miocene	Entry location for Pacific water, shallow end of depth transect
BOW-14B	54°02.0′N, 179°00.5′E	2166	555	600	Hemipelagic silty clay with siliceous microfossils	late Miocene	Entry location for Pacific water, deep site on the ridge
BOW-15A	54°49.7′N, 176°55.0′E	837	165	165	Hemipelagic silty clay with siliceous and calcareous microfossils	middle Pliocene	Shallow end of depth transect
Gateway							
GAT-3C (alternate)	59°03.0′N, 179°12.2′W	3209	~500	745	Silty clay with siliceous microfossils	late Miocene	Gateway to the Arctic, deep end of depth transect
GAT-4C	57°33.4′N, 175°49.0′W	1975	745	745	Hemipelagic silty clay with siliceous and calcareous microfossils	late Miocene	Gateway to the Arctic
NAV-1B (alternate)	60°9.192′N, 179°28.202′W	1130	150	150	Intermittently laminated hemipelagic silty clay with siliceous and calcareous microfossils	Pleistocene	Late Pleistocene history of Bering Sea at submillennial timescales
Kamchatka Strait (Russia)							
KST-1B	55°55.6′N, 164°54.9′E	3435	200	200	Hemipelagic silty clay with siliceous microfossils	Pliocene	Gateway to the Pacific, western end, deep end of depth transect
Shirshov Ridge (Russia)							
SHR-1B (alternate)	57°19.0′N, 170°06.4′E	963	200	200	Hemipelagic silty clay with siliceous and calcareous microfossils	Pliocene	Sea ice and water mass distribution in northeast region
SHR-3B	56°26.1′N, 170°37.2′E	2232	200	200	Hemipelagic silty clay with siliceous microfossils	Pliocene	Sea ice and water mass distribution, distal to Pacific water
Umnak Plateau							
UMK-4D	54°40.2′N, 169°58.9′W	1900	200	200	Hemipelagic silty clay with siliceous and calcareous microfossils	Pliocene	Sea ice and water mass distribution, distal to Pacific water
UMK-3B (alternate)	54°25.1′N, 170°14.6′W	1898	200	200	Hemipelagic silty clay with siliceous and calcareous microfossils	Pliocene	Sea ice and water mass distribution, distal to Pacific water

Table T2. Primary operations plan. Plan includes sites in Russian territorial waters.

Expedition 323 Bering Sea

Operations Plan and Time Estimate - Plan A

Site No.	Location (Latitude Longitude)	Seafloor Depth (mbrf)	Operations Task Description (mbsf)	Transit (days)	Drilling (days)	Logging (days)
Victoria, BC			Total Time in Port: 5.0 days			
			Transit 1761 nmi to UMK-4D @ 10 kt	7.3		
UMK-4D (USA)	54° 40.2'N 169° 58.9'W	1911	Hole A: APC to ref. ~200 mbsf. APCT/DVTP measurements		1.3	
			Hole B: APC to ref. ~200 mbsf.		0.9	
			Hole C: APC to ref. ~25 mbsf - Microbiology coring		0.2	
			Hole D: APC to ref. ~200 mbsf, Downhole Logging Triple Combo, and FMS-Sonic		1.2	0.5
			Total Time On-Site: 4.0 days			
			Transit 344 nmi to BOW-12B @ 10 kt	1.4		
BOW-12B (USA)	53° 24.0'N 179° 31.3'W	1324	Hole A: APC to ref. ~200 mbsf. APCT/DVTP measurements		1.0	
			Hole B: APC to ref. ~200 mbsf.		0.7	
			Hole C: APC to ref. ~200 mbsf. XCB to ref ~500 mbsf.		2.4	
			Hole D: Drill to ~500 mbsf. RCB to ~700 mbsf. Downhole logging: Triple Combo, FMS-Sonic and VSI		2.5	1.3
			Total Time On-Site: 8.0 days			
			Transit 65 nm to BOW-14B @ 10 kt	0.3		
BOW-14B (USA)	54° 2.0'N 179° 0.5.0'E	2177	Hole A: APC to ref. ~200 mbsf. APCT/DVTP measurements		1.2	
			Hole B: APC to ref. ~200 mbsf.		0.9	
			Hole C: APC to ref. ~200 mbsf. XCB to ref. ~555 mbsf.		3.3	
			Total Time On-Site: 5.4 days			
			Transit 87 nmi to BOW-15A @ 10 kt	0.3		
BOW-15A (USA)	54° 49.7.0'N 176° 55.0'E	848	Hole A: APC to ref. ~165 mbsf. APCT/DVTP measurements		0.7	
			Hole B: APC to ref. ~165 mbsf.		0.5	
			Hole C: APC to ref. ~165 mbsf.		0.5	
			Hole D: APC to ref. ~25 mbsf - Microbiology coring		0.2	
			Total Time On-Site: 2.0 days			
			Transit 292 nmito GAT-4C @ 10 kt	1.2		
GAT-4C (USA)	57° 33.4.0'N 175° 49.0'W	1986	Hole A: APC to ref. ~200 mbsf. APCT/DVTP measurements		1.1	
			Hole B: APC to ref. ~200 mbsf.		0.9	
			Hole C: ABC to ref. ~200 mbsf, XCB to ref. ~500 mbsf.		2.9	
			Hole D: APC to ref. ~25 mbsf - Microbiology coring		0.2	
			Hole E: Drill to ~500 mbsf. RCB to ~700 mbsf. Downhole logging: Triple Combo, FMS-Sonic and VSI		2.8	1.1
			Total Time On-Site: 8.9 days			
			Transit 448 nm to SHR-3B @ 10 kt	1.8		
SHR-3B (Russia)	56° 26.1.0'N 170° 37.2.0'E	2243	Hole A: APC to ref. ~200 mbsf. APCT/DVTP measurements		1.2	
			Hole B: APC to ref. ~200 mbsf.		0.9	
			Hole C: APC to ref. ~25 mbsf - Microbiology coring		0.2	
			Hole D: APC to ref. ~200 mbsf. - Downhole logging: Triple combo and FMS-Sonic		1.1	0.6
			Total Time On-Site: 4.0 days			
			Transit 193 nmi to KST-1B @ 10 kt	0.8		
KST-1B (Russia)	55° 55.6.0'N 164° 54.9.0'E	3446	Hole A: APC to ref. ~190 mbsf. APCT/DVTP measurements		1.5	
			Hole B: APC to ref. ~190 mbsf.		1.1	
			Hole C: APC to ref. ~190 mbsf.		0.2	
			Hole D: APC to ref. ~25 mbsf - Microbiology coring		1.3	
			Total Time On-Site: 4.1 days			
			Transit 1695 nmi from KST-1B to Yokohama, Japan @ 10 kt	6.6		
Yokohama, Japan						
			Subtotal :	**19.6**	**32.9**	**3.5**
			Total Operating Days :	**56.0**		
			Port Call Days :	**5.0**		
			Grand Total Expedition :	**61.0**		

Notes:

1. The JOIDES Resolution will cross 8 time zones during transits gaining 8 hours of time during the expedition, but it will advance one day when crossing the international dateline
2. VSI (checkshots) in Sites GAT-4C and BOW-12B are not yet approved
3. (mbrf) = meters below the rig floor

Table T3. Backup operations plan. Plan only includes sites in U.S. territorial waters.

Expedition 323 Bering sea

Operations Plan and Time Estimate - Plan B

Site No.	Location (Lat/Long)	Seafloor Depth (mbrf)	Operations Task Description (mbsf)	Transit (days)	Drilling (days)	Logging (days)
Victoria, BC			Total Time in Port: 5.0 days			
			Transit 1761 nmi to UMK-4D @ 10 kt	7.3		
UMK-4D	54° 40.2.0'N	1911	Hole A: APC to ref. ~200 mbsf. APCT/DVTP measurements		1.3	
(USA)	169° 58.9.0'W		Hole B: APC to ref. ~200 mbsf.		0.9	
			Hole C: APC to ref. ~25 mbsf - Microbiology coring		0.2	
			Hole D: APC to ref. ~200 mbsf, Downhole Logging Triple Combo, and FMS-Sonic		1.3	0.5
			Total Time On-Site: 4.1 days			
			Transit 344 nmi to BOW-12B @ 10 kt	1.4		
BOW-12B	53° 24.0'N	1324	Hole A: APC to ref. ~200 mbsf. APCT/DVTP measurements		1.0	
(USA)	179° 31.3.0'W		Hole B: APC to ref. ~200 mbsf.		0.7	
			Hole C: APC to ref. ~200 mbsf. XCB to ref ~500 mbsf.		2.5	
			Hole D: Drill to ~500 mbsf. RCB to ~700 mbsf. Downhole logging: Triple Combo, FMS-Sonic and VSI		2.6	1.3
			Total Time On-Site: 8.1 days			
			Transit 65 nmi to BOW-14B @ 10 kt	0.3		
BOW-14B	54° 2.0'N	2177	Hole A: APC to ref. ~200 mbsf. APCT/DVTP measurements		1.2	
(USA)	179° 0.5.0'E		Hole B: APC to ref. ~200 mbsf.		0.9	
			Hole C: APC to ref. ~200 mbsf. XCB to ref. ~555 mbsf.		3.3	
			Total Time On-Site: 5.5 days			
			Transit 87 nmi to BOW-15A @ 10 kt	0.3		
BOW-15A	54° 49.7.0'N	848	Hole A: APC to ref. ~165 mbsf. APCT/DVTP measurements		0.7	
(USA)	176° 55.0'E		Hole B: APC to ref. ~165 mbsf.		0.5	
			Hole C: APC to ref. ~165 mbsf.		0.5	
			Hole D: APC to ref. ~25 mbsf - Microbiology coring		0.2	
			Total Time On-Site: 2.0 days			
			Transit 292 nmi to GAT-4C @ 10 kt	1.2		
GAT-4C	57° 33.4.0'N	1986	Hole A: APC to ref. ~200 mbsf. APCT/DVTP measurements		1.2	
(USA)	175° 49.0'W		Hole B: APC to ref. ~200 mbsf.		0.9	
			Hole C: ABC to ref. ~200 mbsf, XCB to ref. ~500 mbsf.		2.9	
			Hole D: APC to ref. ~25 mbsf - Microbiology coring		0.2	
			Hole E: Drill to ~500 mbsf. RCB to ~700 mbsf. Downhole logging: Triple Combo, FMS-Sonic and VSI		2.8	1.1
			Total Time On-Site: 9.1 days			
			Transit 139 nmi to GAT-3C @ 10 kt	0.6		
GAT-3C	59° 3.0'N	3220	Hole A: APC to ref. ~200 mbsf. APCT/DVTP measurements		1.6	
(USA)	179° 12.2.0'W		Hole B: APC to ref. ~200 mbsf.		1.2	
			Hole C: APC to ref. ~25 mbsf - Microbiology coring		0.2	
			Hole D: APC to ref. ~200 mbsf. XCB to ref. 400 mbsf. Downhole logging: Triple Combo and FSM-Sonic		3.0	0.9
			Total Time On-Site: 6.9 days			
			Transit 2261 nmi from GAT-3C to Yokohama, Japan @ 10 kt	9.3		
Yokohama, Japan						
			Subtotals:	**20.3**	**32.0**	**3.8**
			Total Operating Days:	**56.0**		
			Port Call Days:	**5.0**		
			Grand Total Expedition:	**61.0**		

Notes:

1. The JOIDES Resolution will cross 8 time zones during transits gaining 8 hours of time during the expedition, but it will advance one day when crossing the international dateline
2. VSI (checkshots) in Sites GAT-4C and BOW-12B are not yet approved
3. (mbrf) = meters below the rig floor

Table T4. Operations plan for alternate sites.

Expedition 323 Bering Sea

Operations Plan and Time Estimates - Alternate Sites

Site No.	Location (Lat/Long)	Seafloor Depth (mbrf)	Operations Task Description (mbsf)	Drilling (days)	Logging (days)
			GAT-3C		
GAT-3C (USA)	59° 03.00'N 179° 12.20'W	3220	Hole A: APC to ref. ~200 mbsf. APCT/DVTP measurements	1.6	
			Hole B: APC to ref. ~200 mbsf.	1.2	
			Hole C: APC to ref. ~25 mbsf - Microbiology coring	0.2	
			Hole D: APC to ref. ~200 mbsf, XCB to ref. ~ 400 mbsf. Logging - Triple Combo, & FMS-Sonic	3.0	0.9
			Total Time On-Site: 6.9 days		
			NAV-1B		
NAV-1B (USA)	60° 09.19'N 179° 28.20'W	1140	Hole A: APC to ref. ~150 mbsf. APCT/DVTP measurements	0.8	
			Hole B: APC to ref. ~150 mbsf.	0.6	
			Hole C: APC to ref. ~150 mbsf.	0.6	
			Hole D: APC to ref. ~150 mbsf.	0.5	
			Hole E: APC to ref. ~25 mbsf - Microbiology coring	0.4	
			Total Time On-Site: 2.9 days		
			UMK-3B		
UMK-3B (USA)	54° 25.10'N 170° 14.60'W	1909	Hole A: APC to ref. ~200 mbsf. APCT/DVTP measurements	1.2	
			Hole B: APC to ref. ~200 mbsf.	0.9	
			Hole C: APC to ref. ~25 mbsf - Microbiology coring	0.2	
			Hole D: APC to ref. ~200 mbsf, Downhole Logging Triple Combo, and FMS-Sonic	1.2	0.5
			Total Time On-Site: 4.0 days		
			SHR-1B		
SHR-1B (Russia)	57° 19.00'N 170° 06.40'W	974	Hole A: APC to ref. ~200 mbsf. APCT/DVTP measurements	1.0	
			Hole B: APC to ref. ~200 mbsf.	0.8	
			Hole C: APC to ref. ~25 mbsf - Microbiology coring	0.1	
			Hole D: APC to ref. ~200 mbsf, Downhole Logging Triple Combo, and FMS-Sonic	1.0	0.4
			Total Time On-Site: 3.3 days		

Figure F1. Planned drill sites and highlights of objectives in the Bering Sea. NPIW = Northern Pacific Intermediate Water. Circles = primary sites, squares = alternate sites.

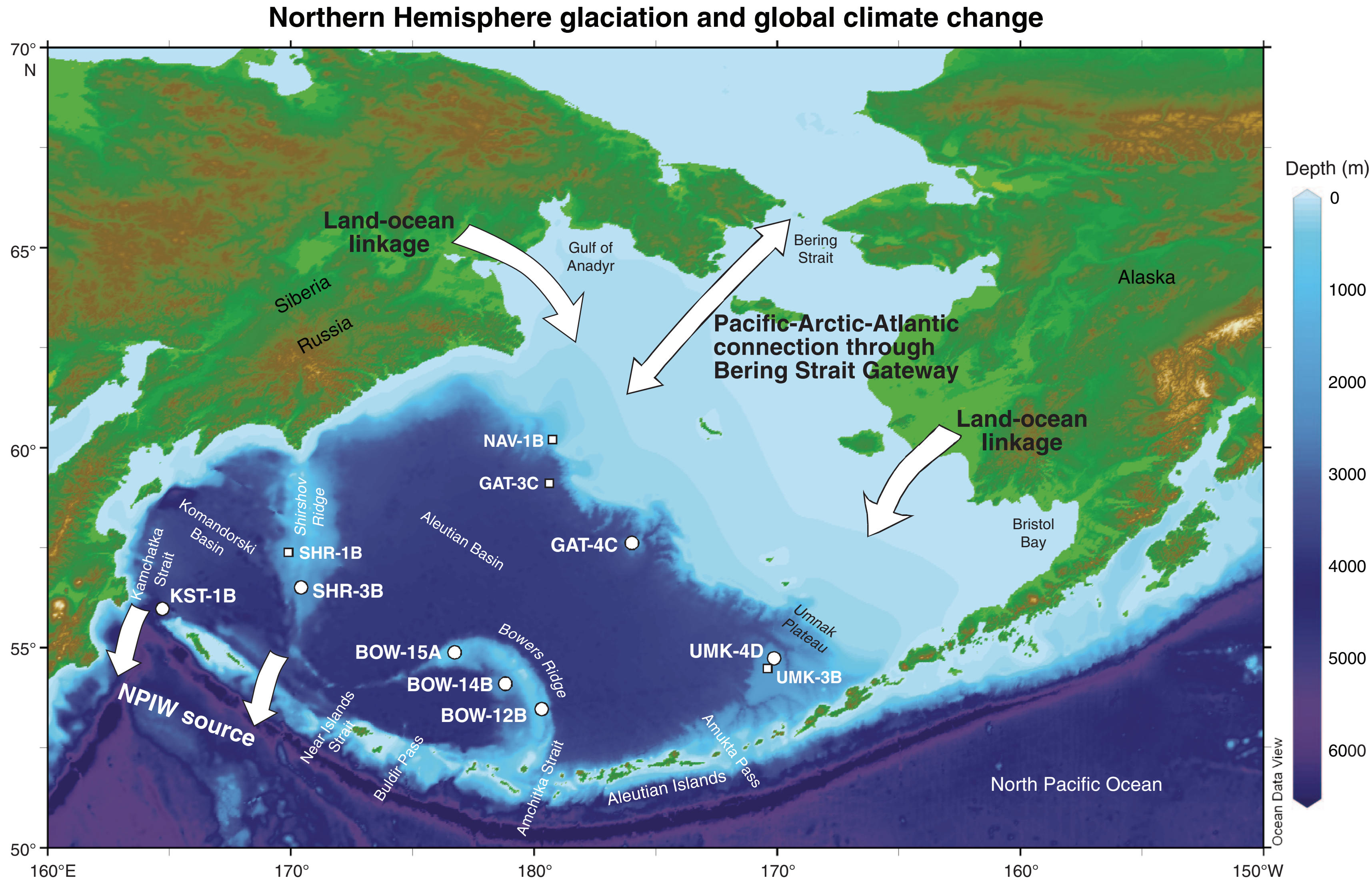

Figure F2. Four regions of planned Bering Sea drilling. Squares = sites drilled during DSDP Leg 19, red circles = primary sites, blue circles = alternate sites. **A.** Kamchatka and Shirshov regions. **B.** Bering/Arctic Gateway. **C.** Bowers Ridge. **D.** Umnak Plateau.

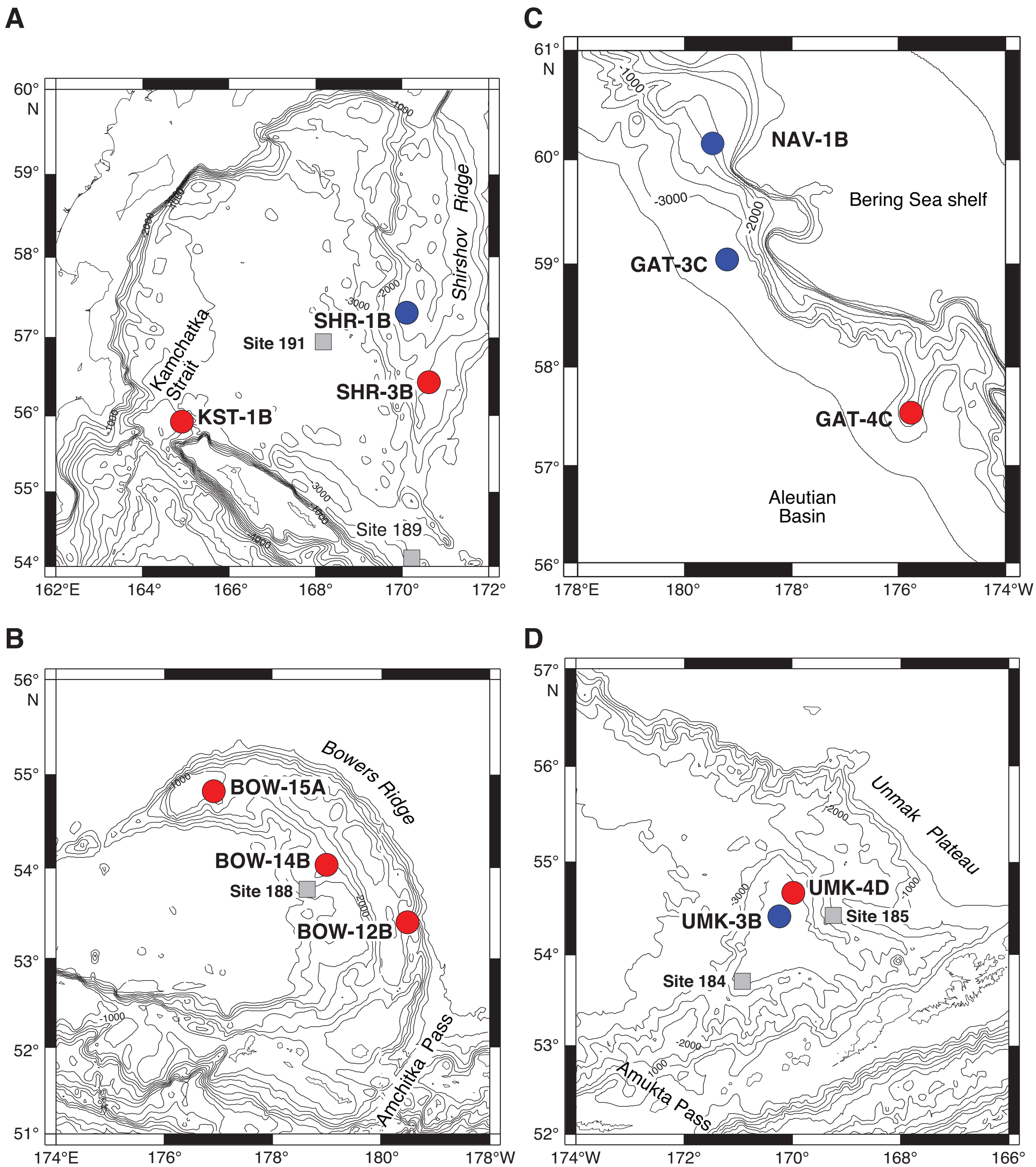

Figure F3. Cross section of straits and passes with volume transport (Sv) in the Aleutian Island arc and the Bering Strait. Note horizontal and vertical scales of the Bering Strait are twice that of the Aleutians for viewing. Aleutians illustration from Stabeno et al. (1999); Bering Strait data from International Bathymetric Chart of the Arctic Ocean (IBCAO) and illustrated in Takahashi (2005).

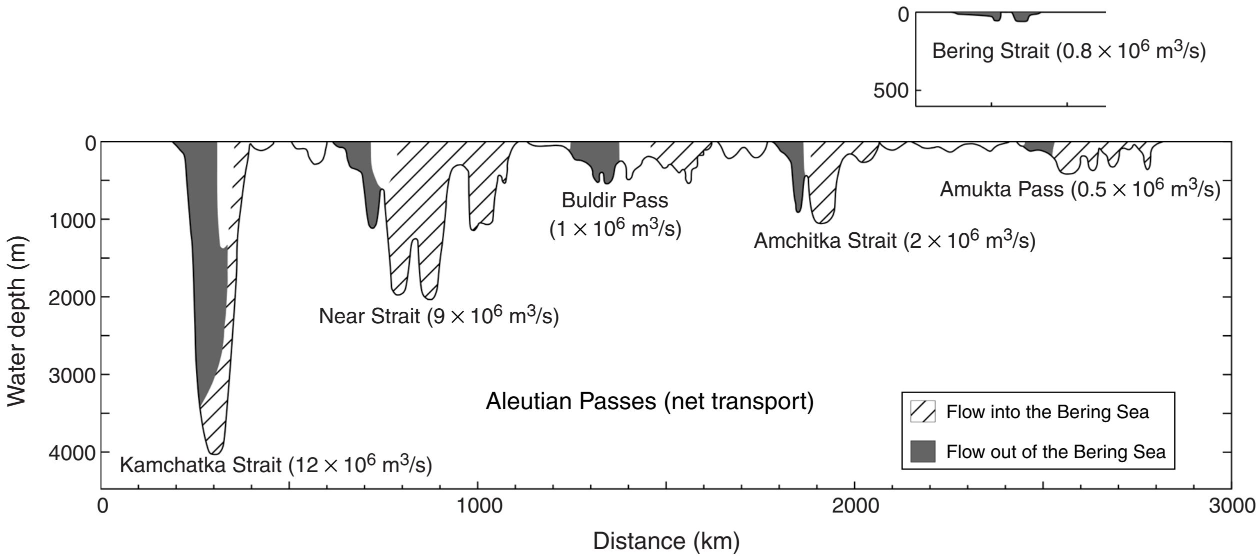

Figure F4. Past sea ice cover and surface circulation system when sea level dropped 100 m below that of today in the Bering Sea and the subarctic Pacific. Dark gray area = paleocontinental shelf, light gray area = paleobathymetry between 400 and 900 m isobaths. Double black arrows = stronger flow than today, gray arrows = weaker flow than today. Circles = cores examined by Katsuki and Takahashi (2005), stars = cores reported from various sources as cited in Katsuki and Takahashi (2005). ES = Emperor Seamount.

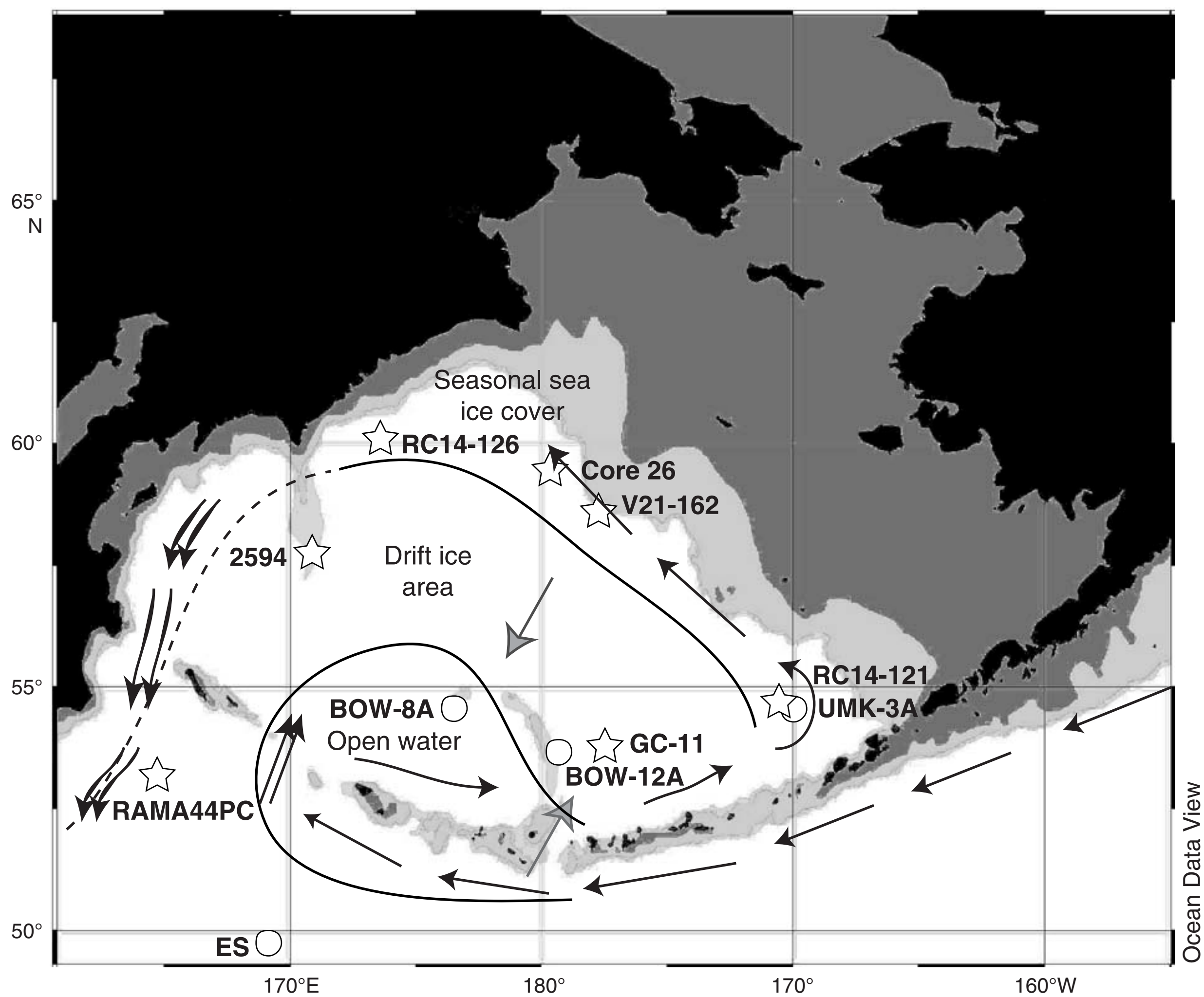

Figure F5. **A.** Relative abundances of *Cycladophora davisiana* during the last 100 k.y. in the Bering Sea, the western subarctic Pacific (circle = Cores BOW-9A, BOW-12A, UMK-3A, and GAT-3A and Site ES [Emperor Seamount, in the subarctic Pacific]), and the Okhotsk Sea (square = Cores PC1, PC2, and PC4; data from Okazaki et al., 2003). **B.** Distribution patterns of *Cycladophora davisiana*: the present (redrawn from Lombari and Boden, 1985), marine isotope stage (MIS) 1, the Last Glacial Maximum (LGM), and MIS 5-3. Arrows indicate source regions of past NPIW (Tanaka and Takahashi, 2005).

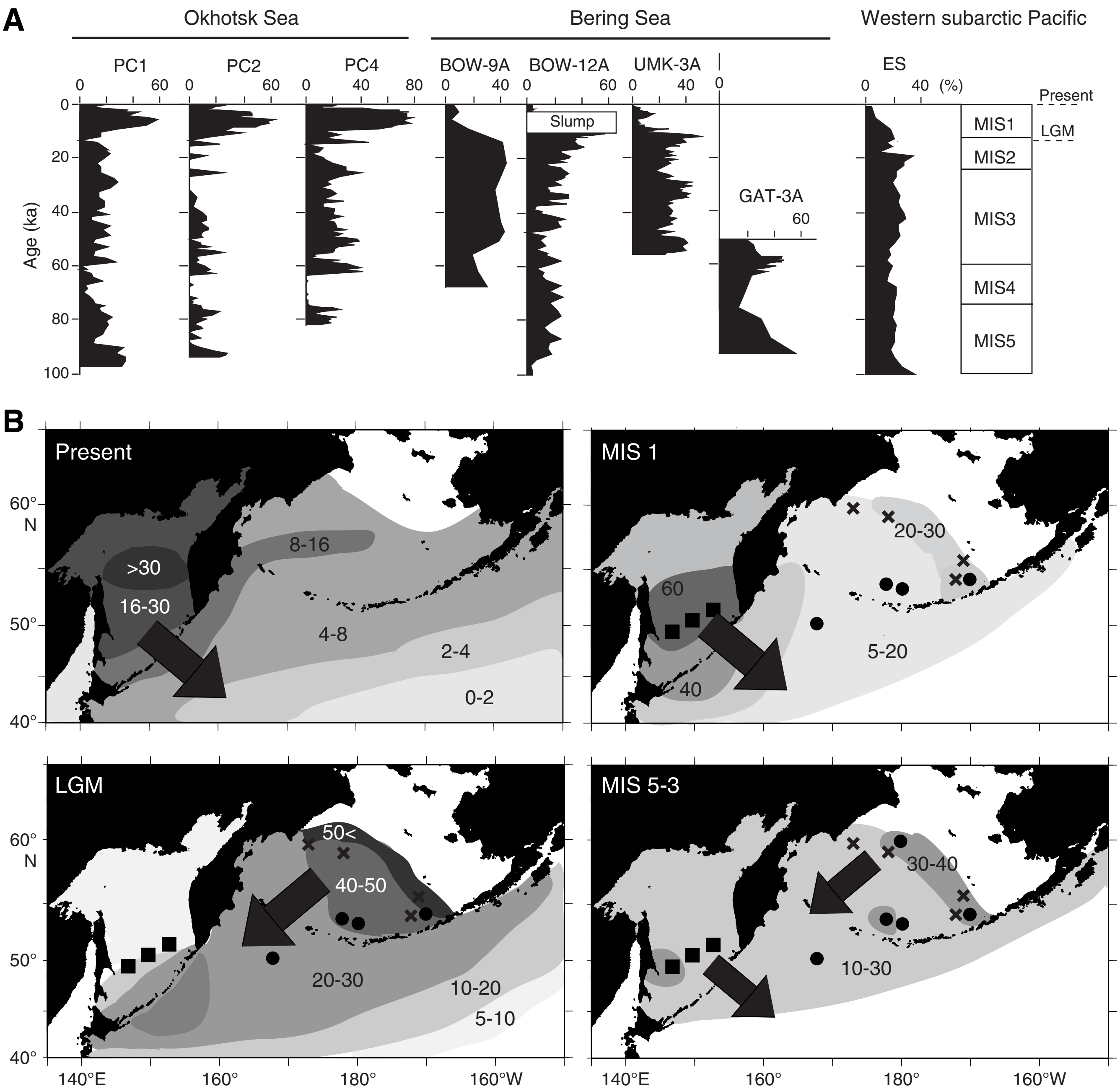

Figure F6. Three navigation tracks of seismic survey cruises over planned drill sites (circles) in the Bering Sea. Refer to **"Site summaries"** for site information, detailed maps, and seismic profiles. Bathymetric contour line created by GMT (**gmt.soest.hawaii.edu**) using the NGDC/NOAA ETOPO2 database (**www.ngdc.noaa.gov/mgg/fliers/01mgg04.html**).

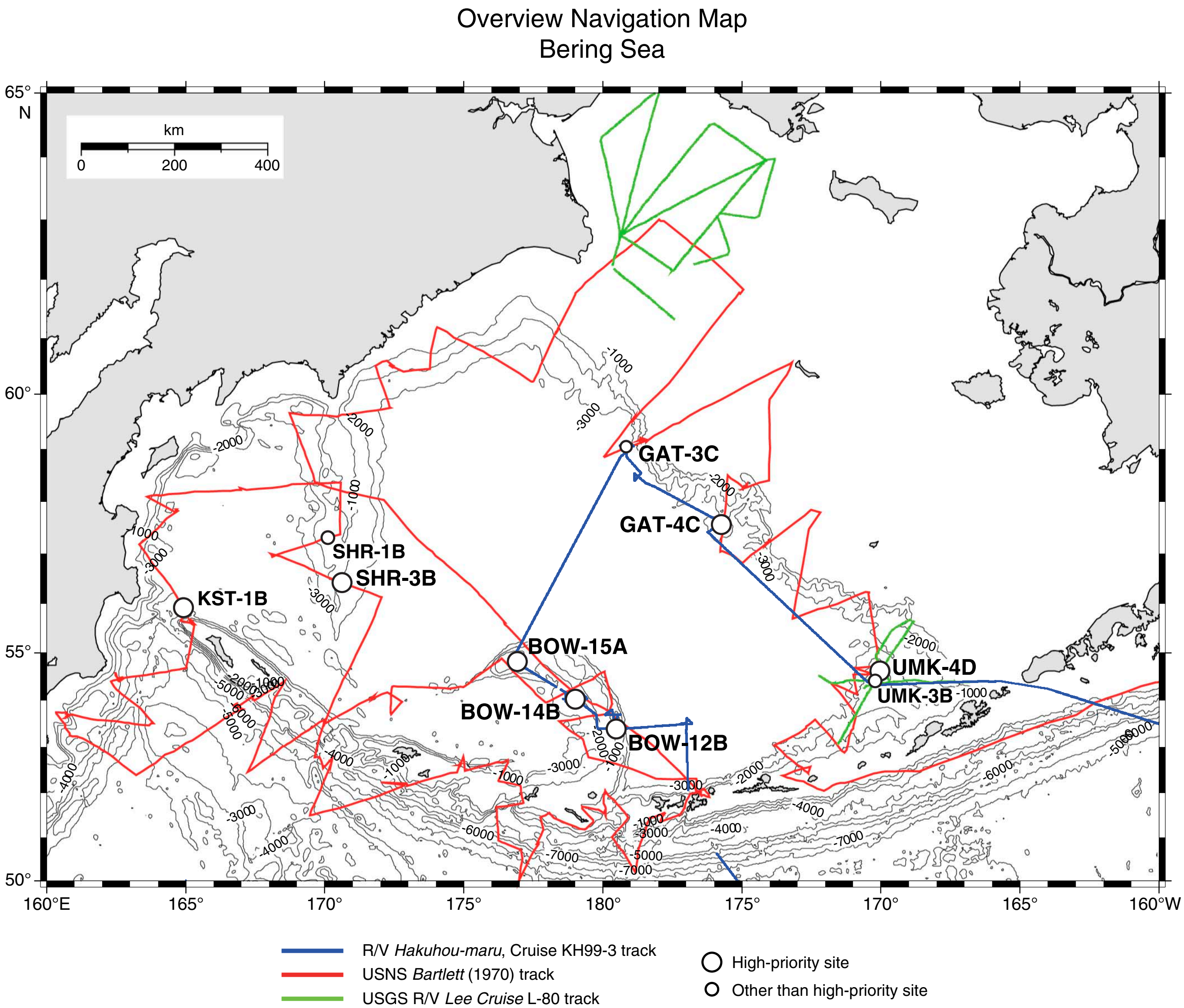

Site summaries

Site BOW-12B (Bowers Ridge): upper Miocene

Priority:	Primary
Position:	53°24.0′N, 179°31.3′W (WGS 84)
Water depth (m)	1313
Target drilling depth (mbsf):	700
Approved maximum penetration (mbsf):	745
Previous drilling in area:	DSDP Site 188
Comments:	Relocated from Site BOW-12A to Shotpoint 910 on Line Stk6-1 during Cruise KH99-3, 1999 (EPSP December 2005)
Survey coverage (track map, seismic profile); sediment cores:	R/V *Hakuhou-maru* Cruise KH99-3 Leg 3 (1999): • Location and track map (Figs. **AF1, AF2**) • Swath bathymetry: Line Stk6-1 (W–E) and Stk6-3 (S–N) (Fig. **AF3**) • MCS profile: Line Stk6-1 (W–E) (Figs. **AF4, AF5**) • Crossing Line Stk6-3 (S–N) (Figs. **AF6, AF7**) • Subbottom profile, 3.5 kHz: Line Stk6-1 (W–E) (Fig. **AF8**) • Piston core (9 m)
Objective (see text for complete details):	Provide records from the shallowest part of vertical depth transect to slightly deep water (2166 m) to evaluate vertical water mass gradients when compared to other sites. Used to represent surface water and climate conditions in the southernmost part of the Bering Sea and to monitor the exchange of North Pacific and Bering Sea water from the upper Miocene through the Pleistocene.
Drilling/coring program:	Triple APC to refusal, XCB and RCB if needed: • Holes A, B, and C: APC with core orientation to refusal (~200 mbsf) • Hole C: XCB to ~500 mbsf • Hole D: drill to ~500 mbsf, RCB to ~700 mbsf; logging Temperature measurements: 3 APCT-3, 2 DVTP if required
Downhole logging program:	Wireline logging: triple combo, FMS-sonic, possible check shot survey
Anticipated lithology:	Hemipelagic silty clay with siliceous and calcareous microfossils

Site summaries (continued)

Site BOW-14B (Bowers Ridge): upper Miocene

Priority:	Primary
Position:	54°02.0′N, 179°00.5′E (WGS 84)
Water depth (m)	2166
Target drilling depth (mbsf):	555
Approved maximum penetration (mbsf):	600
Previous drilling in area:	DSDP Site 188
Comments:	Relocated from Site BOW-14A to Shotpoint 670 on Line Stk5-1 during Cruise KH99-3, 1999. Approved depth of penetration was reduced to 600 mbsf because of concerns about penetrating the strong amplitude event near the original proposed depth of penetration (EPSP December 2005).
Survey coverage (track map, seismic profile); sediment cores:	R/V *Hakuhou-maru* Cruise KH99-3 Leg 3 (1999): • Track map (Figs. **AF9, AF10**) • Swath bathymetry: Line Stk5-1 (W–E) and Stk5-5 (S–N) (Fig. **AF11**) • Subbottom profile, 3.5 kHz: Line Stk5-1 (W–E), Line Stk5-5 (S–N), (Fig. **AF12**) • MCS profile: Line Stk5-1 (W–E) (Figs. **AF13, AF14**) • Crossing Line Stk5-5 (S–N), Shotpoint 2488 (Figs. **AF15, AF16**) • Multiple cores (30 m)
Objective (see text for complete details):	Provide high-resolution records from the deepest part of vertical depth transect in the south Bering Sea; will be used to evaluate vertical water mass gradients when compared to other sites. Monitor exchange of North Pacific and Bering Sea water from the upper Miocene through the Pleistocene.
Drilling/coring program:	Triple APC to refusal, and XCB to 555 mbsf: • Holes A, B, and C: APC with core orientation to refusal (~200 mbsf) • Hole C: XCB to ~555 mbsf; logging Temperature measurements: 3 APCT-3, 2 DVTP if required
Downhole logging program:	Wireline logging: triple combo, FMS-sonic
Anticipated lithology:	Hemipelagic silty clay with siliceous microfossils

Site summaries (continued)

Site BOW-15A (Bowers Ridge): middle Pliocene

Priority:	Primary
Position:	54°49.7′N, 176°55.0′E (WGS 84)
Water depth (m)	837
Target drilling depth (mbsf):	165
Approved maximum penetration (mbsf):	165
Previous drilling in area:	DSDP Site 188
Comments:	Site location and depth of penetration approved by EPSP in December 2005
Survey coverage (track map, seismic profile); sediment cores:	R/V *Hakuhou-maru* Cruise KH99-3 Leg 3 (1999): • Track map (Figs. **AF17, AF18**) • MCS profile: Shotpoint 410 on Line Stk4-1 (N–S) (Figs. **AF19, AF20**) • Crossing Line Stk4-3 (W–E) (Figs. **AF21, AF22**) • Subbottom profile, 3.5 kHz: Line Stk4-1 (W–E) (Fig. **AF23**) • Swath bathymetry: Line Stk4-1 (N–S) and Stk4-3 (W–E) (Fig. **AF24**) • Piston core (9 m)
Objective (see text for complete details):	Provide high-resolution records from the shallowest part of vertical depth transect in the south of the Bering Sea; will be used to evaluate vertical water mass gradients when compared to other sites. Useful in monitoring the exchange of North Pacific and Bering Sea water at shallower depths from the middle Pliocene through the Pleistocene. Reconstruct Pliocene–Pleistocene high-resolution paleoceanography and investigate the Bering/Arctic Gateway history.
Drilling/coring program:	Triple APC in Holes A, B, and C: APC with core orientation to 165 mbsf and in Hole D to 25 mbsf Temperature measurements: 3 APCT-3
Downhole logging program:	No wire-logging currently planned for this site because of shallow penetration
Anticipated lithology:	Hemipelagic silty clay with siliceous and calcareous microfossils

Site summaries (continued)

Site GAT-4C (Gateway): upper Miocene

Priority:	Primary
Position:	57°33.4′N, 175°49.0′W (WGS 84)
Water depth (m)	1975
Target drilling depth (mbsf):	700
Approved maximum penetration (mbsf):	745
Previous drilling in area:	None
Comments:	Relocated from GAT-4B to Shotpoint 351 on Cruise KH99-3, 1999, Line Stk-1 (EPSP December 2005)
Survey coverage (track map, seismic profile); sediment cores:	R/V *Hakuhou-maru* Cruise KH99-3 Leg 3 (1999): • Location and track maps (Figs. **AF25, AF26, AF27**) • MCS profile: Line Stk1 (SW–NE) • Crossing Line Stk2 (SE–NW) (Figs. **AF28, AF29, AF30, AF31**) • 3.5 kHz: Line Stk1 (SW–NE) (Fig. **AF32**) • Swath bathymetry: Lines Stk1 (SW–NE) and Stk2 (SE–NW) (Fig. **AF33**) • Multiple cores (16 cm)
Objective (see text for complete details):	Tripe APC to refusal, XCB and RCB if needed: • Holes A, B, C: APC with core orientation to refusal (~200 mbsf) • Hole C: XCB to ~500 mbsf • Hole D: APC to 25 mbsf • Hole E: drill to ~500 mbsf, RCB to ~700 mbsf Temperature measurements: 3 APCT-3, 2 DVTP if required
Drilling/coring program:	See **BOW-12B**
Downhole logging program:	Wireline logging: triple combo, FMS-sonic, possible check shot survey
Anticipated lithology:	Hemipelagic silty clay with siliceous and calcareous microfossils

Site summaries (continued)

Site GAT-3C (Gateway): upper Miocene

Priority:	Alternate
Position:	59°03.0′N, 179°12.2′W (WGS 84)
Water depth (m)	3209
Target drilling depth (mbsf):	400
Approved maximum penetration (mbsf):	745
Previous drilling in area:	None
Comments:	Relocated from GAT-3B to Shotpoint 2860 on Cruise KH99-3, 1999, Line Stk3-7 (EPSP December 2005)
Survey coverage (track map, seismic profile); sediment cores:	R/V *Hakuhou-maru* Cruise KH99-3 Leg 3 (1999): • Track map (Figs. **AF34, AF35**) • Seismic profiles: Line 3Stk3-7 (W–E); Crossing Line Stk3-5 (S–N) (Figs. **AF36, AF37, AF38, AF39**) • 3.5 kHz: Line Stk3-7 (W–E) (Fig. **AF40**) • Swath bathymetry: Lines Stk3-7 (W–E) and Stk3-5 (S–N) (Fig. **AF41**) • Piston core (9.6 m) USNS *Bartlett* Cruise 02, Leg 093 (1970): • Deep penetration seismic reflection primary line: 256 Day, 1970, 04:56–20:15; begin 58.85100N, 179.94300W; finish 60.57400N, 173.20200W
Objective (see text for complete details):	Reconstruct and monitor evolution of the Arctic/Bering Strait Gateway and Pacific-Atlantic water mass exchange history from the upper Miocene through the Pleistocene. Relatively deeper depth will provide alternate view to GAT-4C for comparison.
Drilling/coring program:	Triple APC to refusal and XCB to 400 mbsf: • Holes A, B, and D: APC with core orientation to refusal (~200 mbsf) • Hole D: XCB to ~400 mbsf • Hole C: APC to 25 mbsf Temperature measurements: 3 APCT-3, 2 DVTP if required
Downhole logging program:	Wireline logging: triple combo, FMS-sonic
Anticipated lithology:	Silty clay with siliceous microfossils

Site summaries (continued)

Site KST-1B (Kamchatka Strait): Pliocene

Priority:	Primary
Position:	55°55.6′N, 164°54.9′E (WGS 84) [Russia]
Water depth (m)	3435
Target drilling depth (mbsf):	190
Approved maximum penetration (mbsf):	200
Previous drilling in area:	DSDP Site 191 (far east in Kamchatka Basin) and Site 192 (far south of this area in the North Pacific)
Comments:	Approved at relocated position at track time 7:03:46 on USNS *Bartlett* Cruise 02, Leg 049, 232 Day, 1970, 22:14–17:32 (EPSP December 2005)
Survey coverage (track map, seismic profile); sediment cores:	USNS *Bartlett Cruise* 02, Leg 049, 232 Day (1970) 22:14–17:32: • Track map (Fig. **AF42**) • Single-channel seismic (Figs. **AF43, AF44**)
Objective (see text for complete details):	Monitor cold dense deep or intermediate water formation in the Bering Sea; gateway to the Pacific Ocean and westernmost and deep end of depth transect.
Drilling/coring program:	Holes A, B, and C: APC with core orientation to 190 mbsf, Hole D to 25 mbsf. Temperature measurements: 3 APCT-3
Downhole logging program:	Wireline logging: triple combo, FMS-sonic
Anticipated lithology:	Hemipelagic silty clay with siliceous microfossils

Site summaries (continued)

Site SHR-3B (Shirshov Ridge): Pliocene

Priority:	Primary
Position:	56°26.1′N, 170°37.2′E (WGS 84) [Russia]
Water depth (m)	2232
Target drilling depth (mbsf):	200
Approved maximum penetration (mbsf):	200
Previous drilling in area:	DSDP Site 191 (farther southwest) and 192 (farther south)
Comments	Approved at relocated position at track time 8:20 on USNS *Bartlett* Cruise 02, Leg 055, 236 Day, 1970, 07:00–09:00 (EPSP December 2005)
Survey coverage (track map, seismic profile); sediment cores:	USNS *Bartlett Cruise* 02, Leg 055, 236 Day (1970) 14:00-13:15: • Track maps (Figs. **AF45, AF46, AF47**) • Single-channel seismic (Figs. **AF48, AF49**) • Seismic velocity: DSDP Site 189 measurement; ref. interval velocity by USGS R/V *Lee* Cruise L6-80, Line 6 • Multiple cores (16 cm)
Objective (see text for complete details):	Monitor deep and intermediate water masses flowing out of the Bering Sea to the Pacific and surface conditions in the western Bering Sea. Reconstruct Pliocene-Pleistocene high-resolution paleoceanography and investigate Bering/Arctic Gateway history and sea ice and water mass distribution in the northeast region.
Drilling/coring program:	Holes A, B, and D: APC with core orientation to 200 mbsf, Hole C to 25 mbsf Temperature measurements: 3 APCT-3
Downhole logging program:	Wireline logging: triple combo, FMS-sonic
Anticipated lithology:	Hemipelagic silty clay with siliceous microfossils

Site summaries (continued)

Site SHR-1B (Shirshov Ridge): Pliocene

Priority:	Alternate
Position:	57°19.0′N, 170°06.4′E (WGS 84) [Russia]
Water depth (m)	963
Target drilling depth (mbsf):	200
Approved maximum penetration (mbsf):	200 Approved at relocated position (previously SHR-1A) (EPSP December 2005)
Previous drilling in area:	DSDP Sites 191 (farther southwest) and 192 (farther south)
Comments:	Approved at relocated position at track time 0:30 on USNS *Bartlett* Cruise 02, Leg 054, 235 Day, 1970, 23:14–01:20 (EPSP December 2005)
Survey coverage (track map, seismic profile); sediment cores:	USNS *Bartlett* Cruise 02, Leg 054, 235 Day (1970) 23:14–14:00: • Track maps (Figs. **AF45, AF46**) • Single-channel seismic (Figs. **AF50, AF51**) • Seismic velocity: DSDP Site 189 measurement; ref. interval velocity by R/V *Lee* Cruise L6-80, Line 6
Objective (see text for complete details):	Monitor subsurface water mass flowing out of the Bering Sea to the Pacific; could expand vertical extent of reconstruction of subsurface water mass conditions. Reconstruct Pliocene–Pleistocene high-resolution paleoceanography and investigate Bering/Arctic Gateway history and sea ice and water mass distribution in the northeast region.
Drilling/coring program:	Holes A, B, and D: APC with core orientation to 200 mbsf, Hole C to 25 mbsf Temperature measurements: 3 APCT-3
Downhole logging program:	Wireline logging: triple combo, FMS-sonic
Anticipated lithology:	Hemipelagic silty clay with siliceous and calcareous microfossils

Site summaries (continued)

Site UMK-4D (Umnak Plateau): Pliocene–Pleistocene

Priority:	Primary
Position:	54°40.2′N, 169°58.9′W (WGS 84)
Water depth (m)	1900
Target drilling depth (mbsf):	200
Approved maximum penetration (mbsf):	200
Previous drilling in area:	DSDP Site 185
Comments:	Relocated from Site UMK-4C to Shotpoint 3275 on Line 2 of USGS R/V *Lee* Cruise L6-80 (EPSP December 2005)
Survey coverage (track map, seismic profile); sediment cores:	USGS R/V *Lee* Cruise L6-80 (1980): • Single-channel seismic: Line 2 (Figs. **AF52, AF53**) • Crossing Line 5 (Figs. **AF54, AF55**) • Seismic velocity: DSDP Site 185 measurement; ref. interval velocity by R/V *Lee* Cruise L6-80, Line 6 R/V *Hakuhou-maru* Cruise KH99-3 Leg 3 (1999): • Regional overview map with track line (Fig. **AF55**) • 3.5 kHz (Fig. **AF56**) • Swath bathymetry (Fig. **AF57**) • Multiple cores (30 cm)
Objective (see text for complete details):	Monitor surface water exchange from the Pacific into the Bering Sea and surface conditions in the easternmost part of the Bering Sea. Reconstruct Pliocene–Pleistocene high-resolution paleoceanography and investigate Bering/Arctic Gateway history and sea ice and water mass distribution, distal to Pacific water.
Drilling/coring program:	Holes A, B, and D: APC with core orientation to ~200 m, Hole C to 25 mbsf Temperature measurements: 3 APCT-3
Downhole logging program:	Wireline logging: triple combo, FMS-sonic
Anticipated lithology:	Hemipelagic silty clay with siliceous and calcareous microfossils. Estimated bottom age = Pliocene.

Site summaries (continued)

Site UMK-3B (Umnak Plateau): Pliocene–Pleistocene

Priority:	Alternate
Position:	54°25.1′N 170°14.6′W (WGS 84)
Water depth (m)	1898
Target drilling depth (mbsf):	200
Approved maximum penetration (mbsf):	200
Previous drilling in area:	DSDP Site 185
Comments:	Relocated from Site UMK-3A to shot point 2617 on the Line 2 of Cruise L6-80 of USGS R/V *Lee* (EPSP December 2005)
Survey coverage (track map, seismic profile); sediment cores:	USGS R/V *Lee* Cruise L6-80 (1980): • Single channel seismic: Line 2 and crossing Line 6, Shotpoint 721 (Figs. **AF52, AF58, AF59**) • Seismic velocity: DSDP Site 185 measurement; ref. interval velocity by USGS R/V *Lee* Cruise L6-80, Line 6 R/V *Hakuhou-maru* Cruise KH99-3 Leg 3 (1999): • Regional overview map with track line (Fig. **AF55**) • 3.5 kHz • Swath bathymetry (Fig. **AF57**) • Piston core (9.6 m)
Objective (see text for complete details):	Monitor surface water exchange from the Pacific into the Bering Sea and surface conditions in the easternmost part of the Bering Sea. Reconstruct Pliocene–Pleistocene high-resolution paleoceanography and investigate Bering/Arctic Gateway history and sea ice and water mass distribution, distal to Pacific water
Drilling/coring program:	Holes A, B, and D: APC with core orientation to 200 mbsf, Hole C to 25 mbsf Temperature measurements: 3 APCT-3
Downhole logging program:	Wireline logging: triple combo, FMS-sonic
Anticipated lithology:	Hemipelagic silty clay with siliceous and calcareous microfossils. Estimated bottom age = Pliocene.

Site summaries (continued)

Site NAV-1B: Pleistocene

Priority:	Alternate
Position:	60°09.19′N, 179°28.20′W
Water depth (m)	1130
Target drilling depth (mbsf):	150
Approved maximum penetration (mbsf):	150
Previous drilling in area:	Piston core *Healy* 02-02-3JPC
Comments:	Relocated from NAV-1A because of an unconformity observed in the seismic profile of *Discoverer* 4-80-BS Line 18 If time is available, coring NAV-1B will provide very high resolution Pleistocene records that could be compared to the Santa Barbara and Cariaco basins and the GISP2 records.
Survey coverage (track map, seismic profile); sediment cores:	• Track map (Fig. **AF60**) • Seismic profiles: CDP1139 on *Farnella*-2-86 BS Line 4A (Fig. **AF61**); 1550Z on *Discoverer* 4-80 BS Line 18 (Fig. **AF62**) • Minisparker (Fig. **AF63**)
Objective (see text for complete details):	Reconstruct high-resolution history of climate of the subarctic Pacific during the late Pleistocene. Study history of North Pacific Intermediate Water formation at submillennial timescales. Investigate oceanic and atmospheric linkage between subarctic Pacific and the rest of the globe during millennial-scale and rapid climate events.
Drilling/coring program:	Quadruple APC (Holes A, B, C, and D) with core orientation to 150 mbsf, Hole E to 25 mbsf
Downhole logging program:	NA
Anticipated lithology:	Hemipelagic silty clay with calcareous and siliceous microfossils

Figure AF1. Specific navigation map of *Hakuhou-maru* Cruise KH99-3 around primary Site BOW-12B with ship time and shotpoint annotation. Crossing of survey lines is at 06:02:15, Shotpoint 863, on Line Stk6-1 (W–E) and 09:42:05, Shotpoint 1537, on Line Stk6-3 (S–N). Site BOW-12B is located at 06:13:20, Shotpoint 910, on Line Stk6-1 (W–E). Squares = navigation map area for close-up seismic profiles in Figure **AF2.** Time annotation in black letters = range of subbottom profile survey in Figure **AF8.**

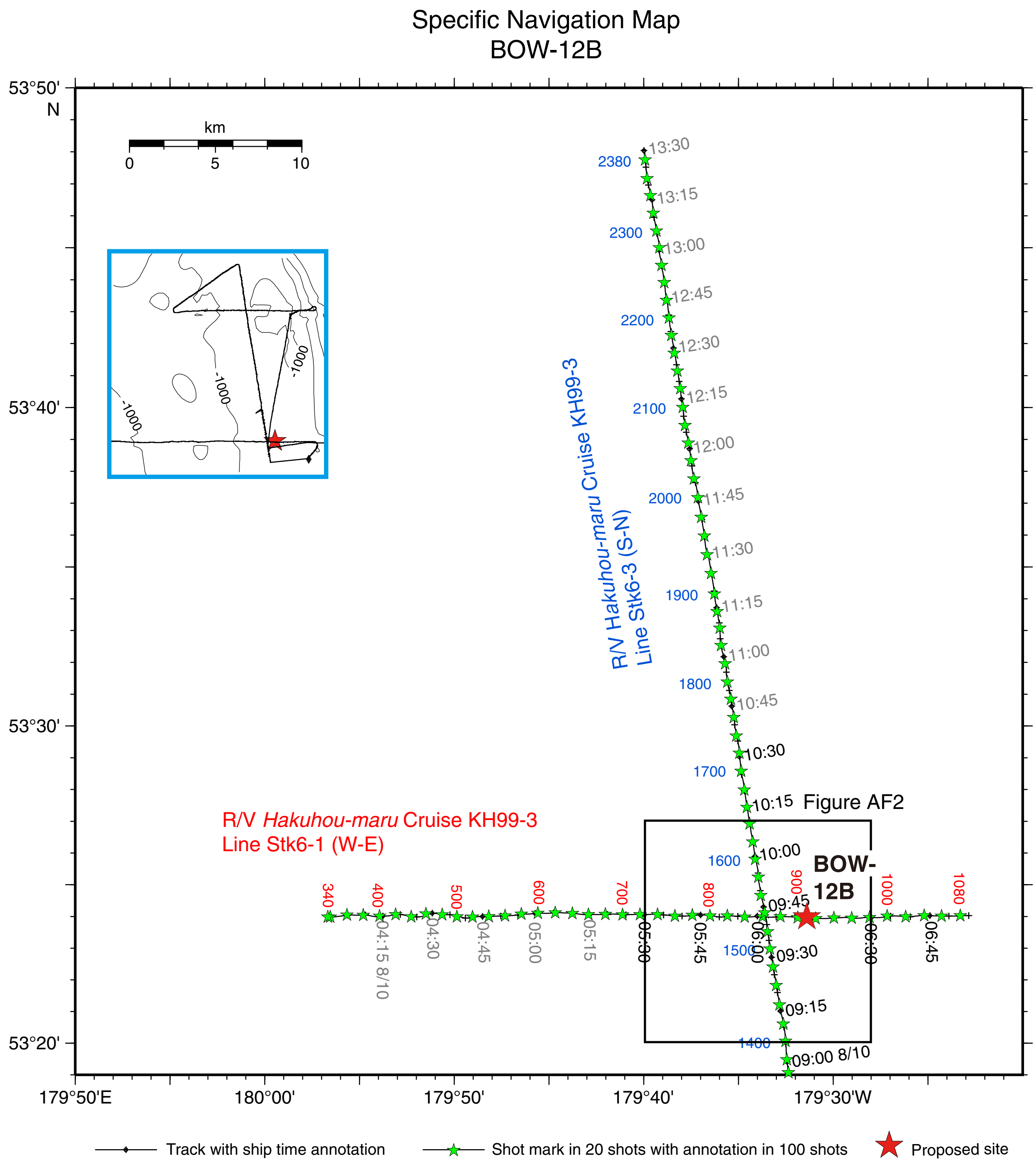

Figure AF2. Close-up navigation map of *Hakuhou-maru* Cruise KH99-3 around Site BOW-12B for close-up seismic profile in Figures **AF4** and **AF12.** Crossing of survey lines is at 06:02:15, Shotpoint 863, on Line Stk6-1 (W–E) and 09:42:05, Shotpoint 1537, on Line Stk6-3 (S–N). Site BOW-12B is located at 06:13:20, Shotpoint 910, on Line Stk6-1 (W–E).

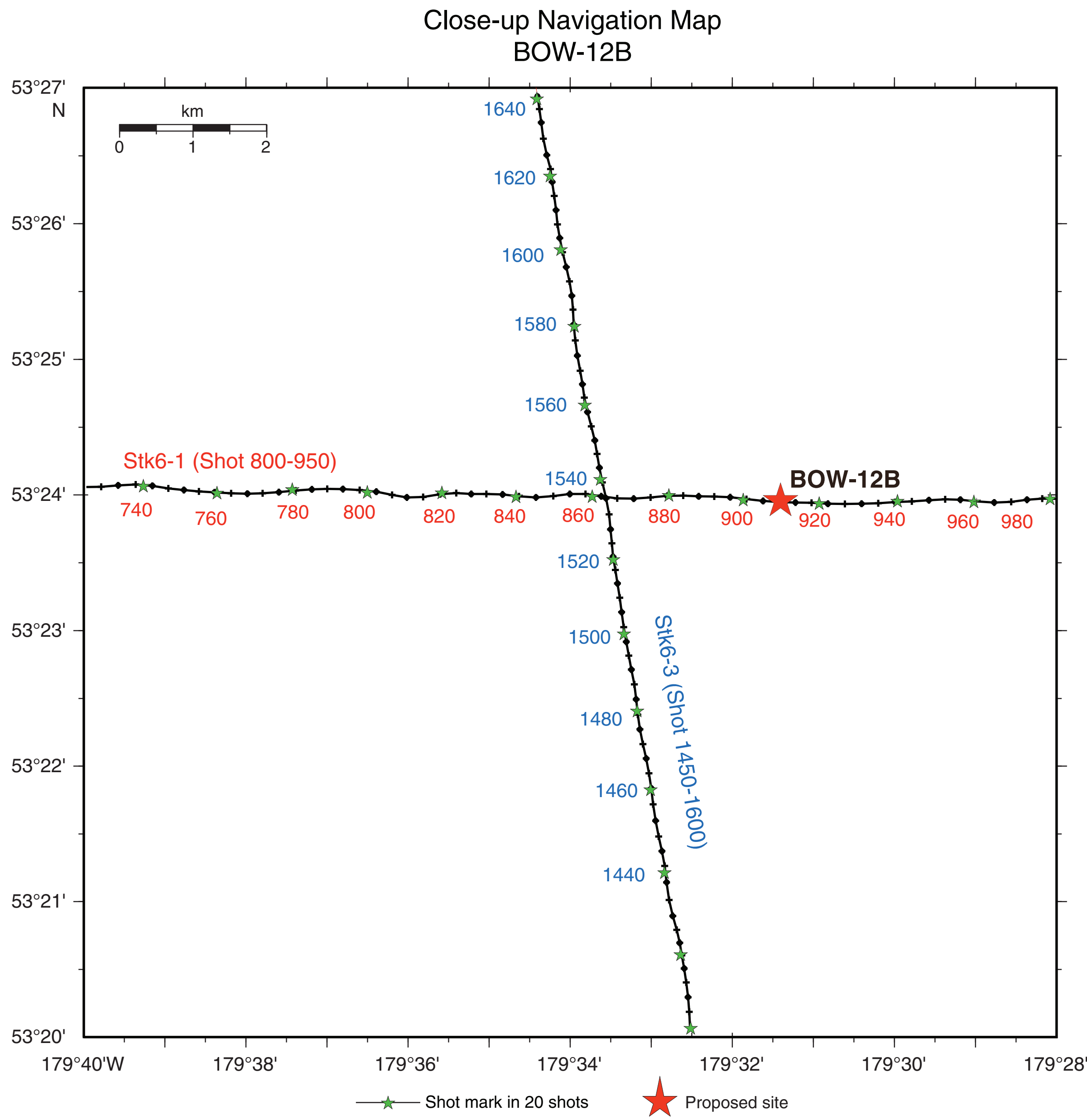

Figure AF3. Swath bathymetric map with track chart of *Hakuhou-maru* Cruise KH99-3 around Site BOW-12B. **A.** Plain image. **B.** Shaded relief image. Crossing of survey lines is at 06:02:15, Shotpoint 863, on Line Stk6-1 (W–E) and 09:42:05, Shotpoint 1537 on Line Stk6-3 (S–N). Site BOW-12B is located at 06:13:20, Shotpoint 910, on Line Stk6-1 (W–E).

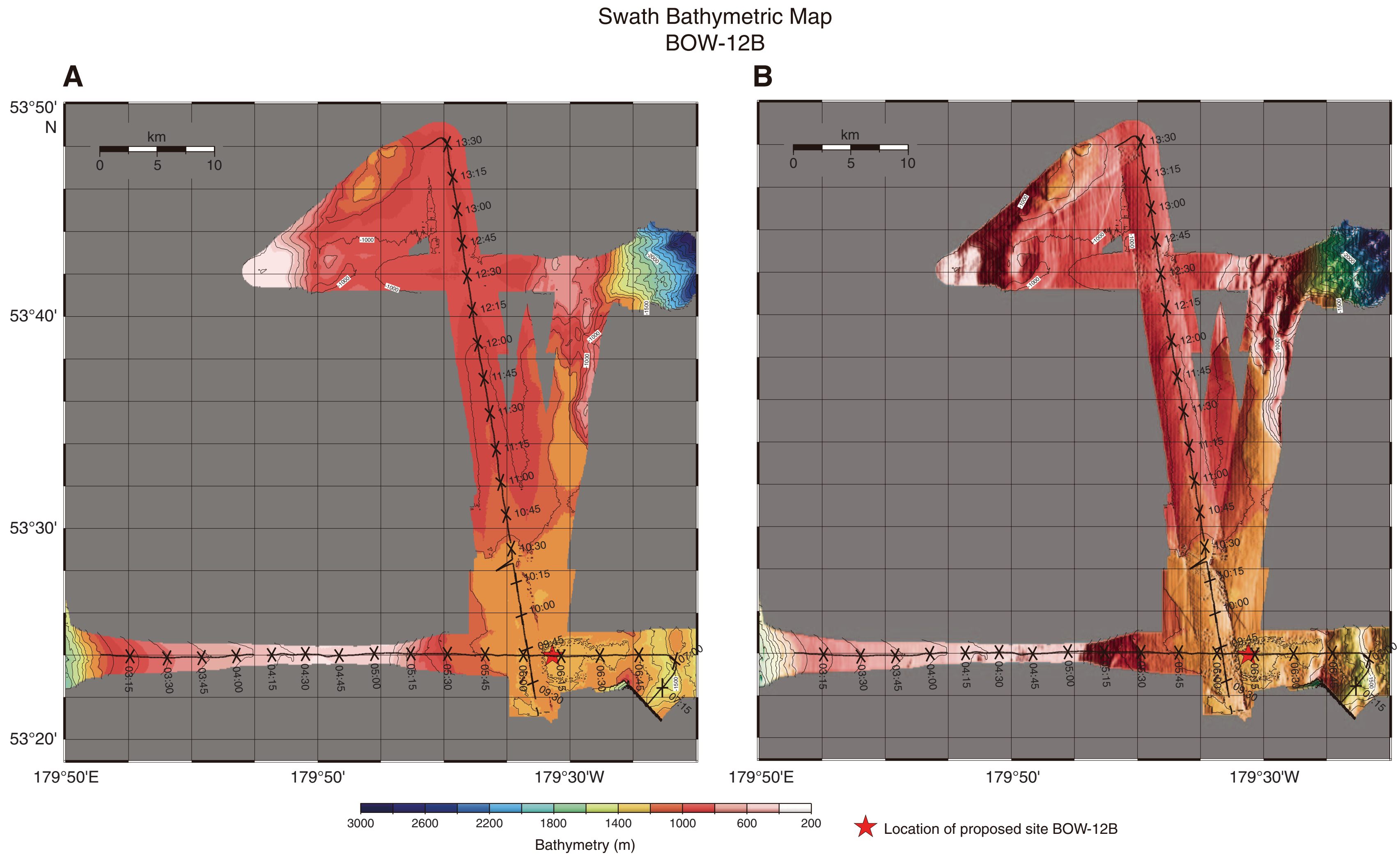

Figure AF4. Seismic profile of *Hakuhou-maru* Cruise KH99-3 Line Stk6-1 (W–E) with location of Site BOW-12B (179°31.3′W, 53°24.0′N; Shotpoint 910; water depth = 1313 m; penetration depth = 745 mbsf).

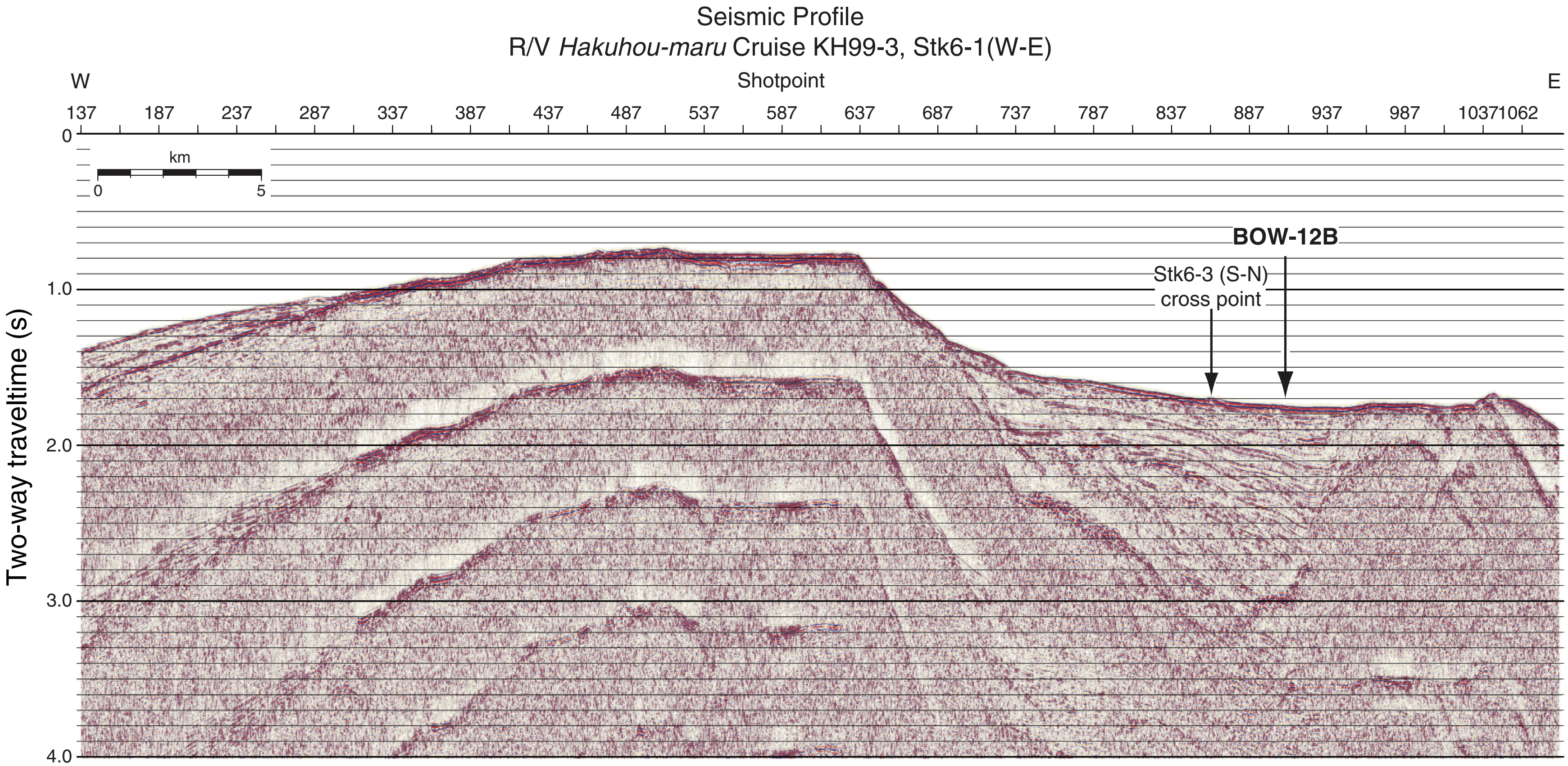

Figure AF5. A. Close-up seismic profile of *Hakuhou-maru* Cruise KH99-3 Line Stk6-1 (W–E) near Site BOW-12B (179°31.3′W, 53°24.0′N; Shotpoint 910; water depth = 1313 m; penetration depth = 700 m coring, 745 m if LWD is planned). Cross point with Line Stk6-3 (S–N) is at Shotpoint 863. **B.** Time-depth curve estimated from results of velocity analyses on Lines Stk6-1 and Stk6-3 around Site BOW-12B.

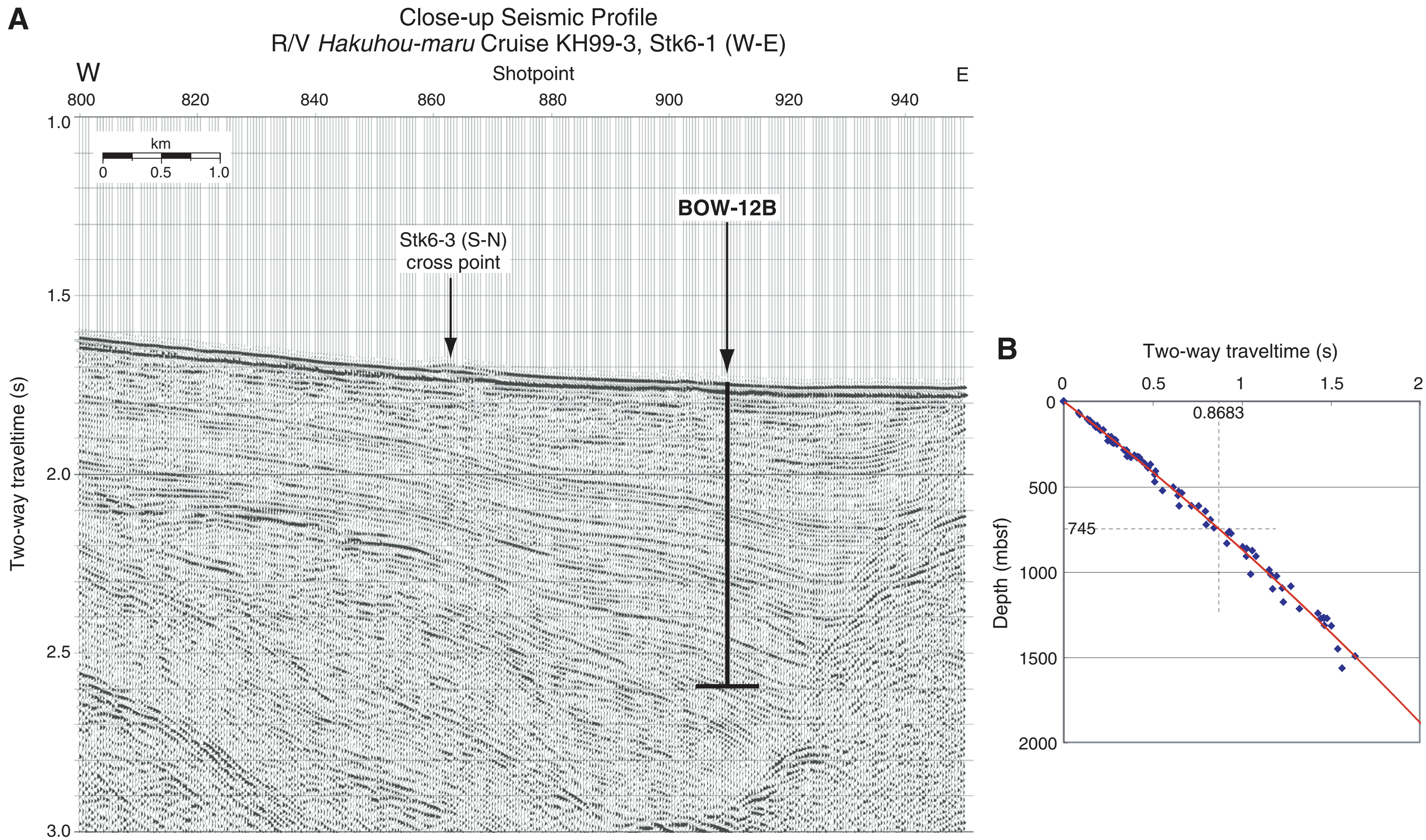

Figure AF6. Seismic profile of *Hakuhou-maru* Cruise KH99-3 Line Stk6-3 (S–N) around Site BOW-12B (179°31.3′W, 53°24.0′N; water depth = 1313 m; penetration depth = 745 mbsf).

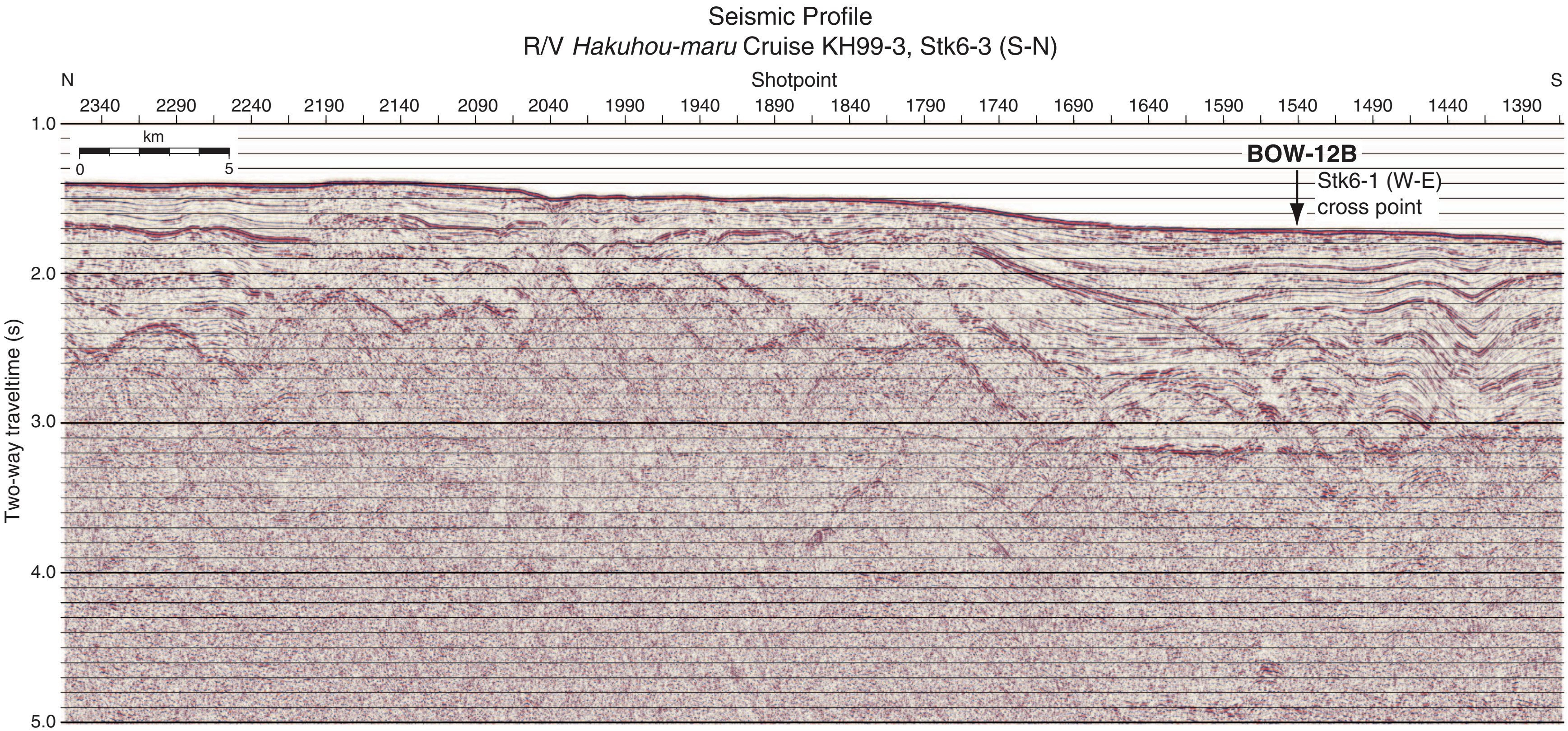

Figure AF7. A. Seismic line of *Hakuhou-maru* Cruise KH99-3 Line Stk6-3 (S–N) near Site BOW-12B. Penetration depth of site is projected from the east on the cross point (see Figure AF2). **B.** Time-depth curve estimated from results of velocity analyses on Lines Stk6-1 and Stk6-3 around Site BOW-12B.

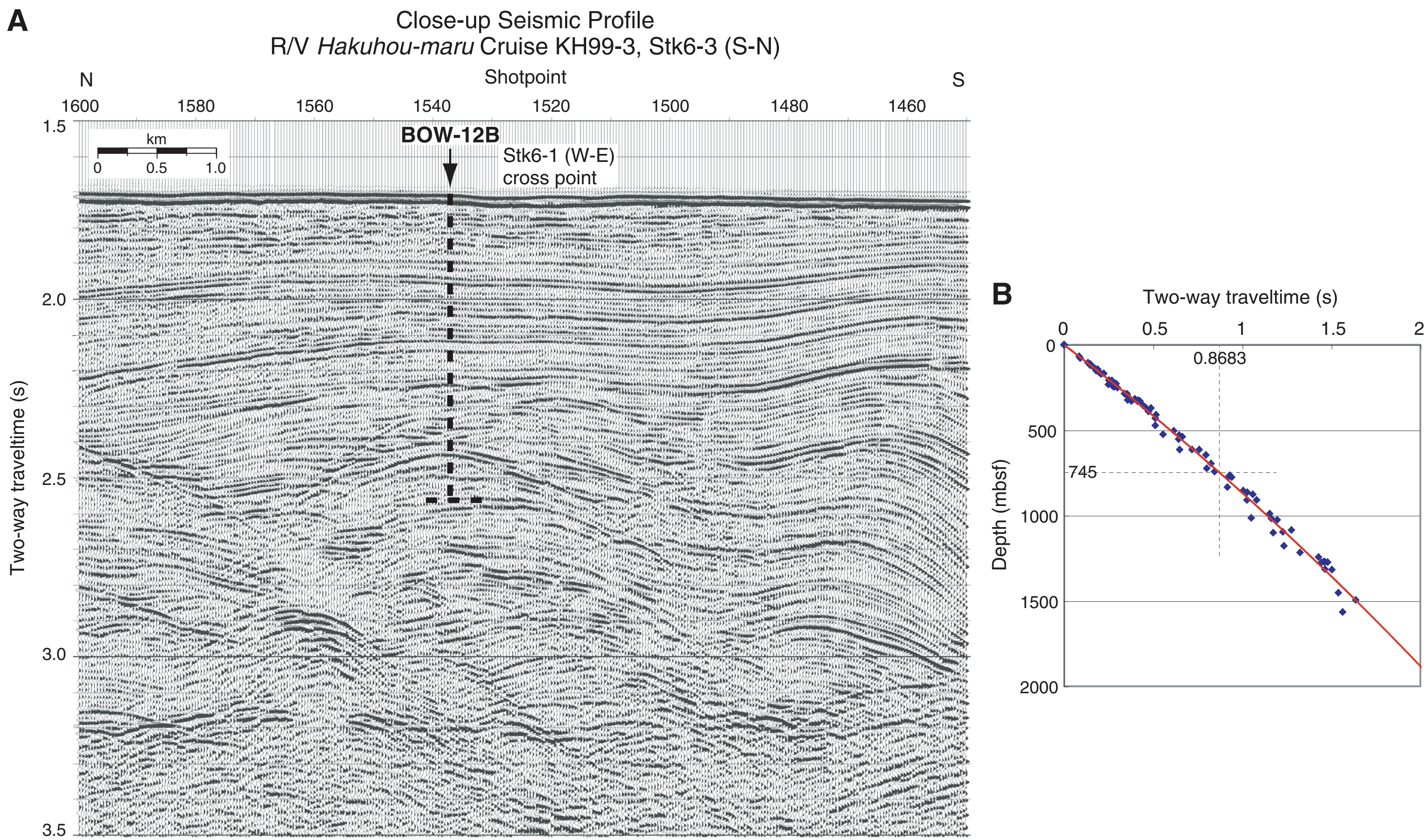

Figure AF8. 3.5 kHz subbottom profile survey from *Hakuhou-maru* Cruise KH99-3. **A.** Line Stk6-1 (W–E) across Site BOW-12B at 06:13:20. **B.** Line Stk6-3 (S–N) around Site BOW-12B. White arrow is projected from the east on the cross point.

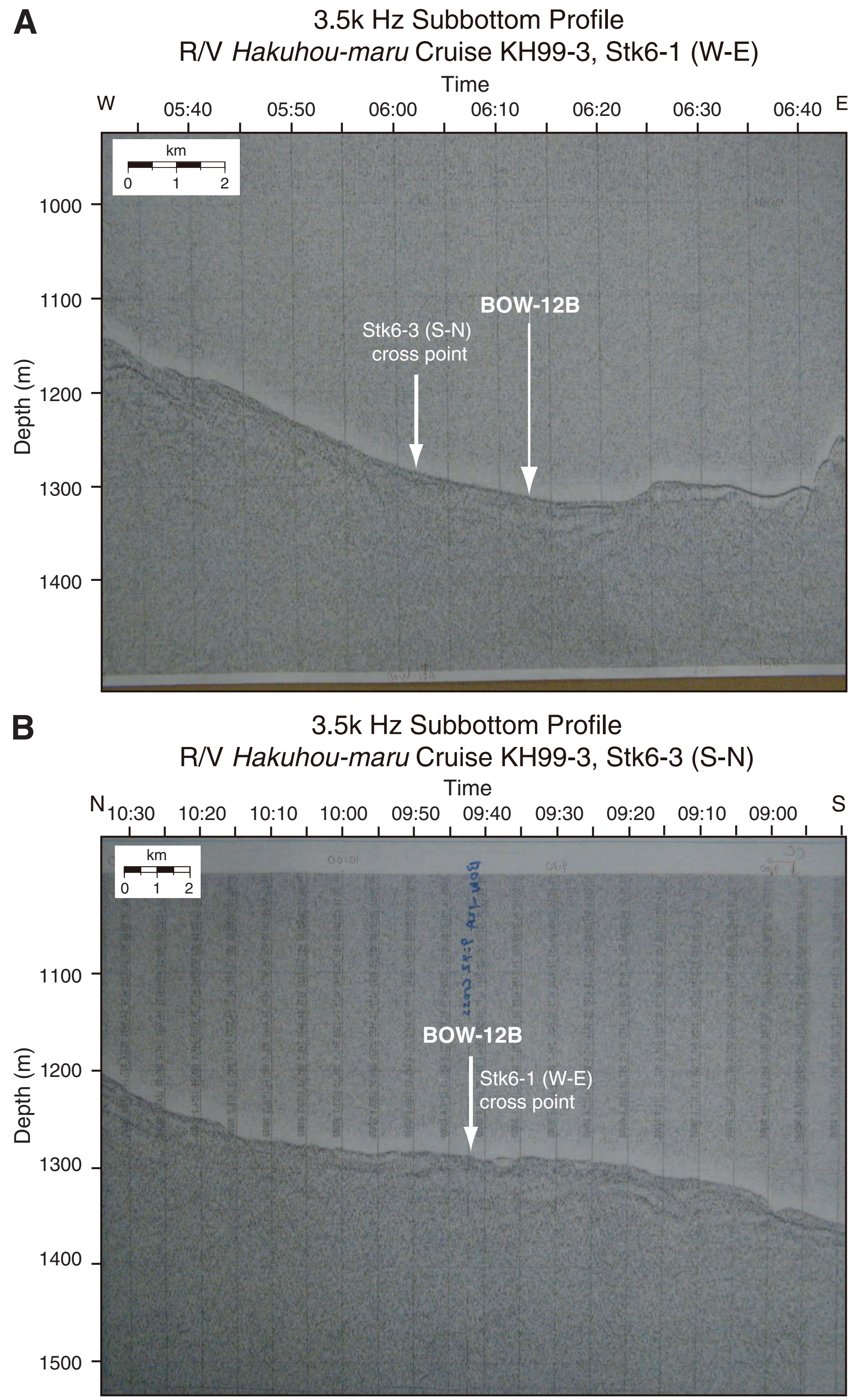

Figure AF9. Specific navigation map of *Hakuhou-maru* Cruise KH99-3 around Site BOW-14B with ship time and shotpoint annotation. Site is located at crossing of survey lines at 10:45:03, Shotpoint 670, on Line Stk5-1 (W–E) and 18:25:13, Shotpoint 2488, on Line Stk5-5 (S–N). Squares = navigation map area for close-up seismic profiles in Figure **AF10.** Time annotation in black letters = range of subbottom profile survey in Figure **AF12.**

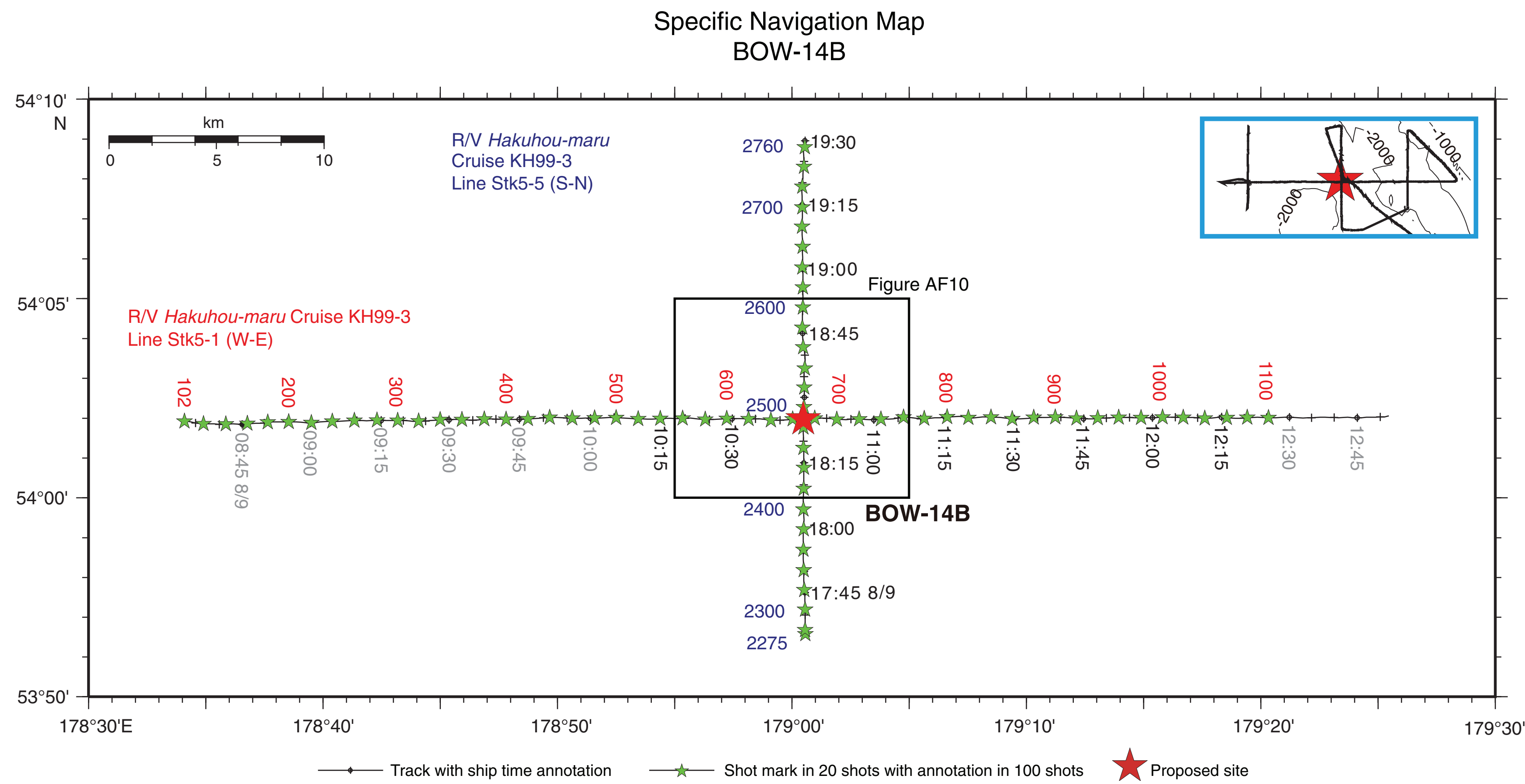

Figure AF10. Close-up navigation map of *Hakuhou-maru* Cruise KH99-3 across Site BOW-14B for close-up seismic profile in Figures **AF14** and **AF16.** Site is located at crossing of survey lines at 10:45:03, Shotpoint 670, on Line Stk5-1 (W–E) and 18:25:13, Shotpoint 2488, on Line Stk5-5 (S–N).

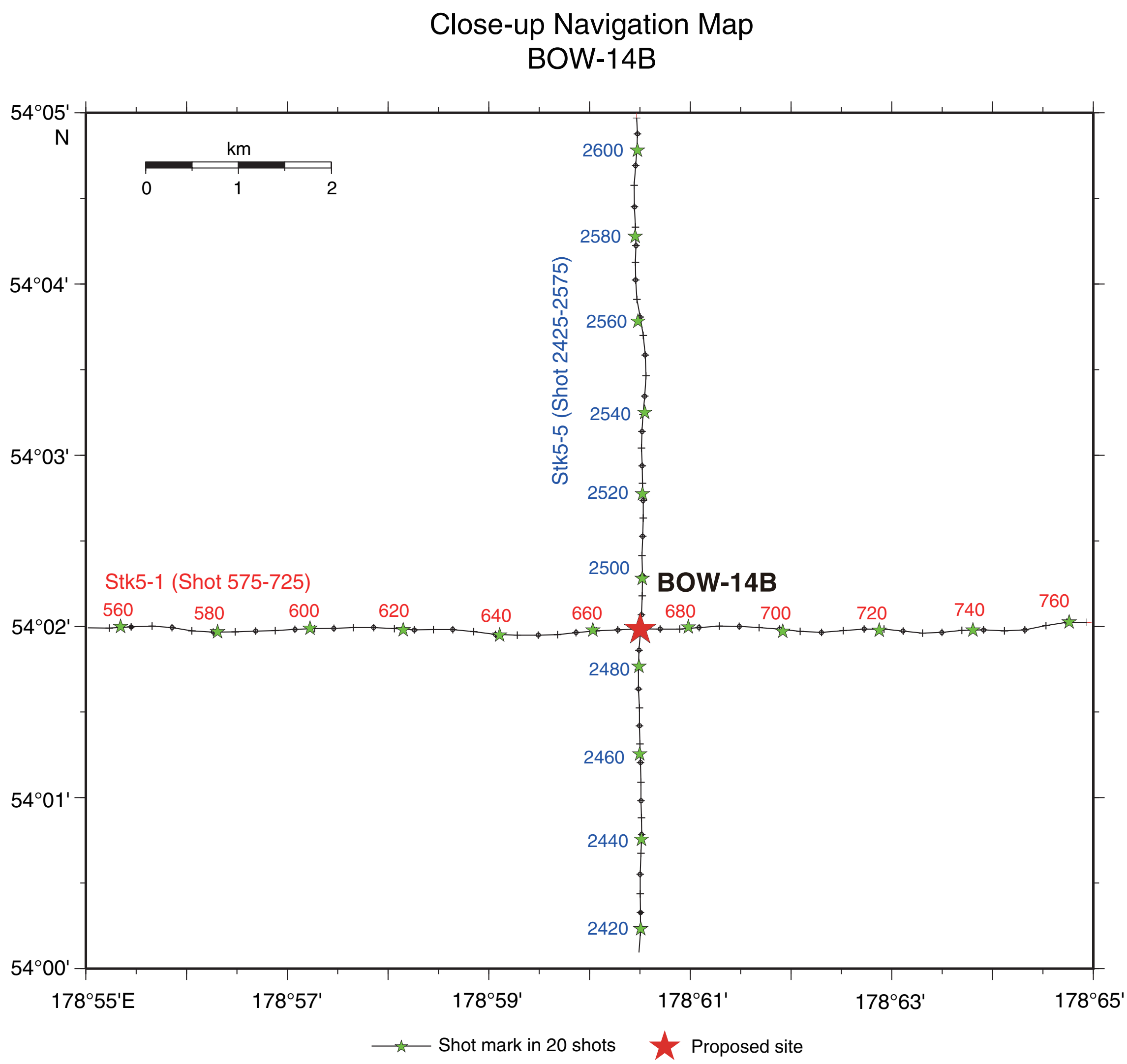

Figure AF11. Swath bathymetric map with track chart from *Hakuhou-maru* Cruise KH99-3 around Site BOW-14B. **A.** Plain image. **B.** Shaded relief image. Site is located at crossing of survey lines at 10:45:03, Shotpoint number 670, on Line Stk5-1 (W–E) and 18:25:13, Shotpoint 2488, on Line Stk5-5 (S–N).

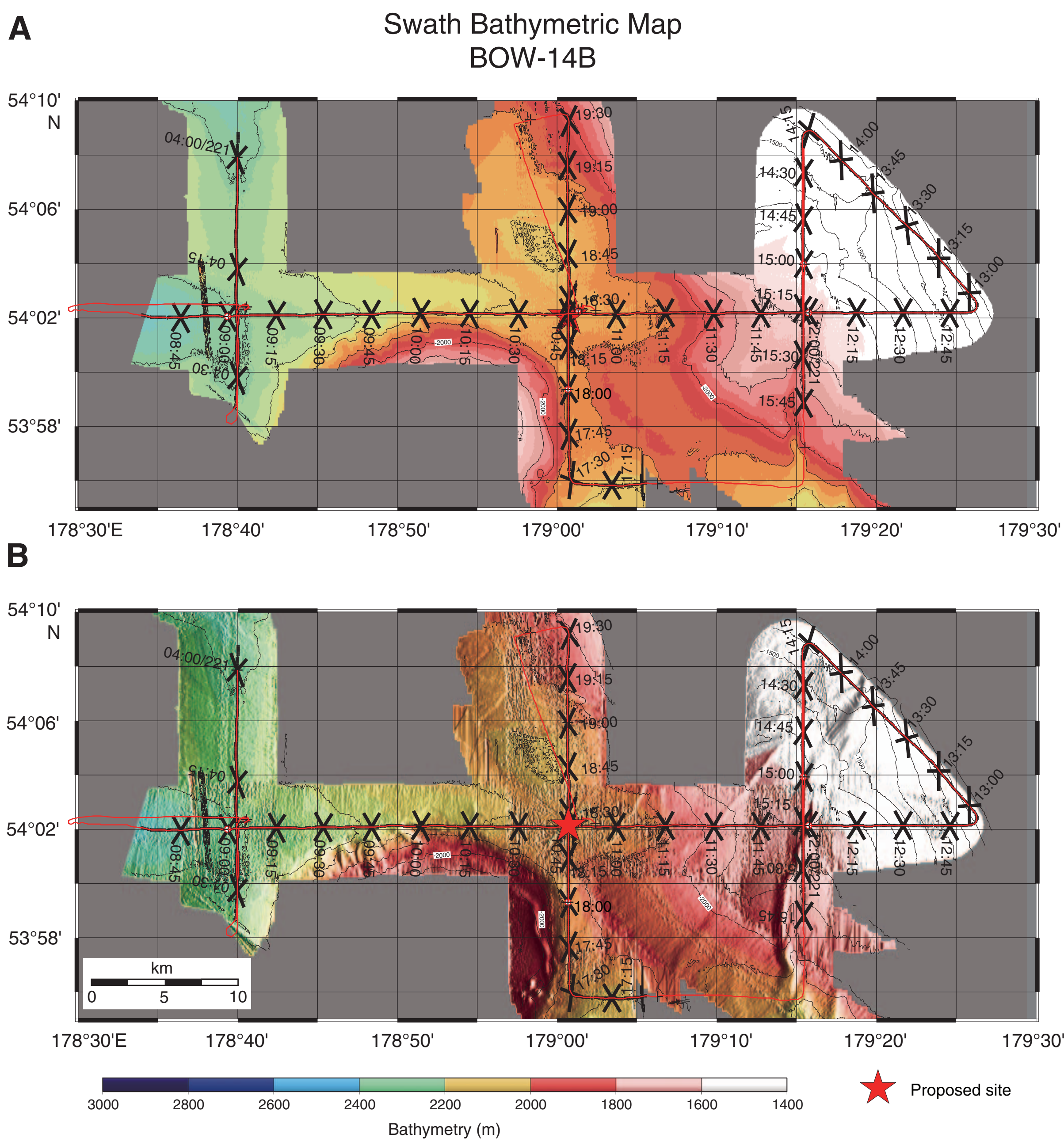

Figure AF12. 3.5 kHz subbottom profile survey from *Hakuhou-maru* Cruise KH99-3. **A.** Line Stk5-1 (W–E) across Site BOW-14B at 10:45:03. **B.** Line Stk5-5 (S–N) across Site BOW-14B at 18:25:13.

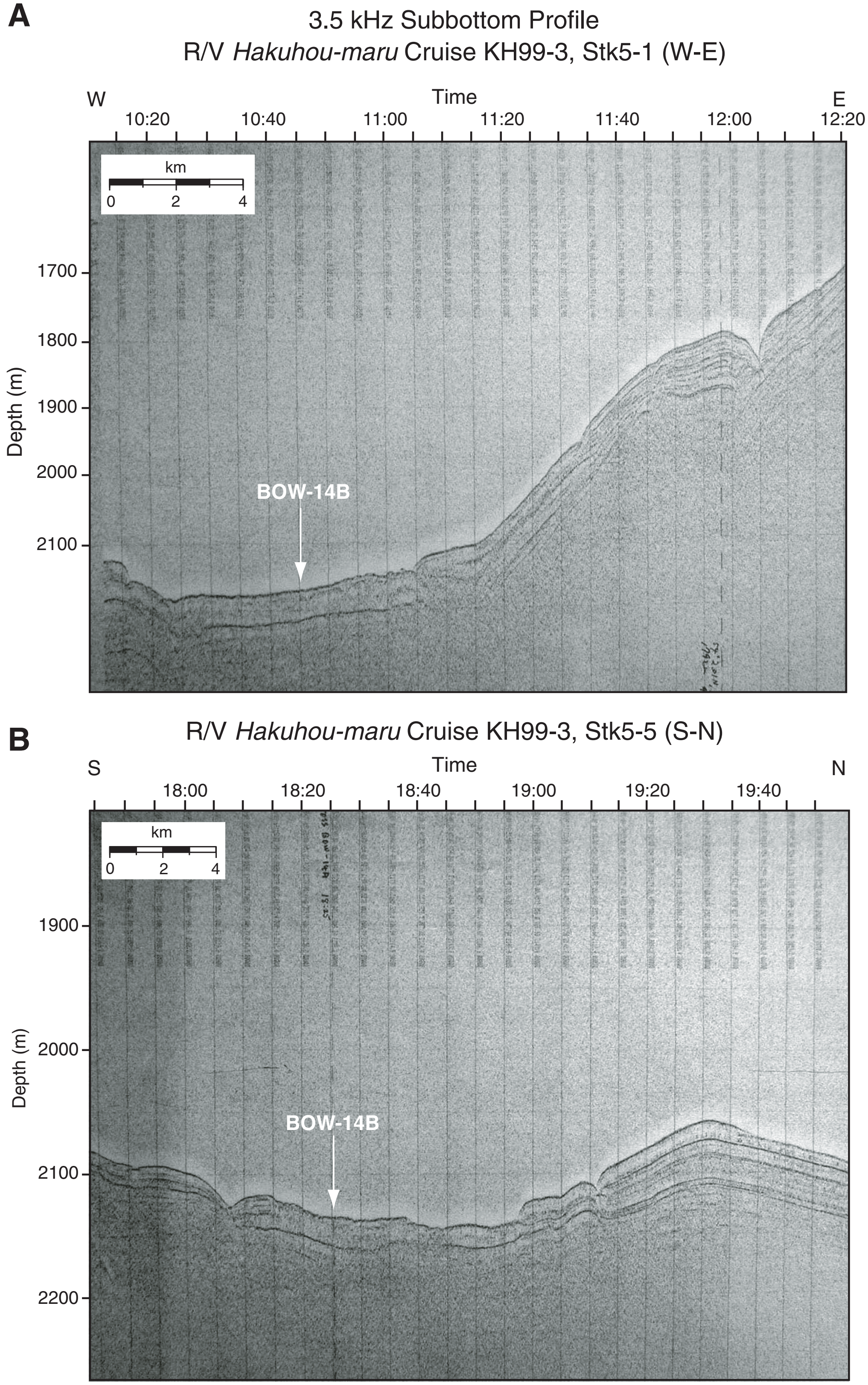

Figure AF13. Seismic profile of *Hakuhou-maru* Cruise KH99-3 Line Stk5-1 (W–E) with location of Site BOW-14B (179°00.5′E, 54°02.0′N; Shotpoint 670, water depth = 2166 m, penetration depth = 600 m).

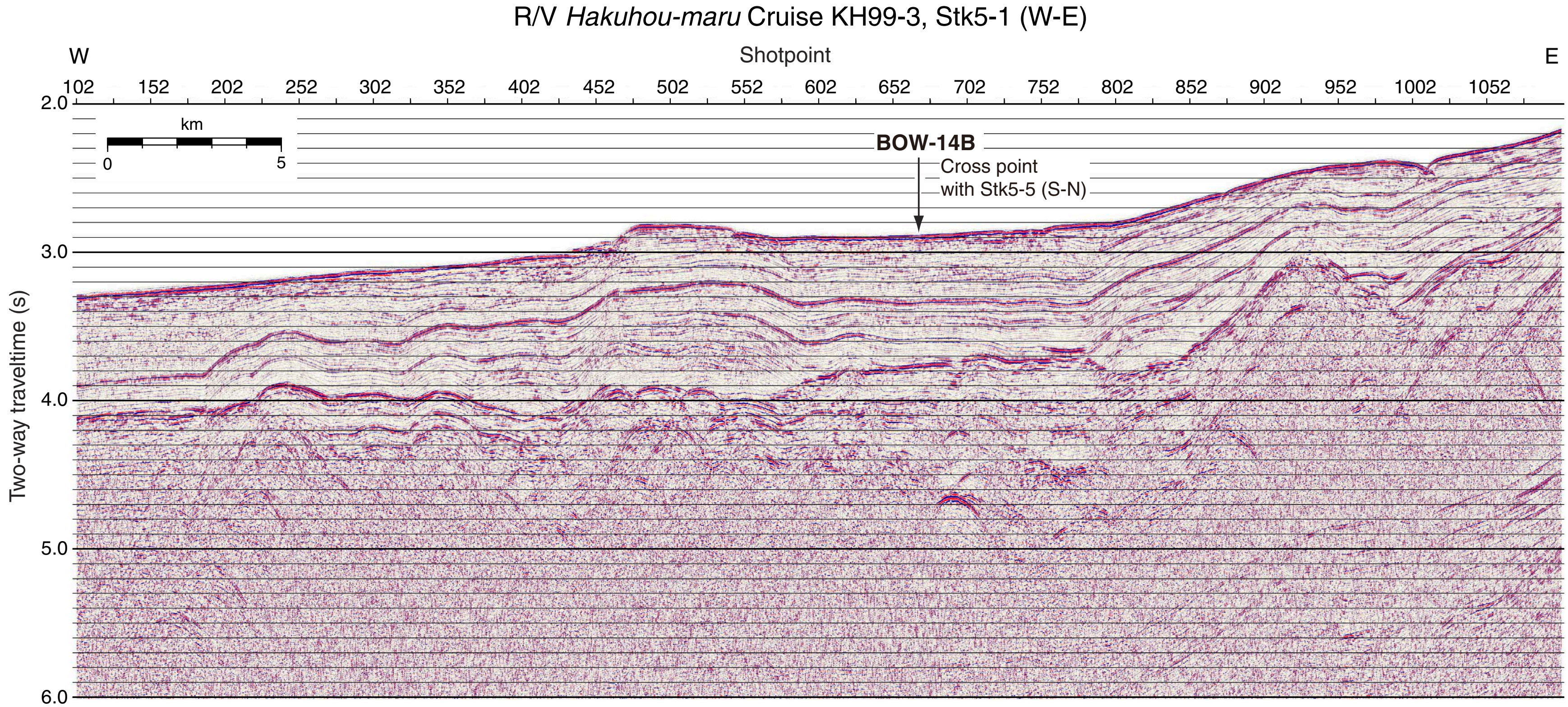

Figure AF14. A. Close-up seismic profile of *Hakuhou-maru* Cruise KH99-3 Line Stk5-1 (W–E) across Site BOW-14B (179°00.5′E, 54°02.0′N; Shotpoint 670; water depth = 2166 m; penetration depth = 55 m coring). **B.** Time-depth curve estimated from results of velocity analyses on Lines Stk5-1 and Stk5-5 around Site BOW-14B.

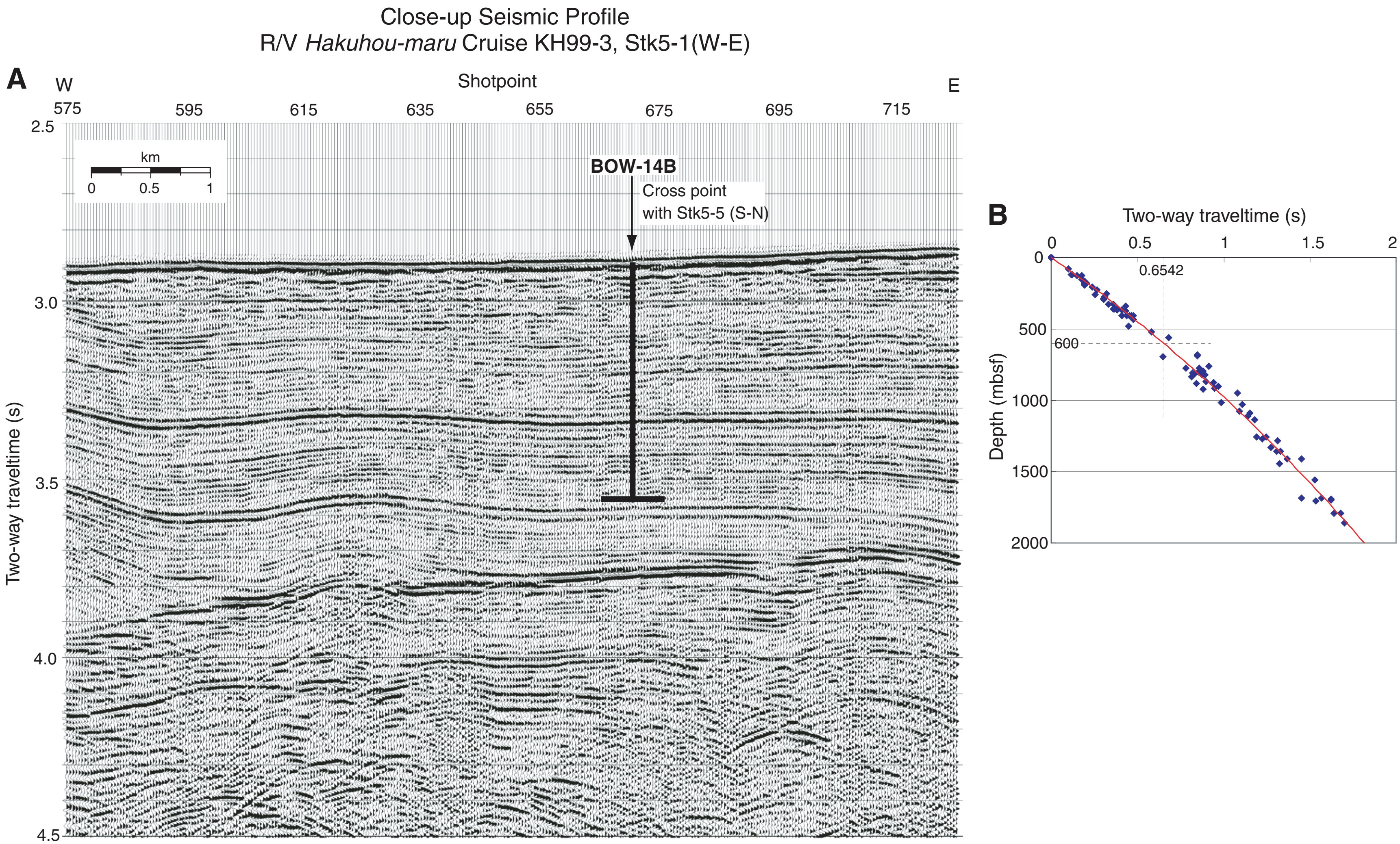

Figure AF15. Seismic profile of *Hakuhou-maru* Cruise KH99-3 Line Stk5-5 (S–N) with location of Site BOW-14B (179°00.5′E, 54°02.0′N; Shotpoint 2488, water depth = 2166 m, penetration depth = 600 m).

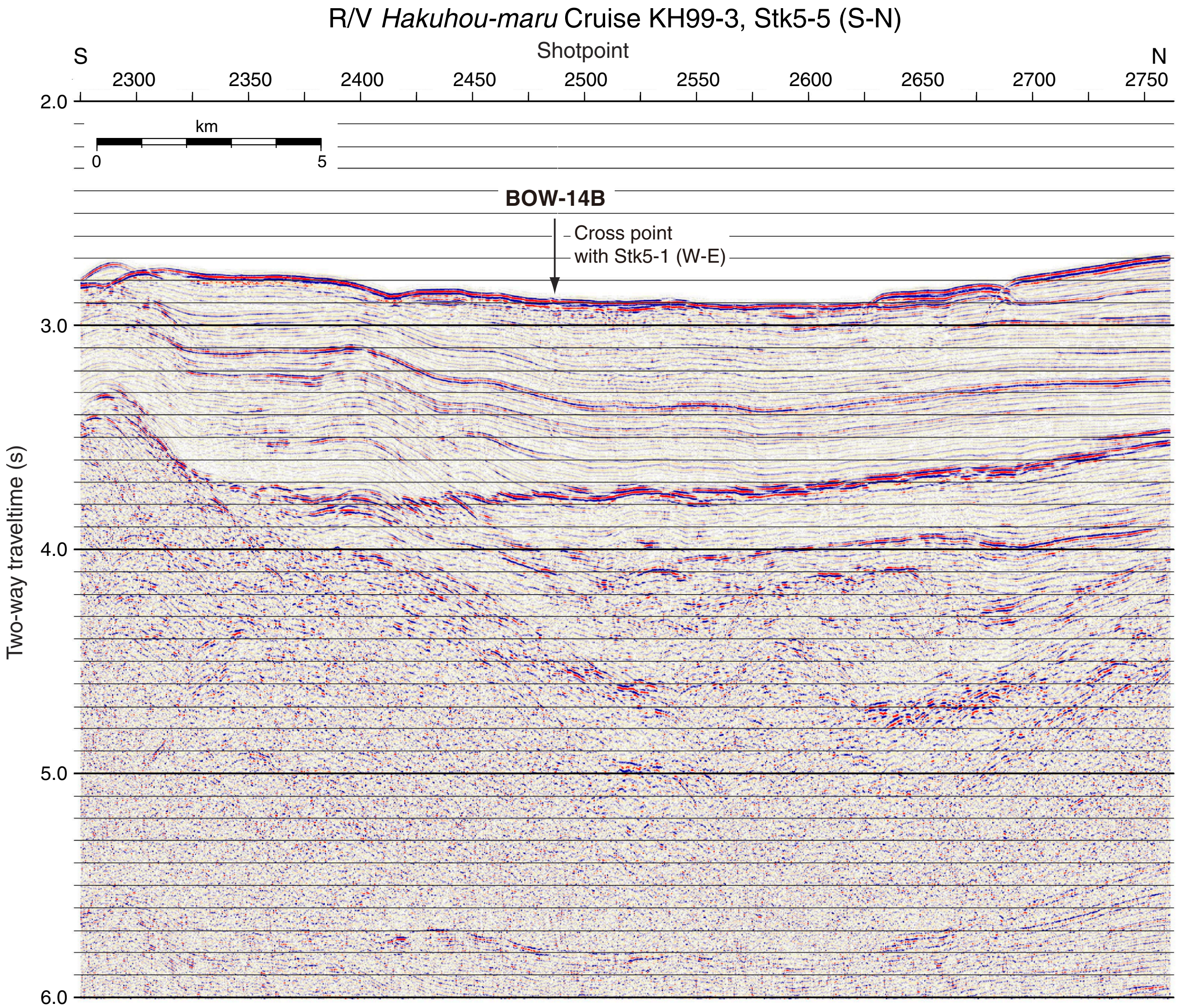

Figure AF16. **A.** Close-up seismic profile of *Hakuhou-maru* Cruise KH99-3 Line Stk5-5 (S–N) near Site BOW-14B (179°00.5′E, 54°02.0′N, Shotpoint 2488; water depth = 2166 m; penetration depth = 555 m coring). **B.** Time-depth curve estimated from results of velocity analyses on Lines Stk5-1 and Stk5-5 around Site BOW-14B.

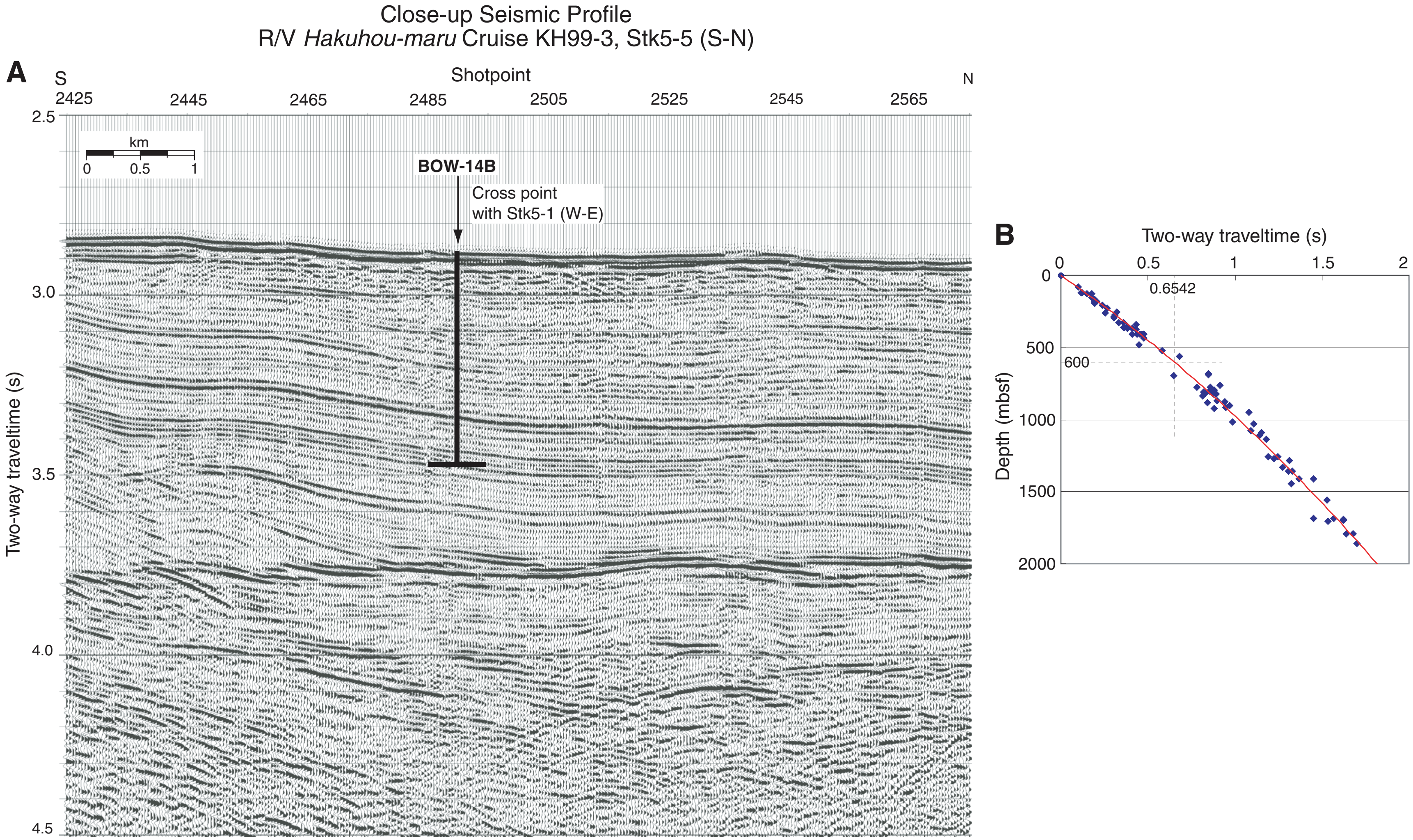

Figure AF17. Specific navigation map of *Hakuhou-maru* Cruise KH99-3 around Site BOW-15A with ship time and shotpoint annotation. Crossing of survey lines is at 19:21:35, Shotpoint 1203, on Line Stk4-3 (W–E) and 16:20:40, Shotpoint 505, on Line Stk4-1 (N–S). Site BOW-15A is located at 15:58:30, Shotpoint 410, on Line Stk4-1 (N–S). Squares = navigation map area for close-up seismic profiles in Figure AF18. Time annotation in black letters = range of subbottom profile survey in Figure AF23.

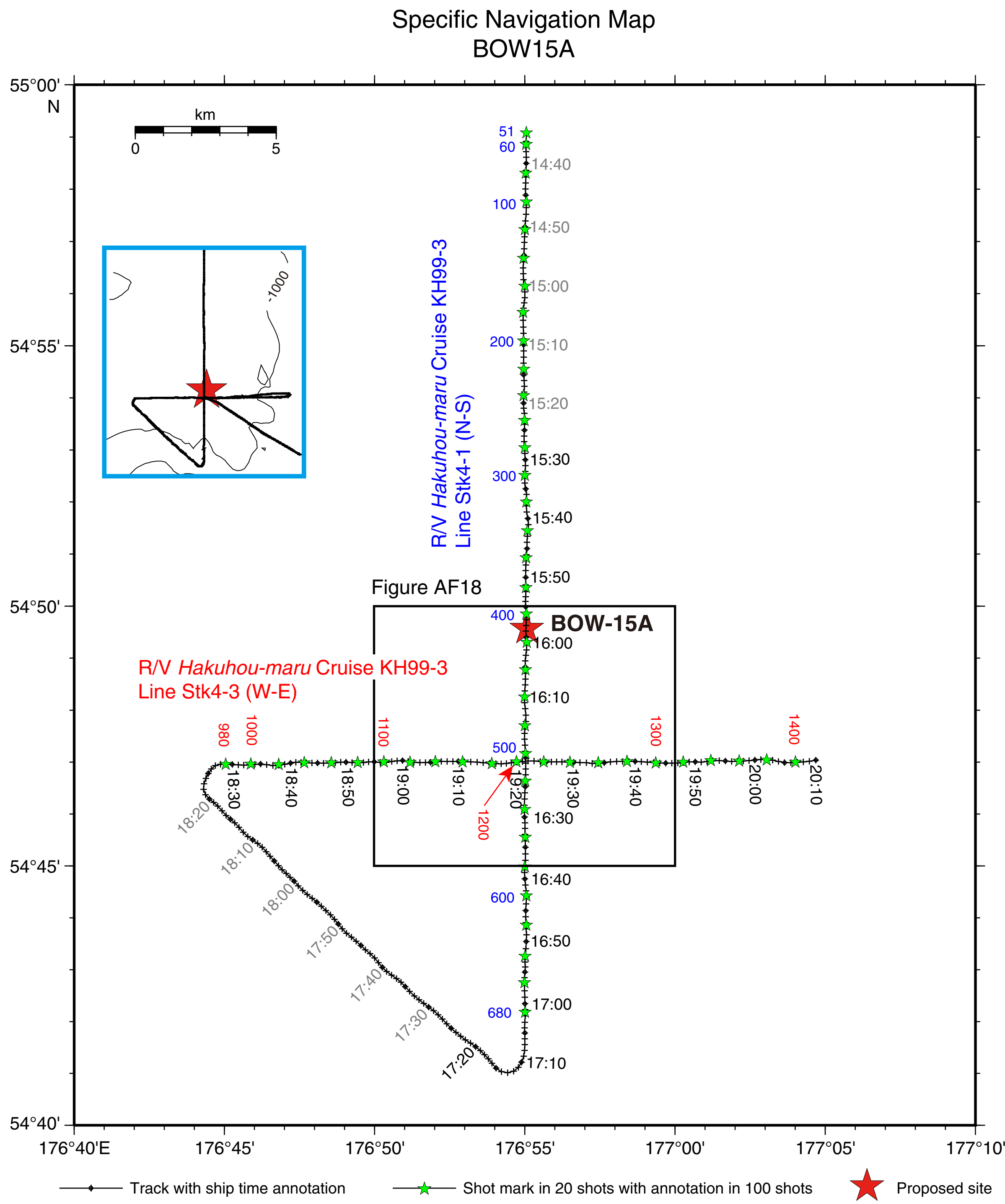

Figure AF18. Close-up navigation map of *Hakuhou-maru* Cruise KH99-3 around Site BOW-15A for close-up seismic profile in Figures **AF20** and **AF22.** Crossing of survey lines is at 19:21:35, Shotpoint 1203, on Line Stk4-3 (W–E) and 16:20:40, Shotpoint 505, on Line Stk4-1 (N–S). Site BOW-15A is located at 15:58:30, Shotpoint 410, on Line Stk4-1 (N–S).

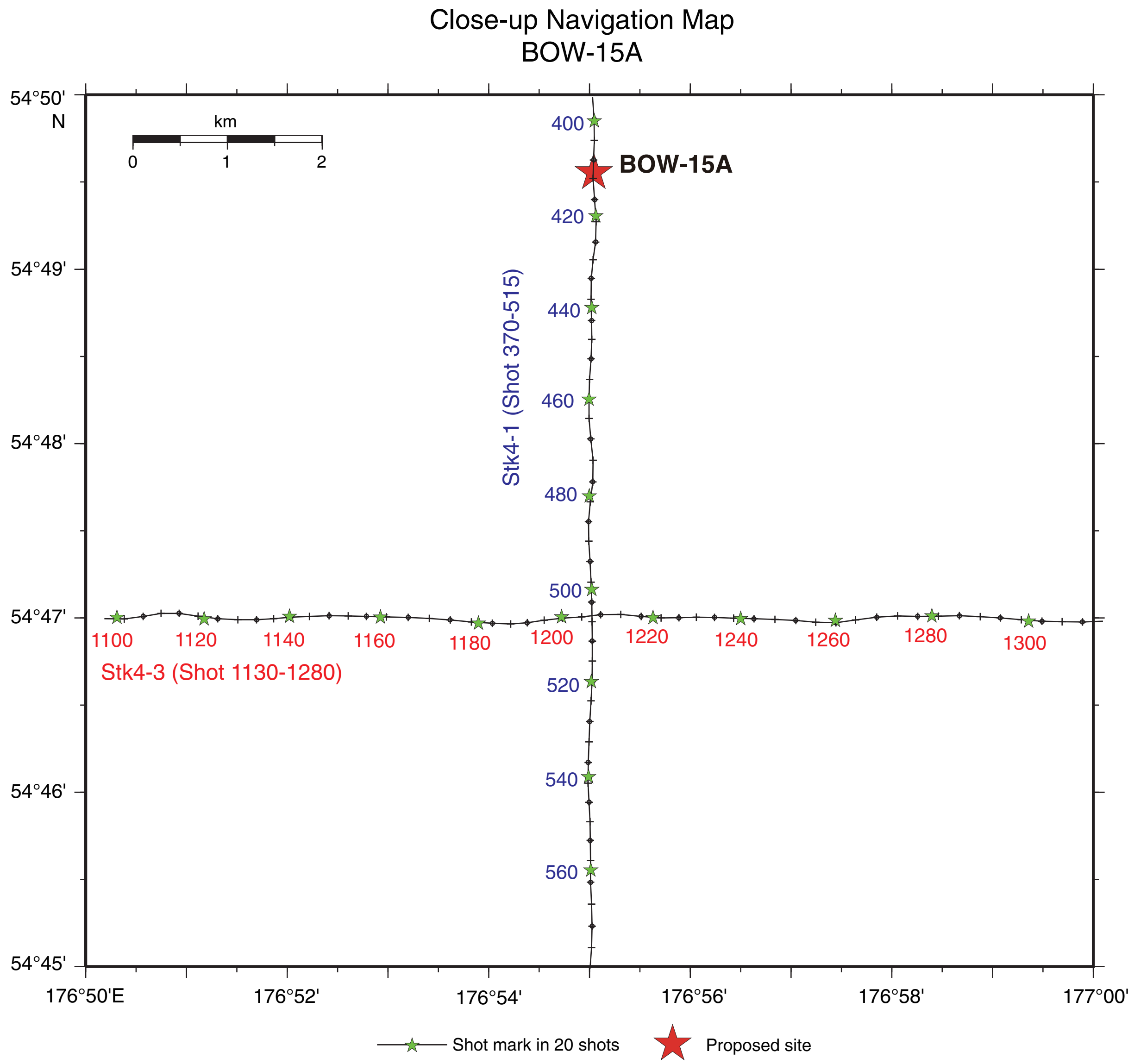

Figure AF19. Seismic profile of *Hakuhou-maru* Cruise KH99-3 Line Stk4-1 (N–S) with location of Site BOW-15A (176°55.0′E, 54°49.7′N; Shotpoint 410; water depth = 837 m; penetration depth = 165 mbsf). Cross point with Line Skt4-3 (W–E) is at Shotpoint 505.

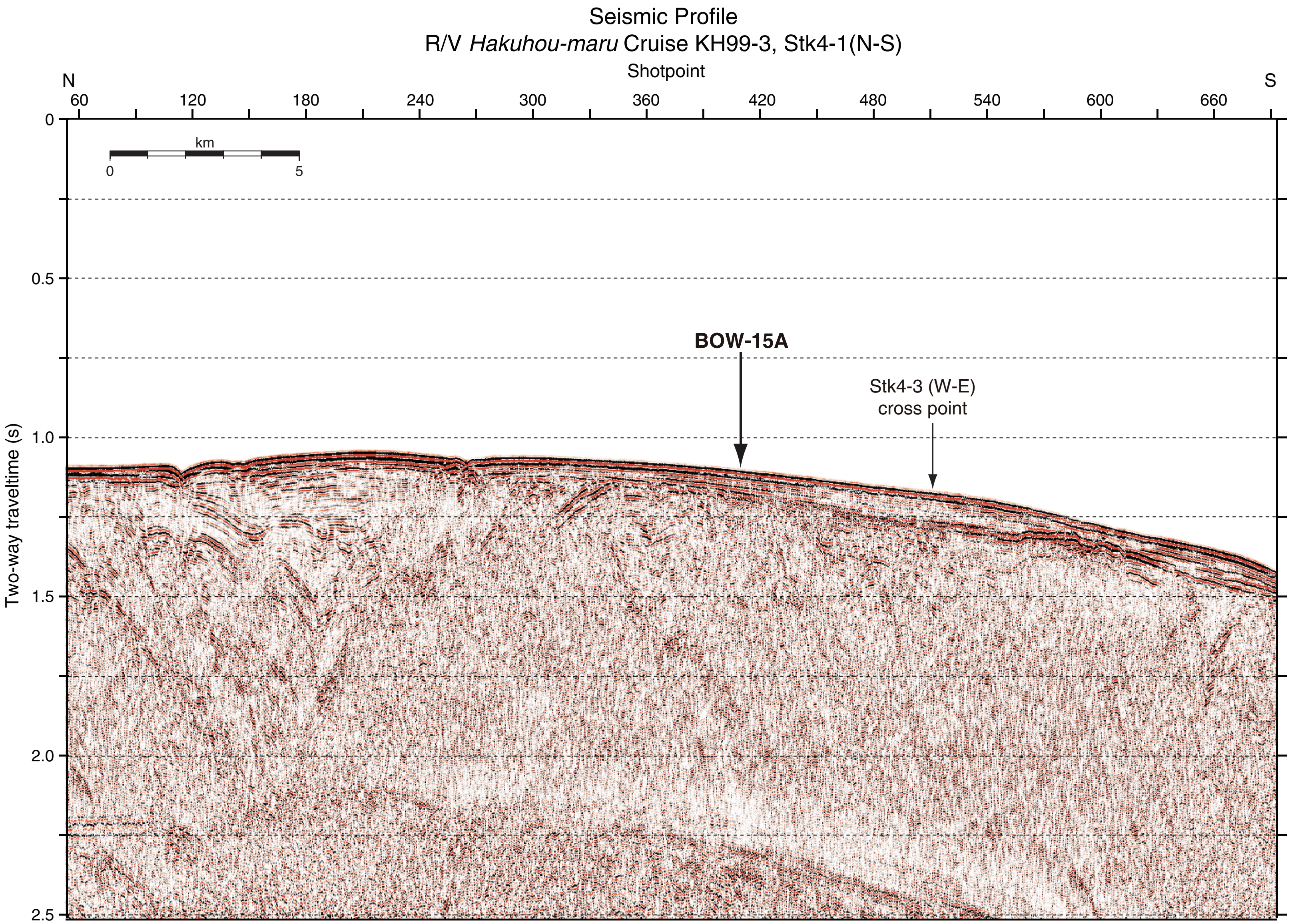

Figure AF20. A. Close-up seismic profile of *Hakuhou-maru* Cruise KH99-3 Line Stk4-1 (N–S) across Site BOW-15A (176°55.0′E, 54°49.7′N; Shotpoint 410; water depth = 837 m; penetration depth = 120 m coring, 165 m if LWD is planned). Cross point with Line Stk4-3 (W–E) is Shotpoint 505. **B.** Time-depth curve estimated from results of velocity analyses on Lines Stk4-1 and Stk4-3 around Site BOW-15A.

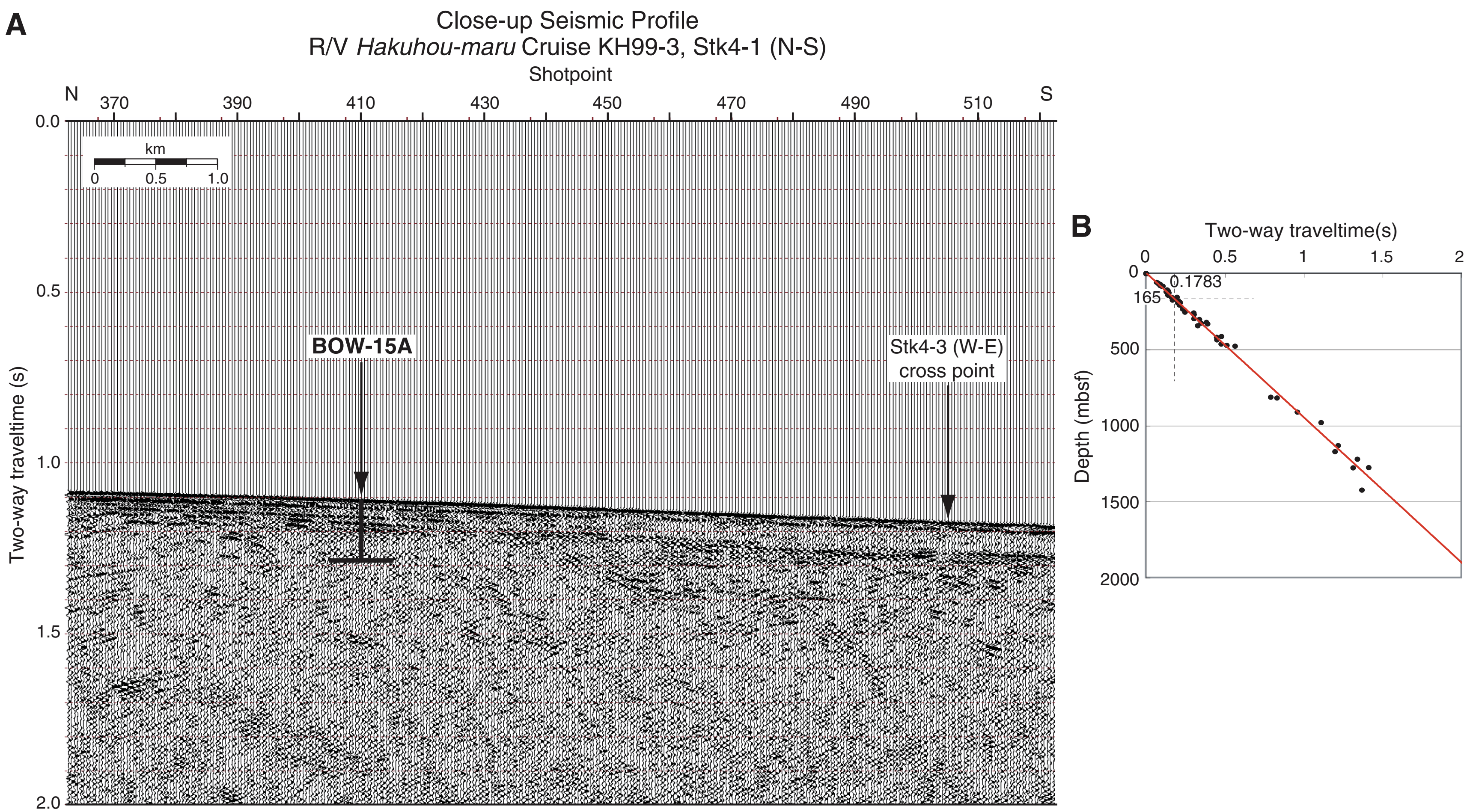

Figure AF21. Seismic profile of *Hakuhou-maru* Cruise KH99-3 Line Stk4-3(W-E) around Site BOW-15A (176°55.0′E, 54°49.7′N; water depth = 837 m; penetration depth = 165 mbsf), projected from the north on the cross point. Cross point with Line Stk4-1 (N–S) is Shotpoint 1203.

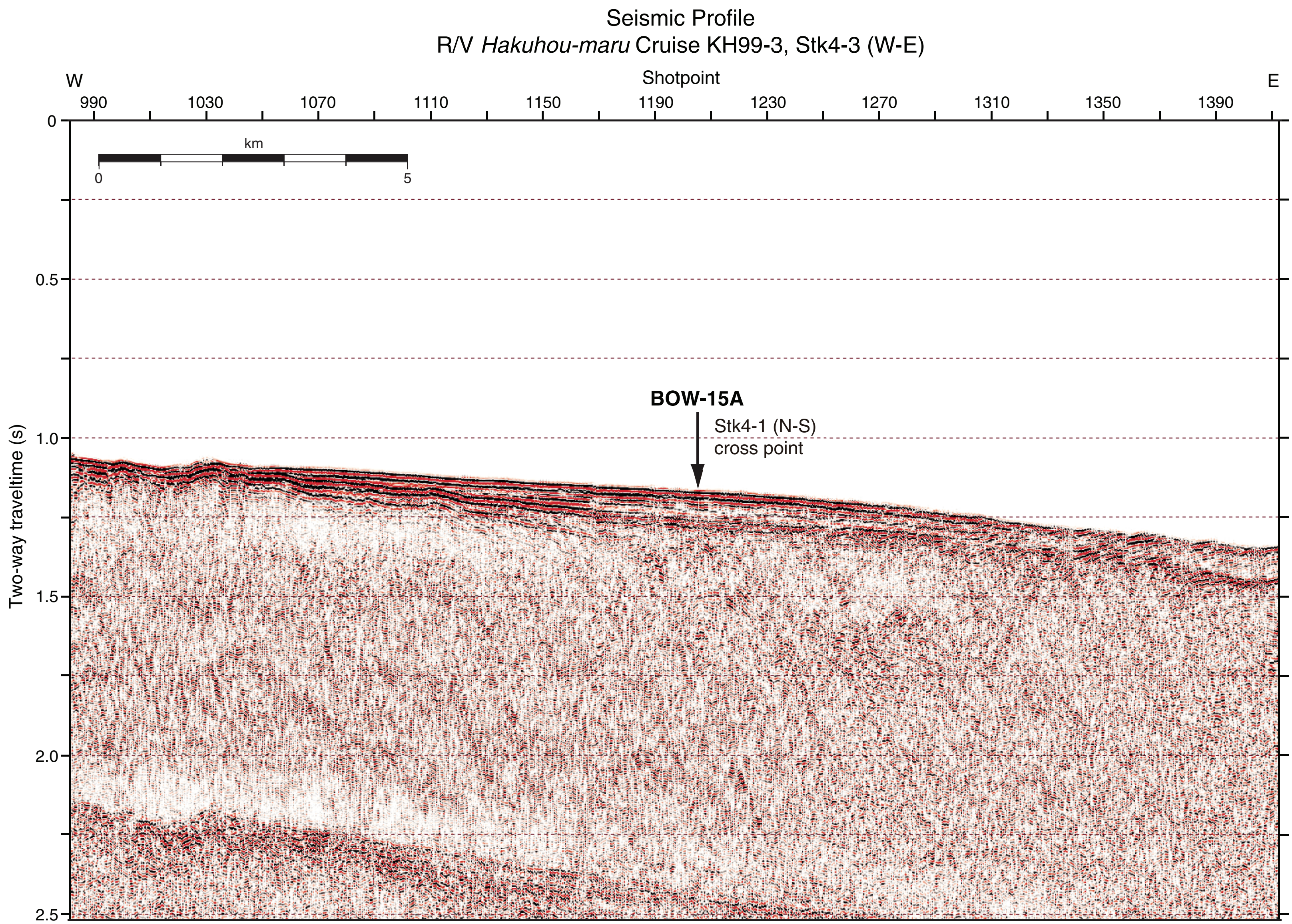

Figure AF22. A. Close-up seismic profile of *Hakuhou-maru* Cruise KH99-3 Line Stk4-3 (W–E) around Site BOW-15A. Cross point with Line Stk4-1 (N–S) is Shotpoint 1203, projected from the north on the cross point. **B.** Time-depth curve estimated from results of velocity analyses on Lines Stk4-1 and Stk4-3 around Site BOW-15A.

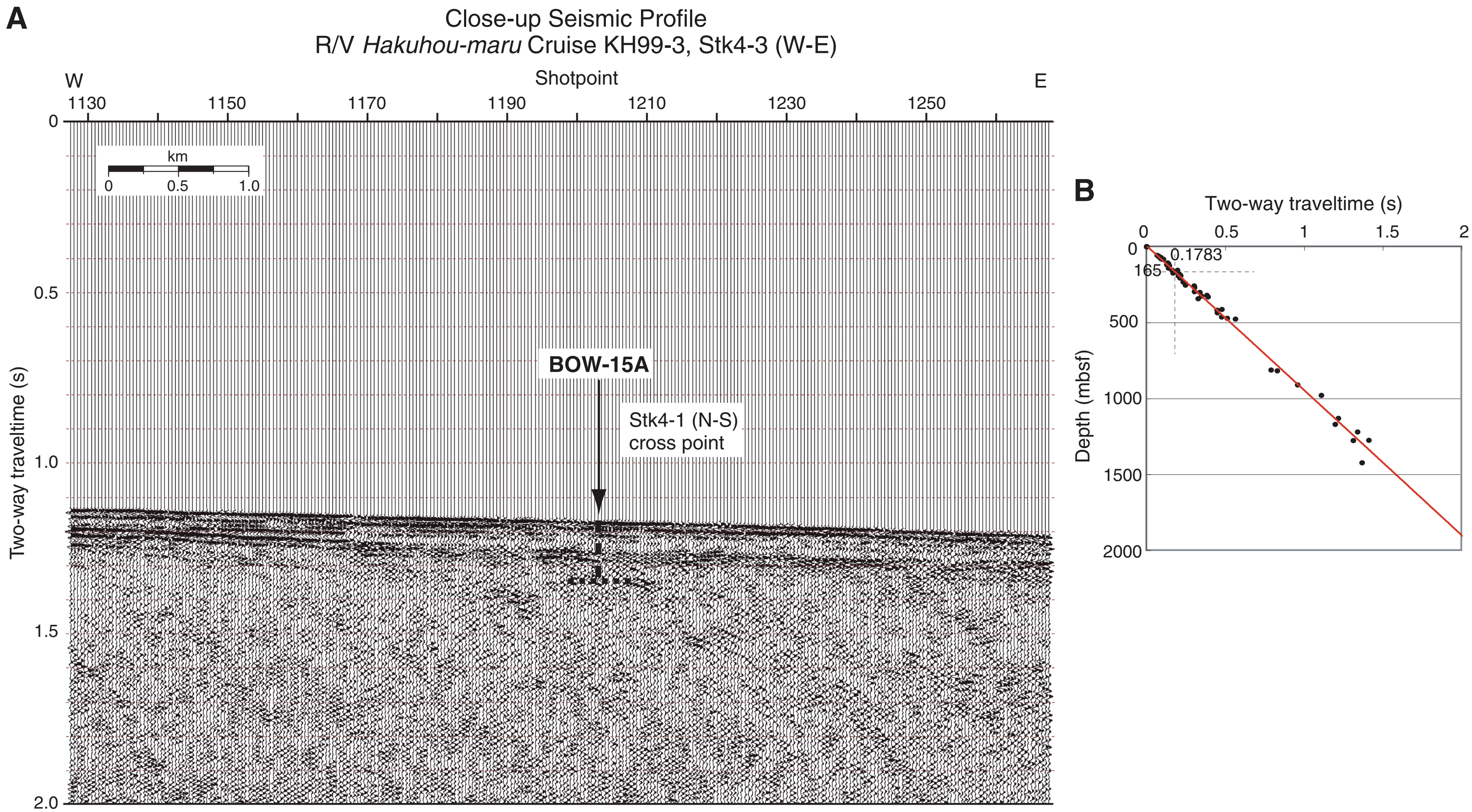

Figure AF23. 3.5 kHz subbottom profile survey from *Hakuhou-maru* Cruise KH99-3. **A.** Line Stk4-3 (W–E) around Site BOW-15A, projected from the north on the cross point. **B.** Line Stk4-1 (N–S) across Site BOW-15A at 15:58:30.

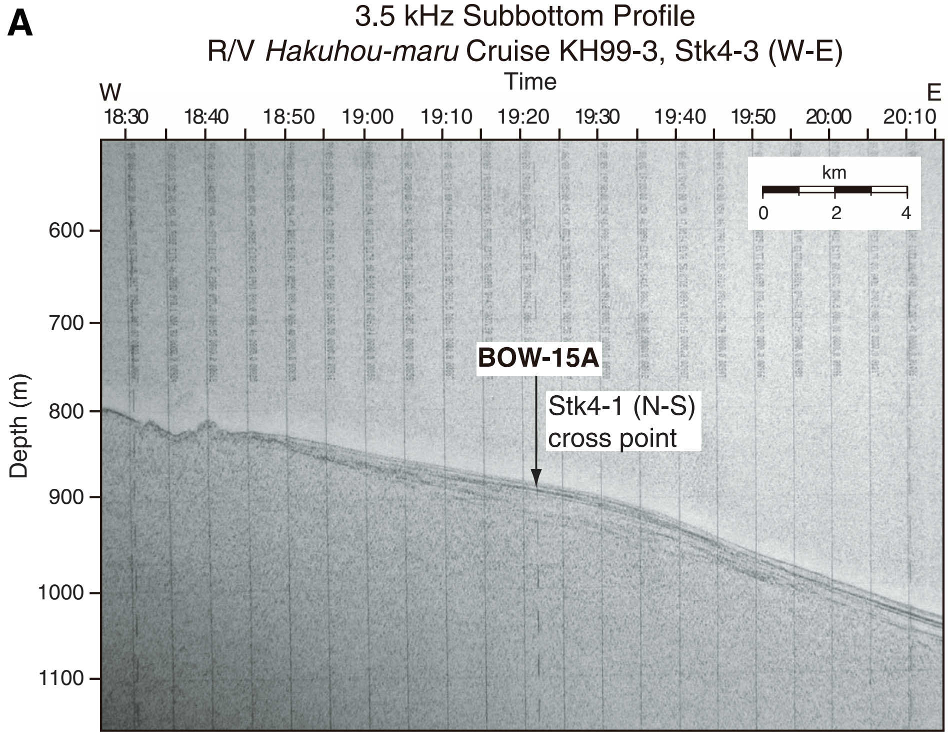

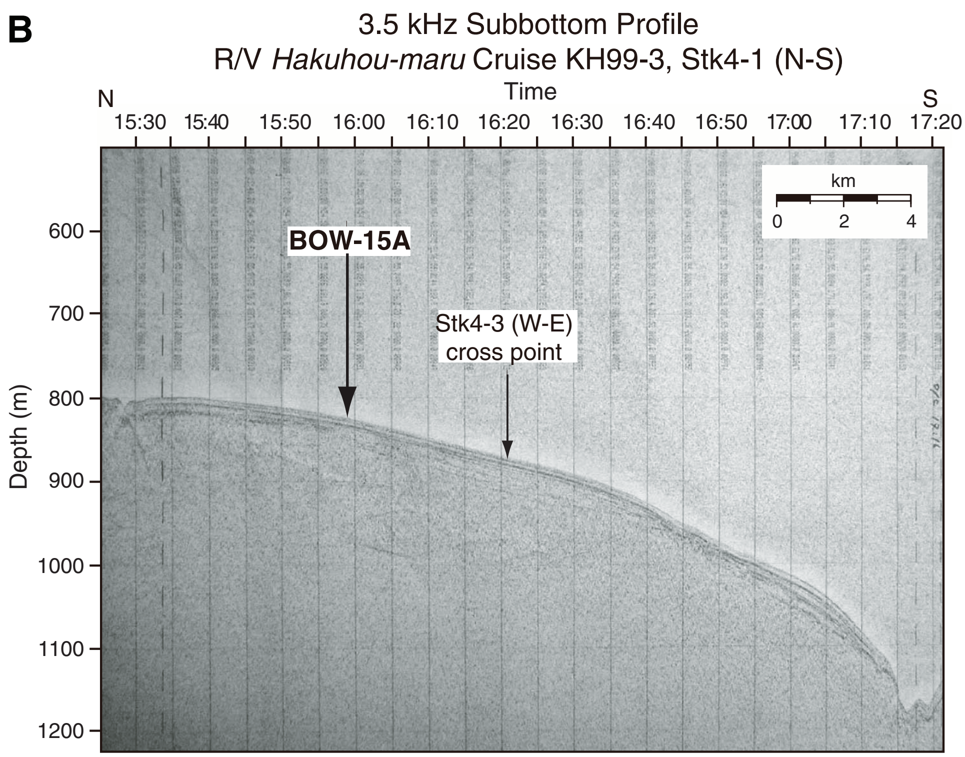

Figure AF24. Swath bathymetric map with track chart at time of *Hakuhou-maru* Cruise KH99-3 around Site BOW-15A. **A.** Plain image. **B.** Shaded relief image. Crossing of survey lines is at 19:21:35, Shotpoint 1203, on Line Stk4-3 (W–E) and 16:20:40, Shotpoint 505, on Line Stk4-1 (N–S). Site BOW-15A is located at 15:58:30, Shotpoint 410, on Line Stk4-1 (N–S).

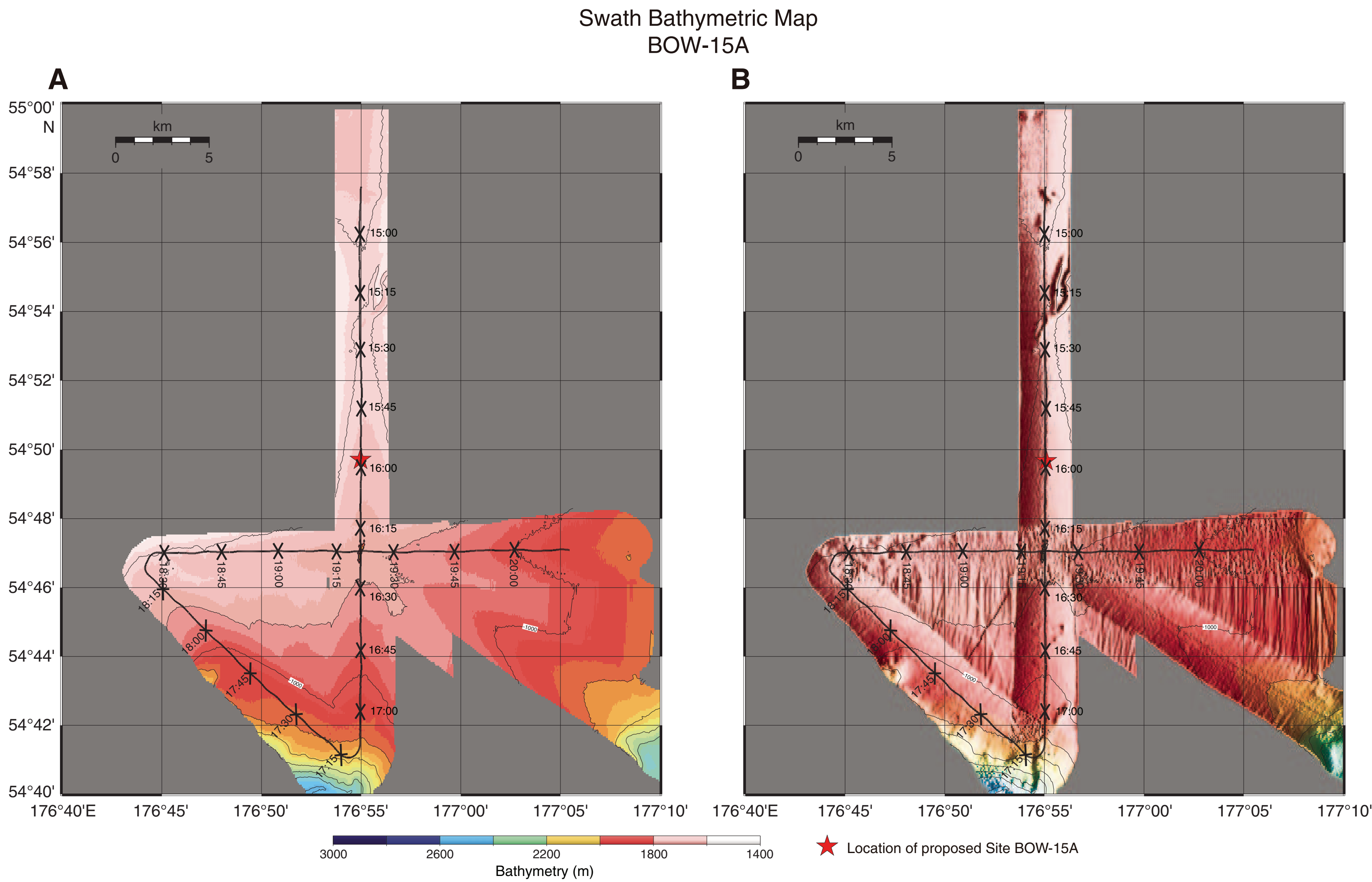

Figure AF25. Regional overview map with track chart of *Hakuhou-maru* Cruise KH99-3 around Sites GAT-3C and GAT-4C. Squares = areas of specific navigation maps around each site. Bathymetric contour lines created by GMT (**gmt.soest.hawaii.edu**) using the NGDC/NOAA ETOPO2 database (**www.ngdc.noaa.gov/mgg/fliers/01mgg04.html**).

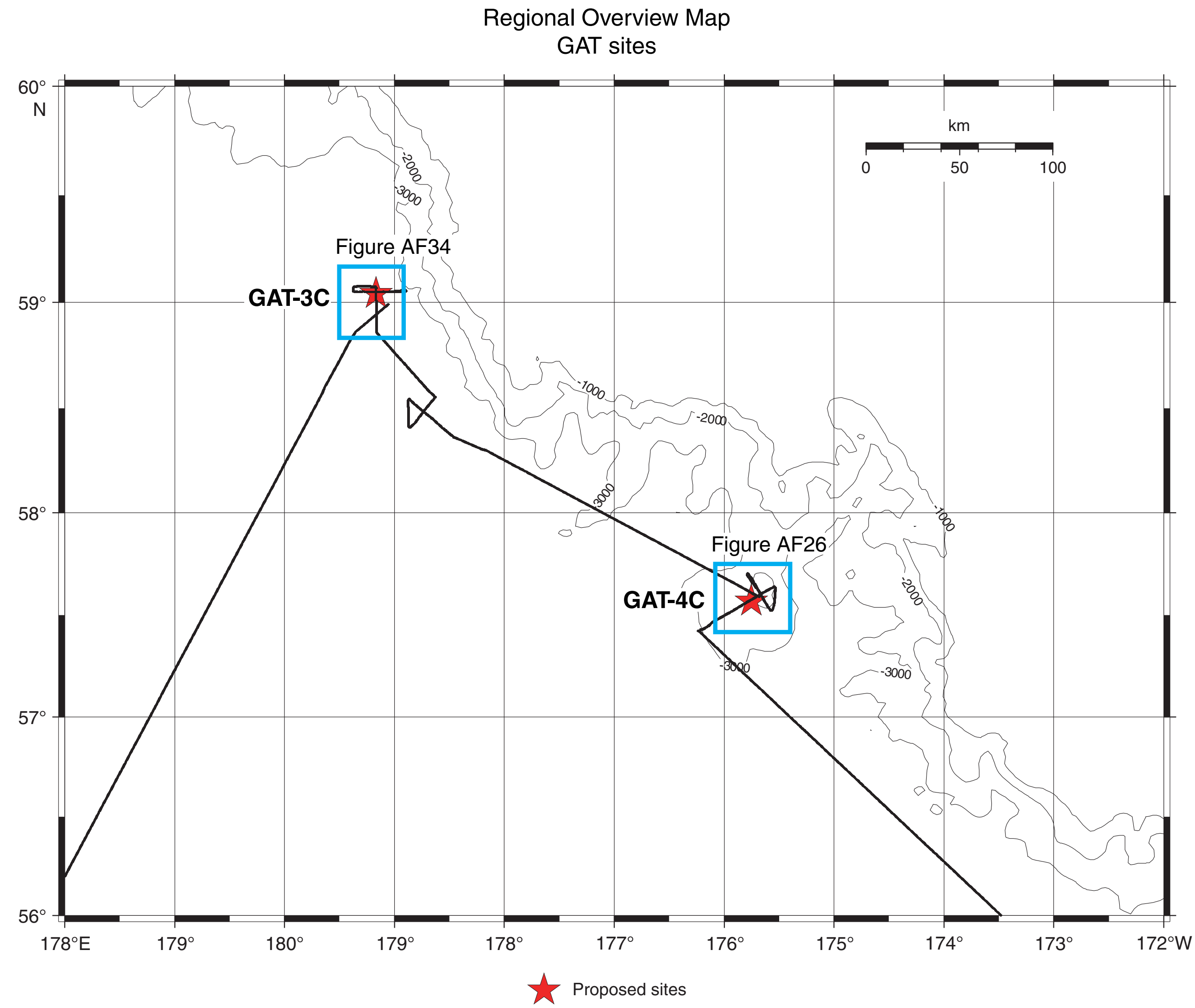

Figure AF26. Specific navigation map of *Hakuhou-maru* Cruise KH99-3 around Site GAT-4C with ship time and shotpoint annotation. Crossing of survey lines is at 23:44:40, Shotpoint 553, on Line Stk1 (SW–NE) and 02:37:55, Shotpoint 400, on Line Stk2 (SE–NW). Site GAT-4C is at 22:50:55, Shotpoint 351, on Line Stk1 (SW–NE). Squares = navigation map area for close-up seismic profiles in Figure **AF27.** Time annotation in black letters = range of subbottom profile survey in Figure **AF31.**

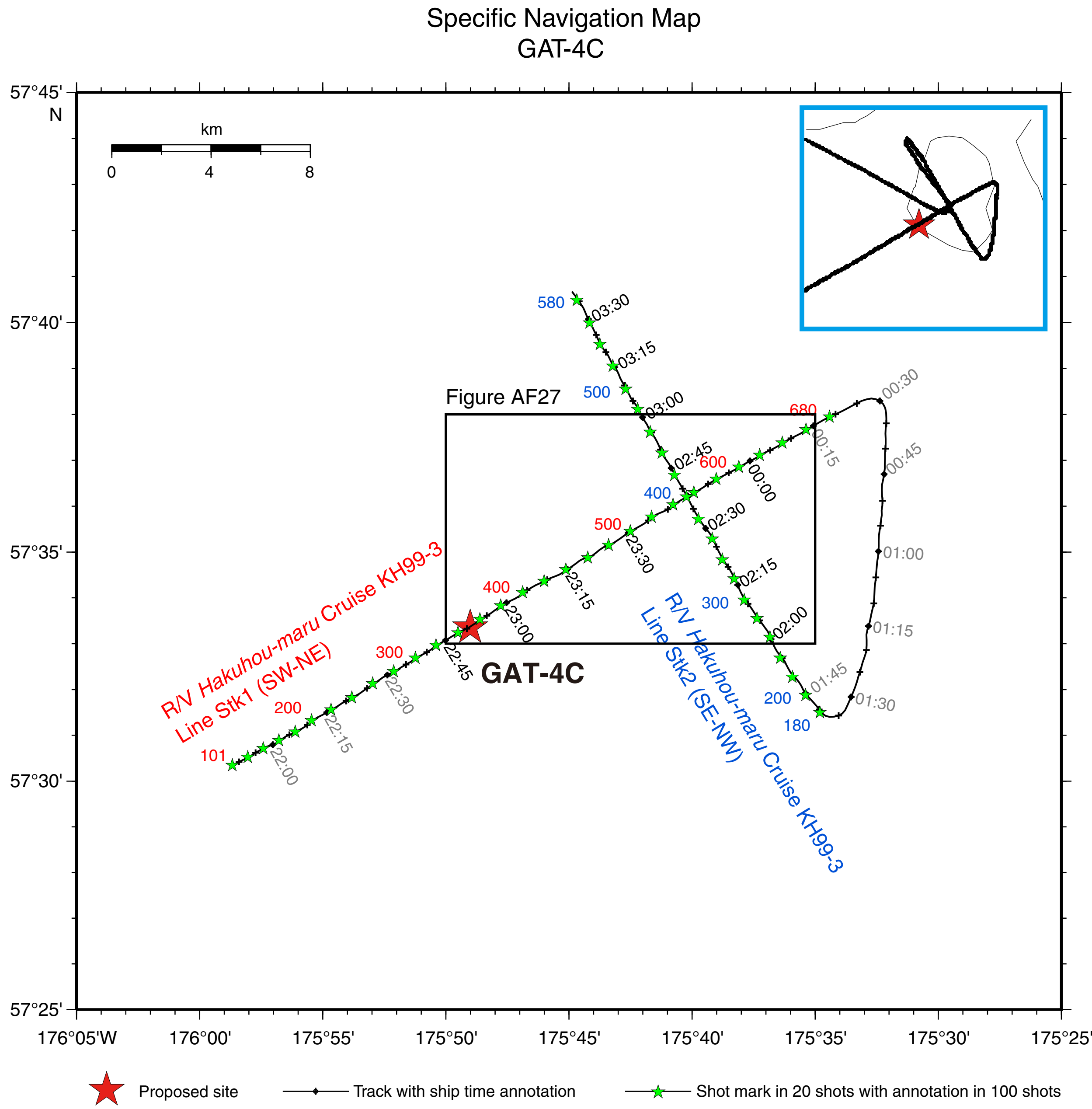

Figure AF27. Close-up navigation map of *Hakuhou-maru* Cruise KH99-3 across Site GAT-4C for close-up seismic profiles in Figures **AF28, AF29,** and **AF31.** Crossing of survey lines is at 23:44:40, Shotpoint 553, on Line Stk1 (SW–NE) and 02:37:55, Shotpoint 400, on Line Stk2 (SE–NW). Site GAT-4C is at 22:50:55, Shotpoint 351, on Line Stk1 (SW–NE).

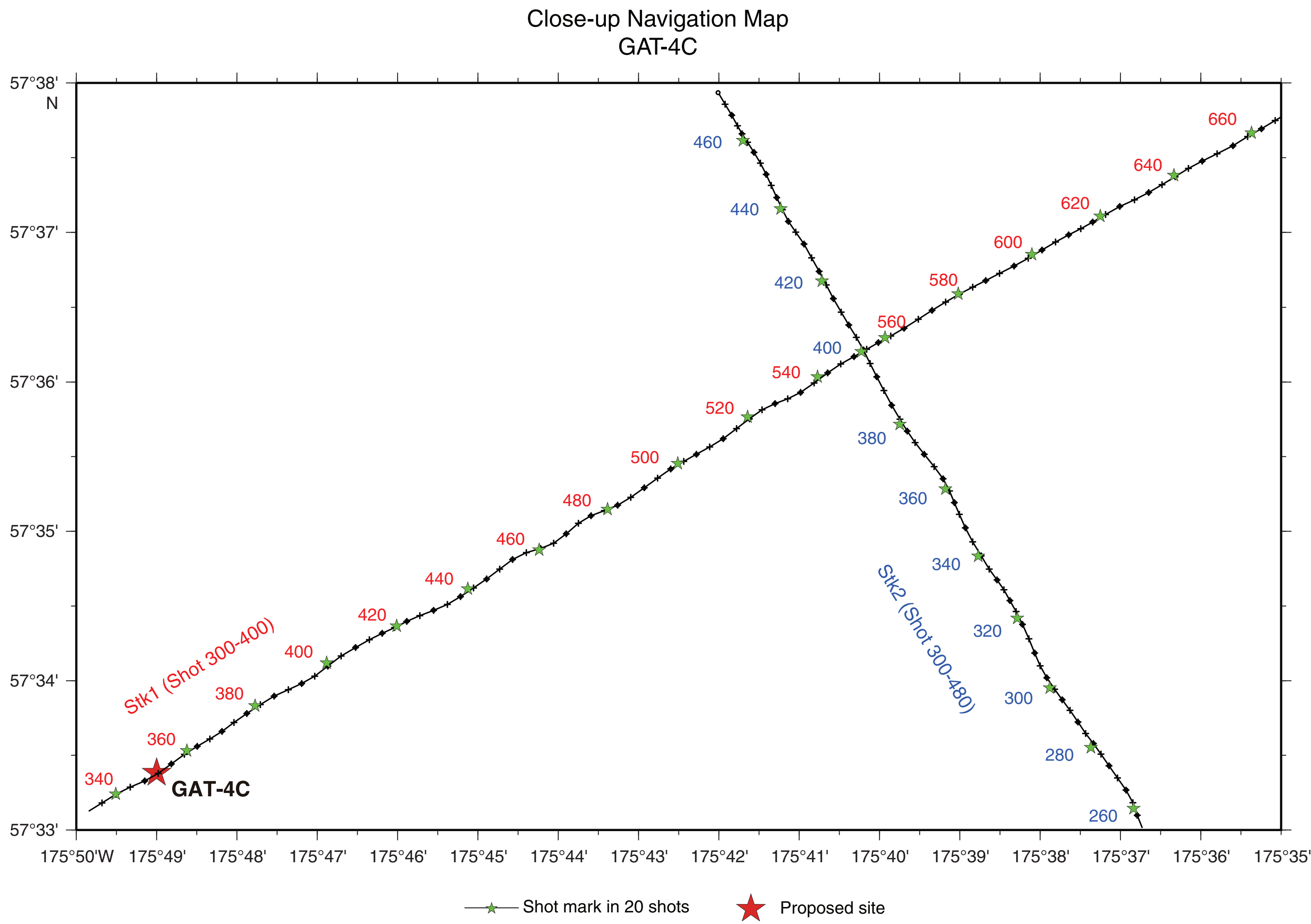

Figure AF28. Seismic profile of *Hakuhou-maru* Cruise KH99-3 Line Stk1 (SW–NE) with location of Site GAT-4C (175°49.0′W, 57°33.4′N; Shotpoint 351; water depth = 1975 m; penetration depth = 745 m) and the observed bottom simulating reflector (BSR).

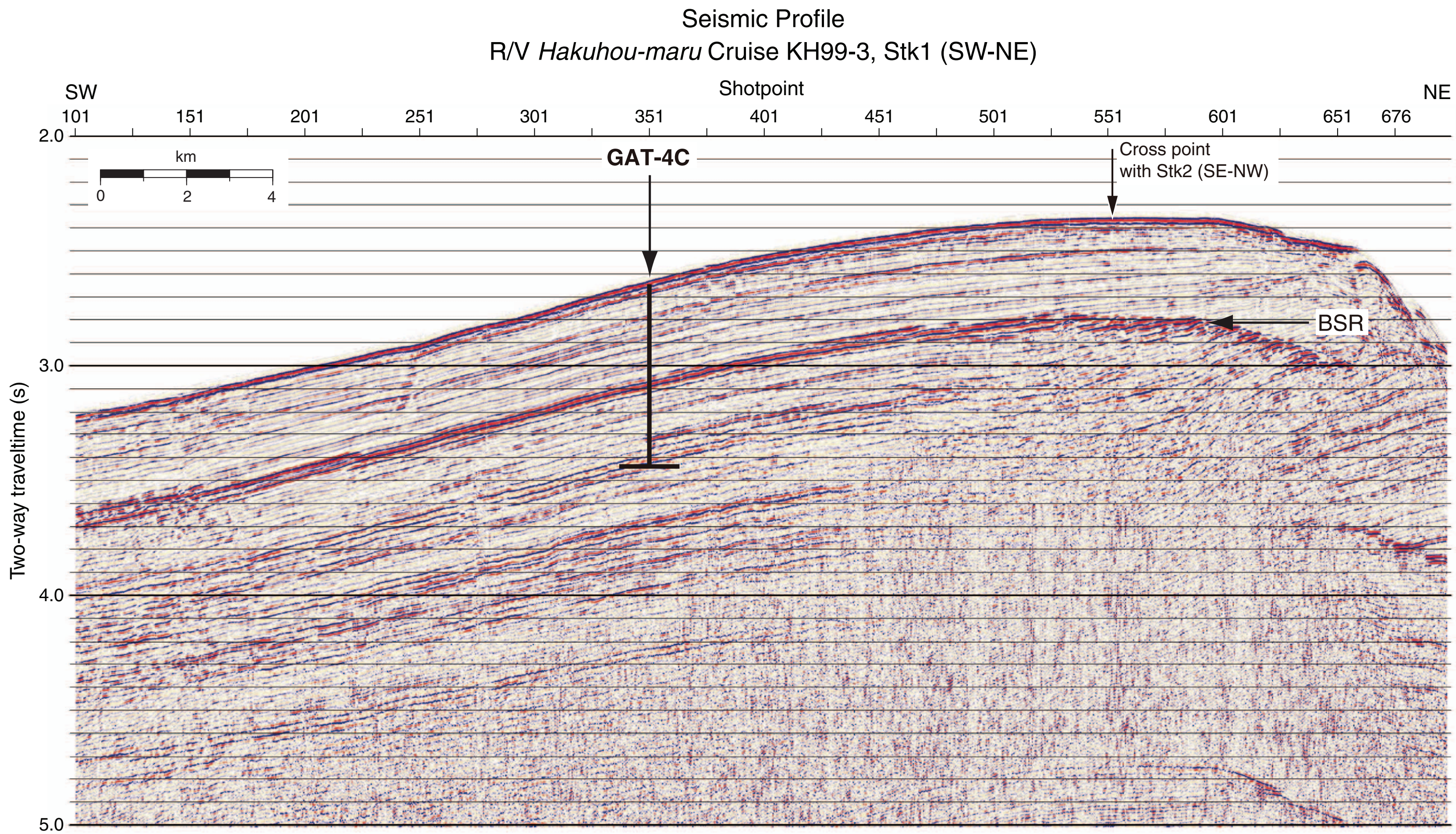

Figure AF29. A. Close-up seismic profile of *Hakuhou-maru* Cruise KH99-3 Line Stk1 (SW–NE) across Site GAT-4C (175°49.0′W, 57°33.4′N; Shotpoint 351; water depth = 1853 m; penetration depth = 700 m coring, 745 m if LWD is planned). **B.** Time-depth curve estimated from results of velocity analyses on Lines Stk-1 and Stk-2 around Site GAT-4C.

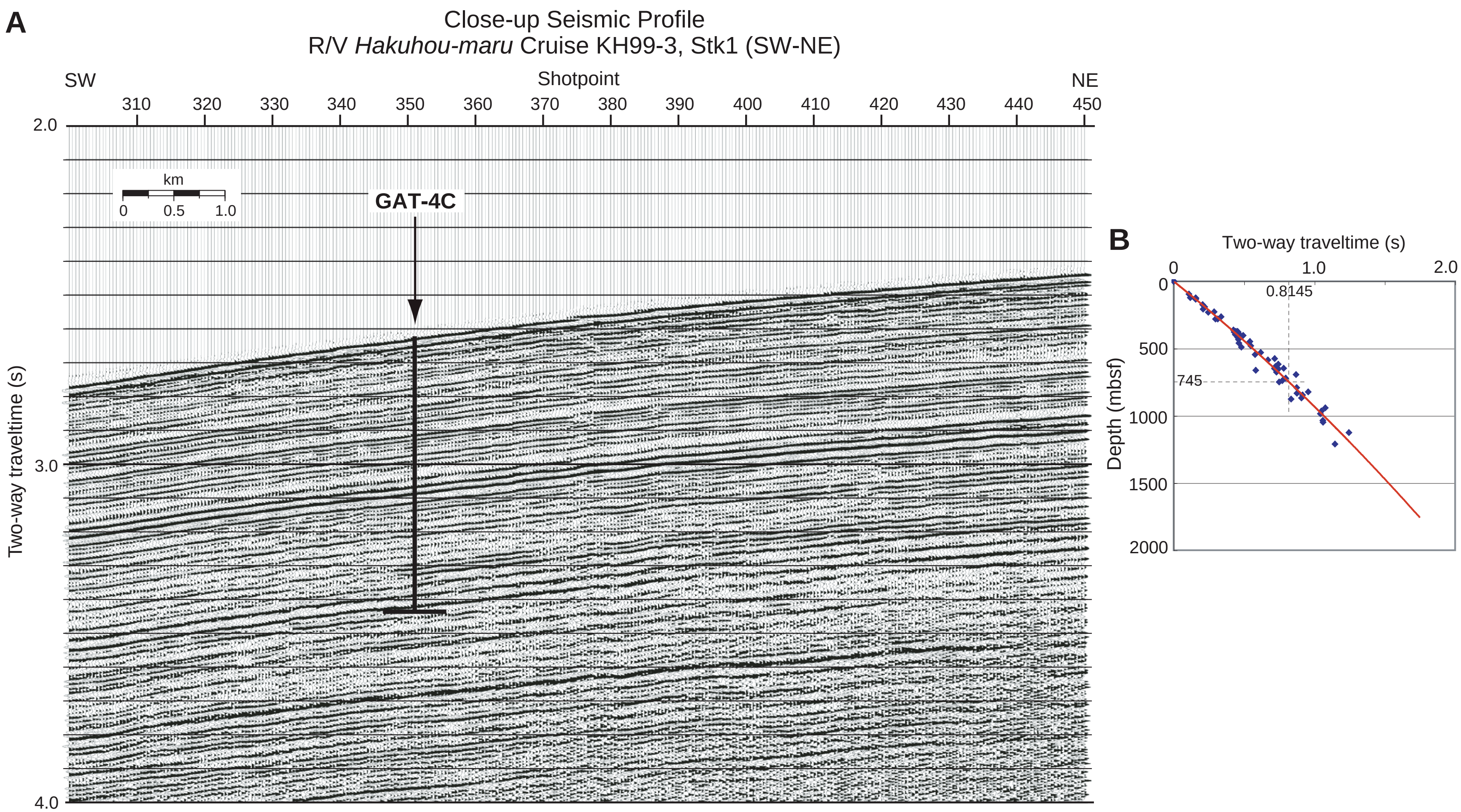

Figure AF30. Seismic profile of *Hakuhou-maru* Cruise KH99-3 Line Stk2 (SE–NW) around Site GAT-4C (175°49.0′W, 57°33.4′N; water depth = 1975 m), projected from the southwest on the cross point.

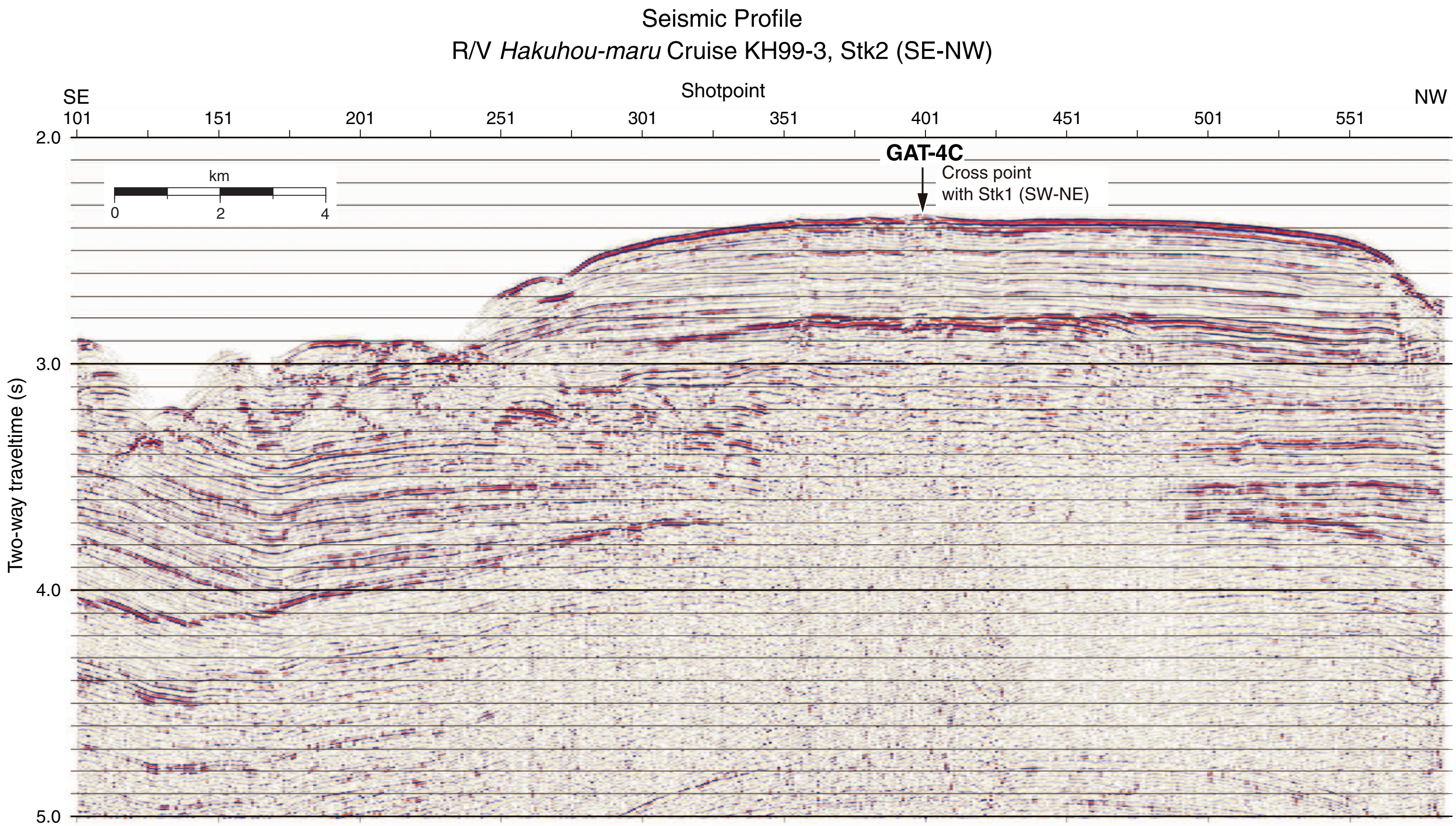

Figure AF31. A. Close-up seismic profile of *Hakuhou-maru* Cruise KH99-3 Line Stk2 (SE–NW) near Site GAT-4C. Penetration depth is projected from the southwest on the cross point (Shotpoint 400; see Fig. AF26). **B.** Time-depth curve estimated from results of velocity analyses on Lines Stk1 and Stk2 around Site GAT-4C.

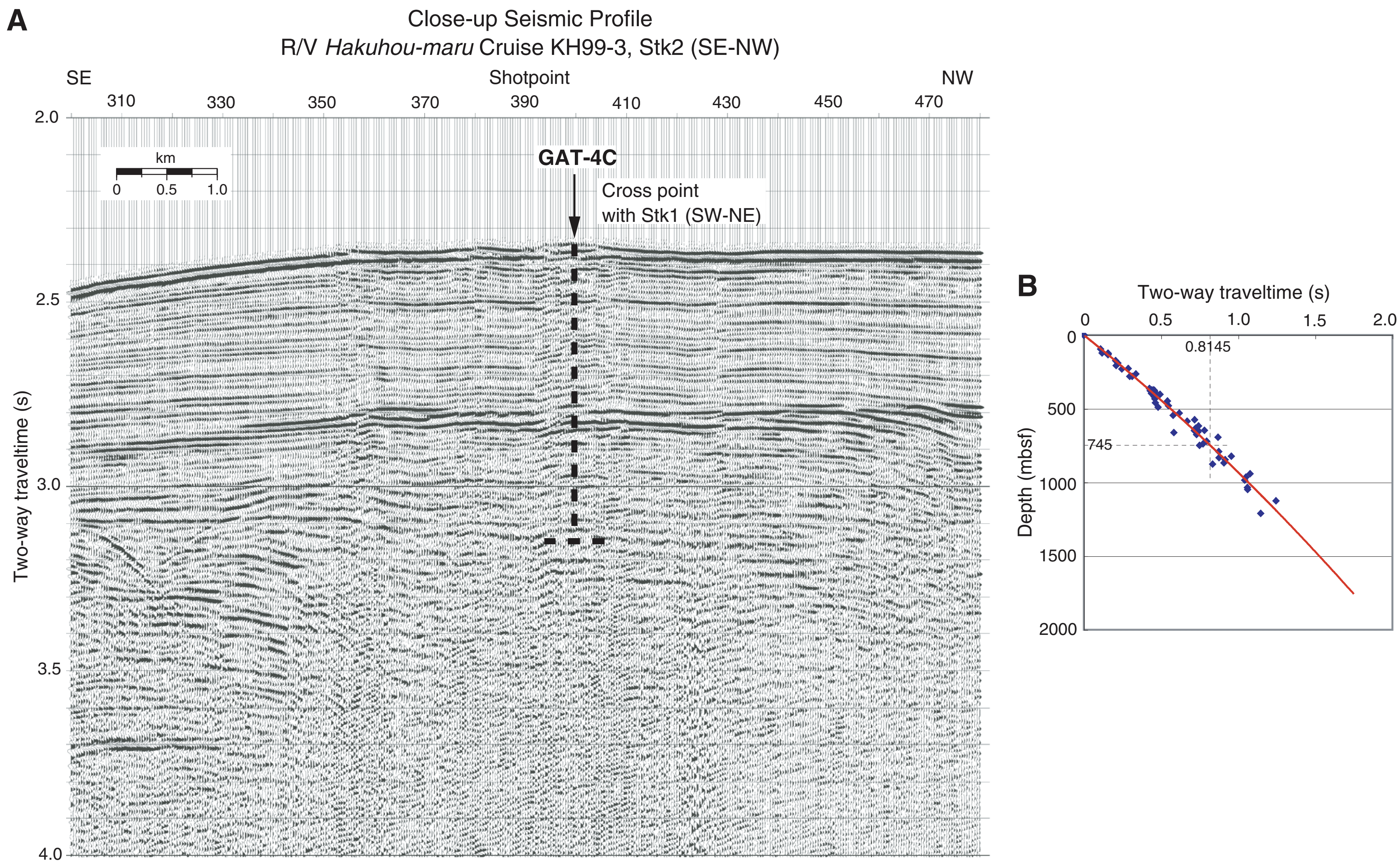

Figure AF32. 3.5 kHz subbottom profile survey from *Hakuhou-maru* Cruise KH99-3. **A.** Line Stk1 (SW–NE) across Site GAT-4C at 22:50:55. **B.** Line Stk2 (SE–NW) around Site GAT-4C, projected from the southwest on the cross point.

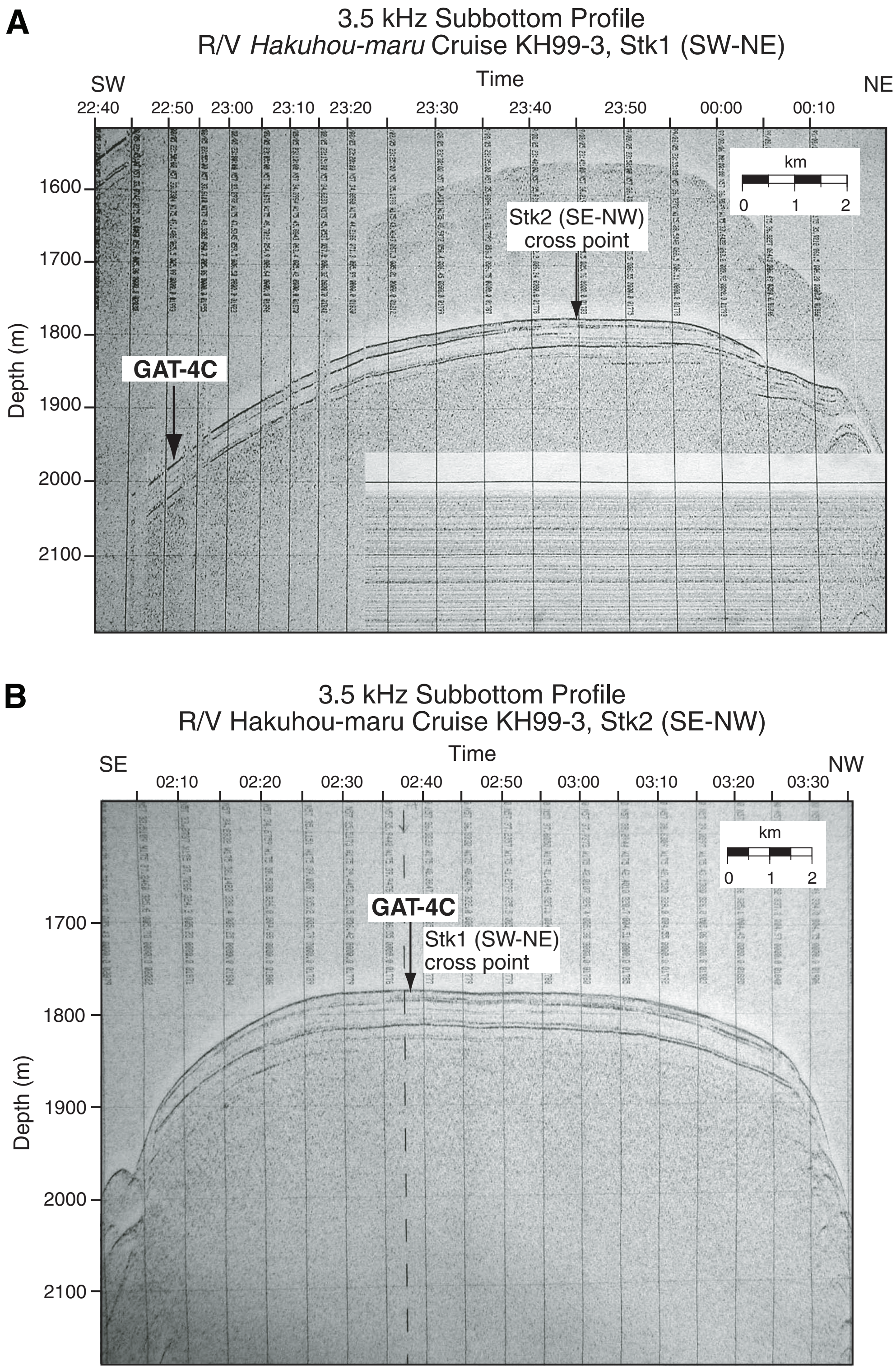

Figure AF33. Swath bathymetric map with track chart at time of *Hakuhou-maru* Cruise KH99-3 around Site GAT-4C. **A.** Plain image. **B.** Shaded relief image. Crossing of survey line is at 23:44:40, Shotpoint 553, on Line Stk1 (SW–NE) and 02:37:55, Shotpoint 400 on Line Stk2 (SE–NW). Site GAT-4C is at 22:50:55, Shotpoint 351, on Line Stk1 (SW–NE).

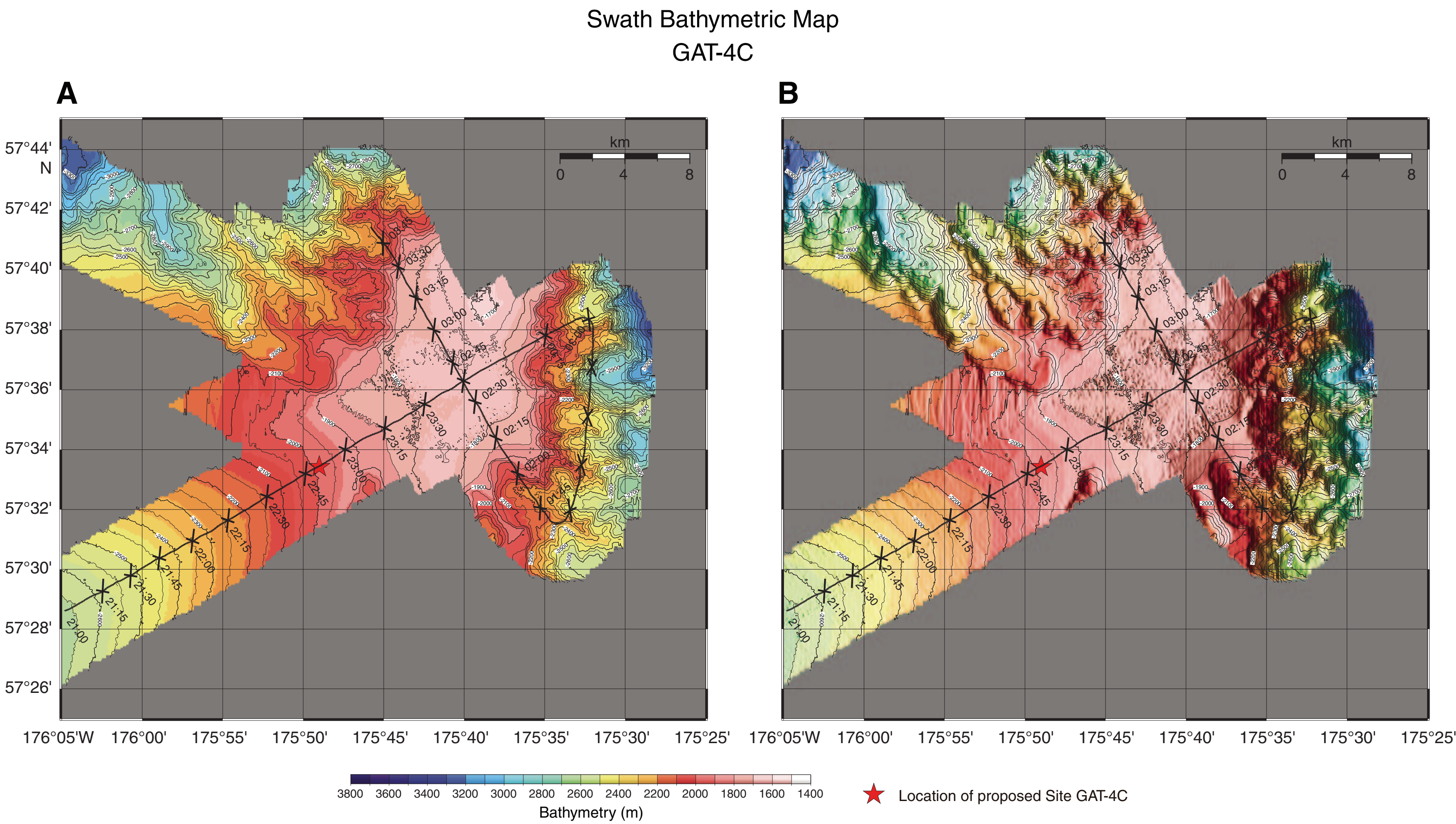

Figure AF34. Specific navigation map of *Hakuhou-maru* Cruise KH99-3 around Site GAT-3C with ship time and shotpoint annotation. Crossing of survey line is at 02:59:56, Shotpoint 2899, on Line Stk3-7 (W–E) and 00:49:55, Shotpoint 2510, on Line Stk3-5 (S–N). Site GAT-3C is at 02:50:45, Shotpoint 2860, on Line Stk3-7 (W–E). Squares = navigation map area for close-up seismic profiles in Figure **AF35.** Time annotation in black letters = range of subbottom profile survey in Figure **AF41.**

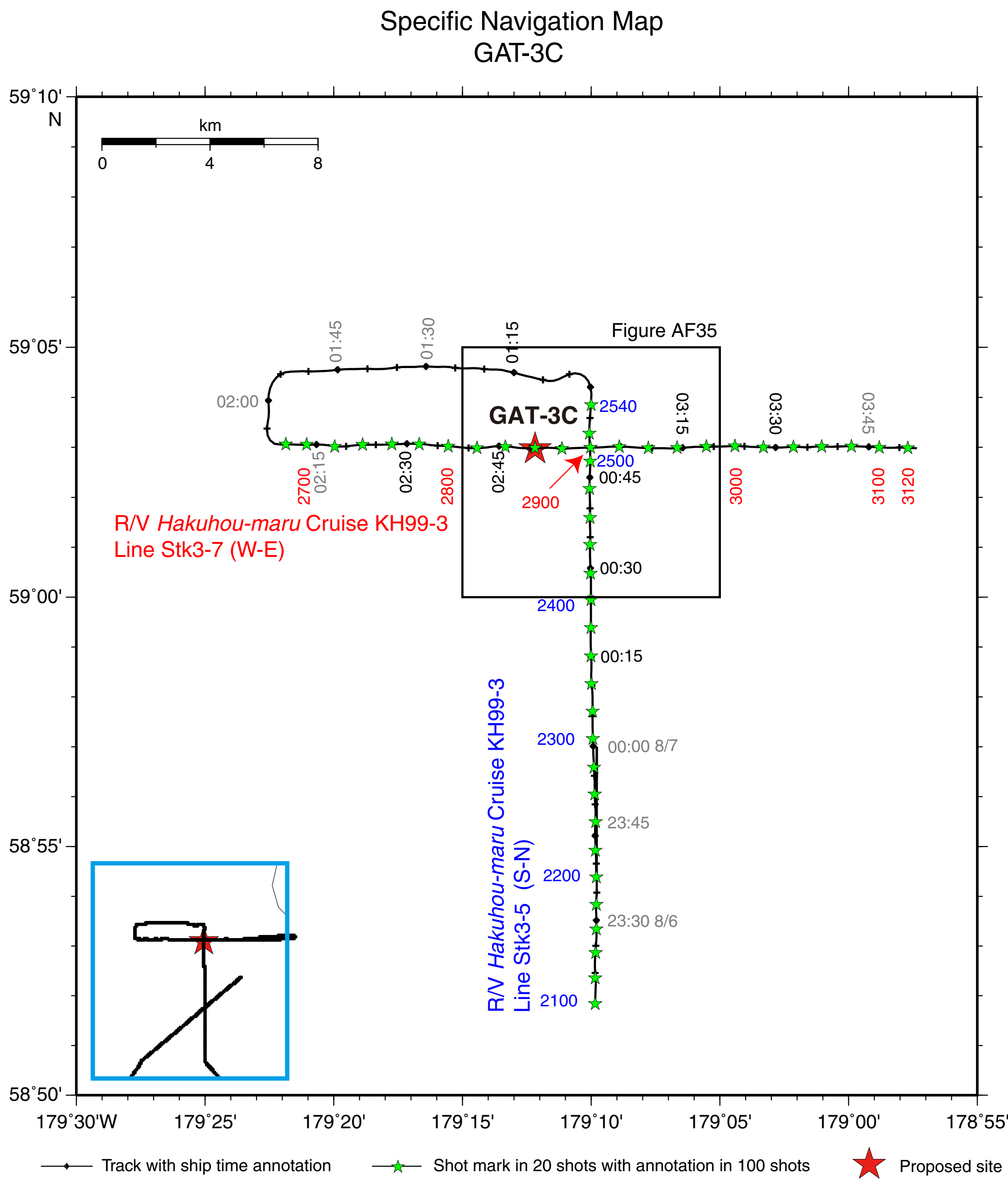

Figure AF35. Close-up navigation map of *Hakuhou-maru* Cruise KH99-3 across Site GAT-3C for close-up seismic profiles in Figures **AF38** and **AF39.** Crossing of survey lines is at 02:59:56, Shotpoint 2899, on Line Stk3-7 (W–E) and 00:49:55, Shotpoint 2510, on Line Stk3-5 (S–N). Site GAT-3C is at 02:50:45, Shotpoint 2860, on Line Stk3-7 (W–E).

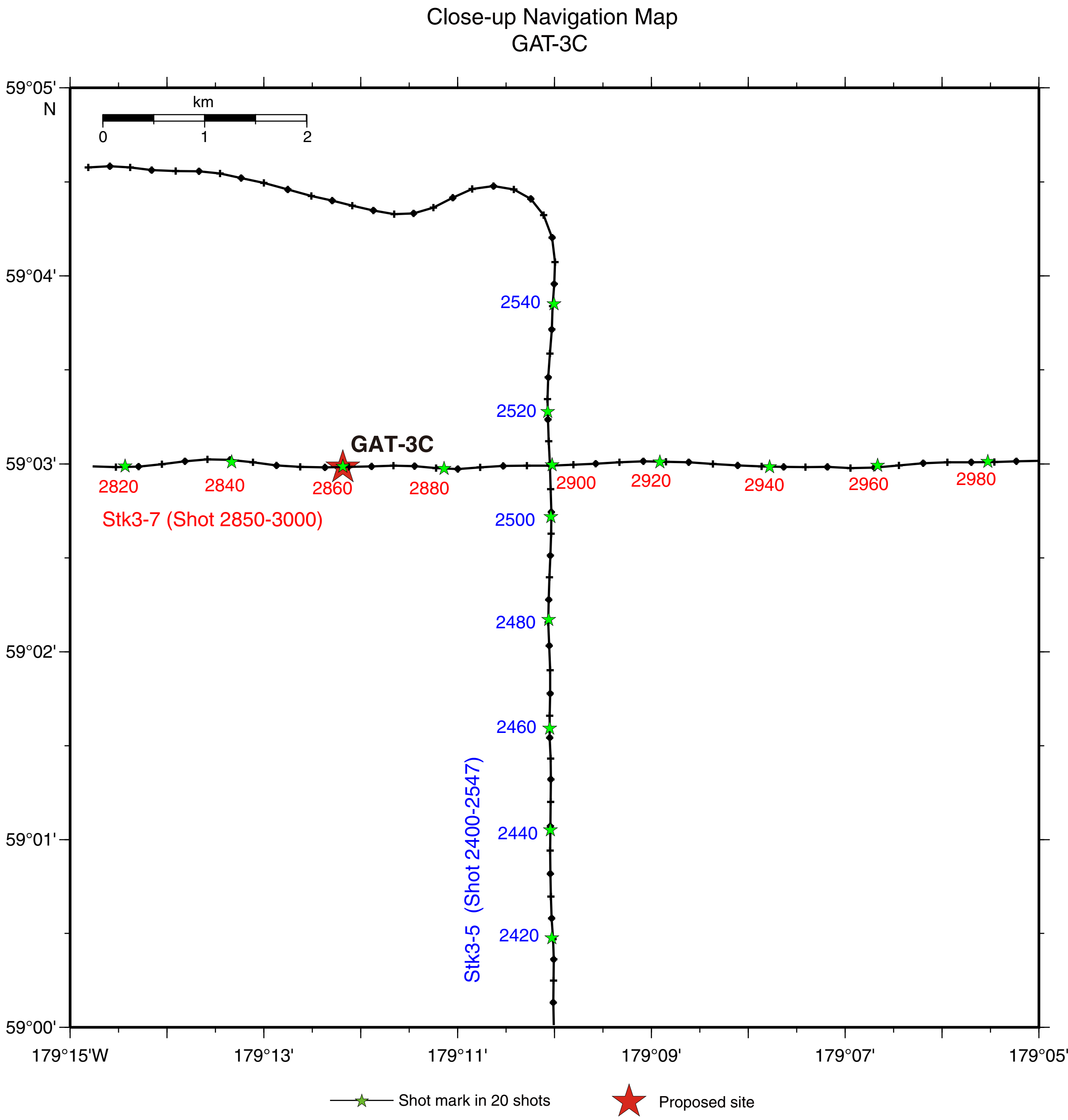

Figure AF36. Seismic profile of *Hakuhou-maru* Cruise KH99-3 Line Stk3-7 (W–E) with location of Site GAT-3C (179°12.2′W, 59°03.0′N; Shotpoint 2860; water depth = 3209 m; penetration depth = 700 m coring, 745 m if LWD is planned).

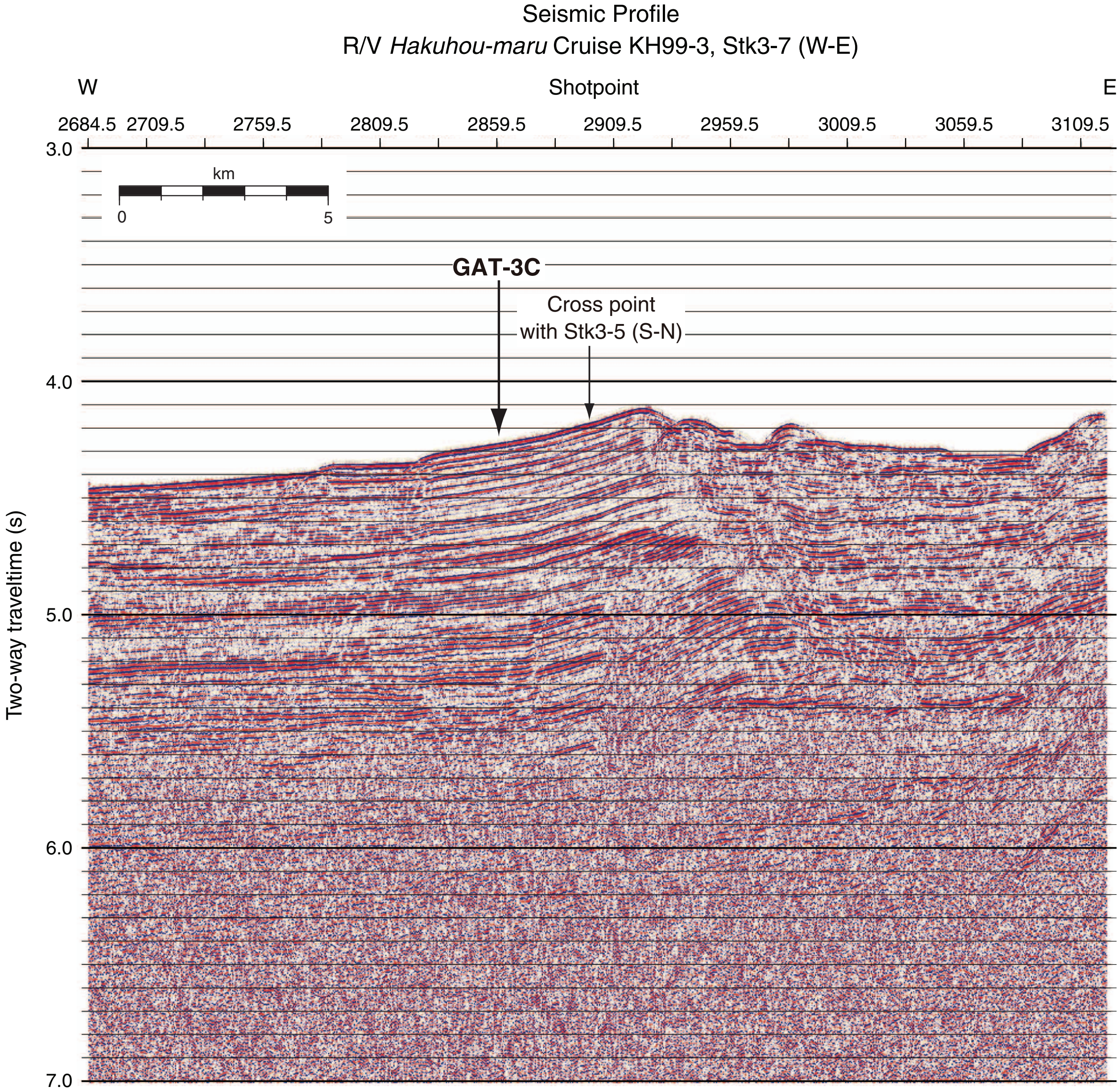

Figure AF37. Seismic profile of *Hakuhou-maru* Cruise KH99-3 Line Stk3-5 (S–N) with location of Site GAT-3C (179°12.2′W, 59°03.0′N; water depth = 3209 m), projected from the west on the cross point.

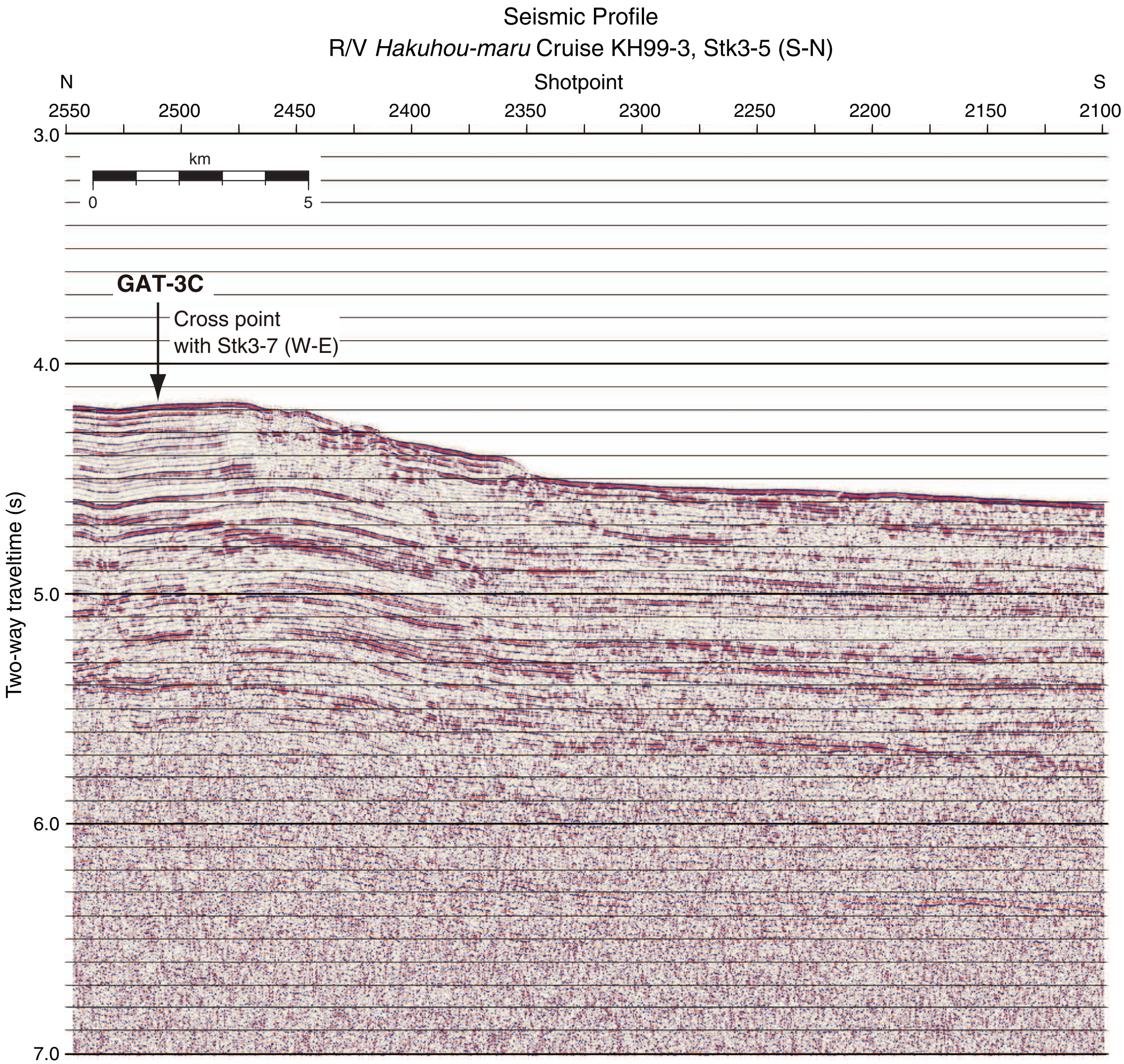

Figure AF38. A. Close-up seismic profile of *Hakuhou-maru* Cruise KH99-3 Line Stk3-7 (W–E) across Site GAT-3C (179°12.2′W, 59°03.0′N; Shotpoint 2860; water depth = 3209 m; penetration depth = 700 m coring, 745 m if LWD is planned). **B.** Time-depth curve estimated from results of velocity analyses on Lines Stk3-5 and Stk3-7 around Site GAT-3C.

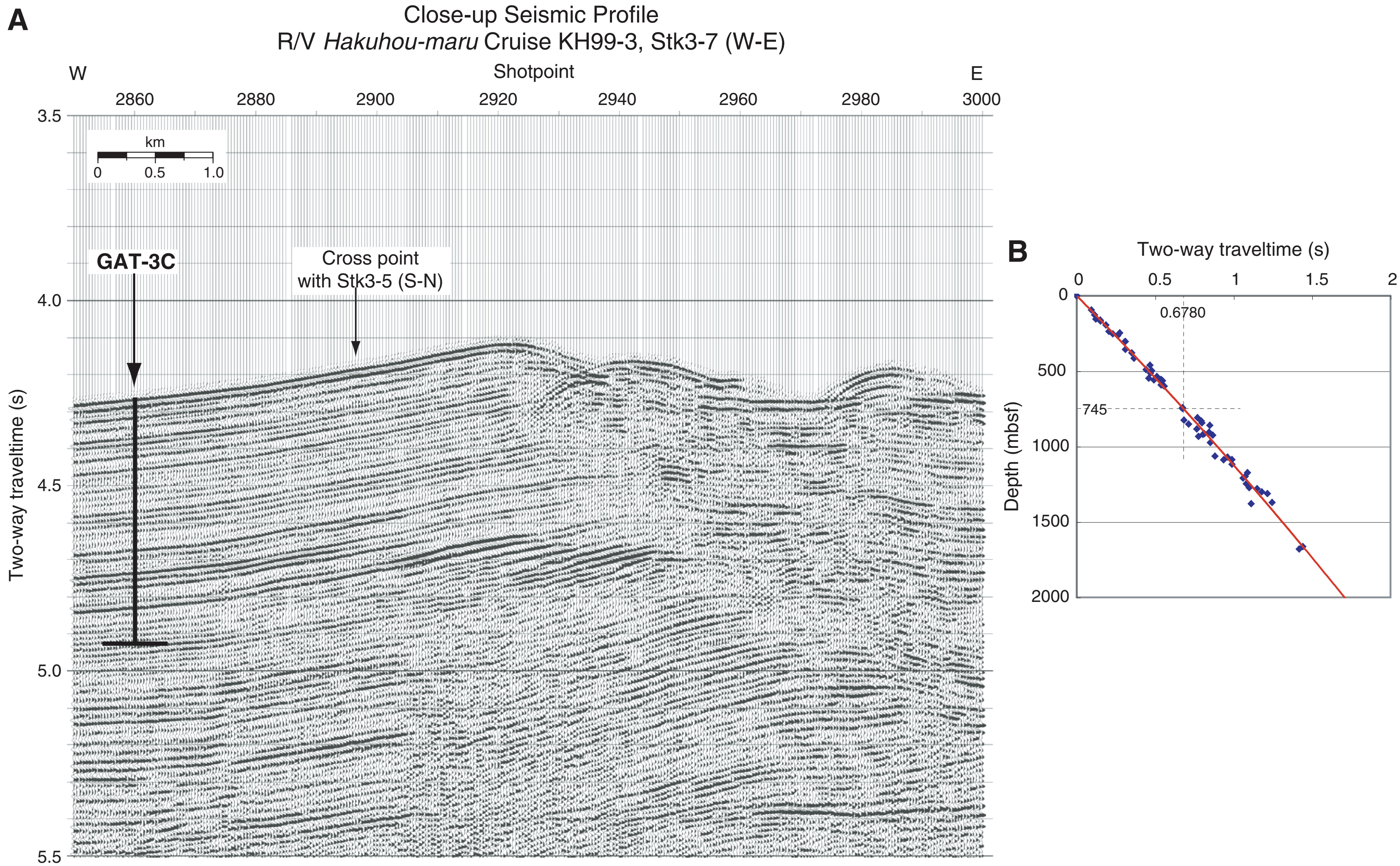

Figure AF39. A. Close-up seismic profile of *Hakuhou-maru* Cruise KH99-3 Line Stk3-5 (S–N) near Site GAT-3C. Penetration depth is projected from the west on the cross point (Shotpoint 2510; see Fig. AF35). **B.** Time-depth curve estimated from results of velocity analyses on Lines Stk3-5 and Stk3-7 around Site GAT-3C.

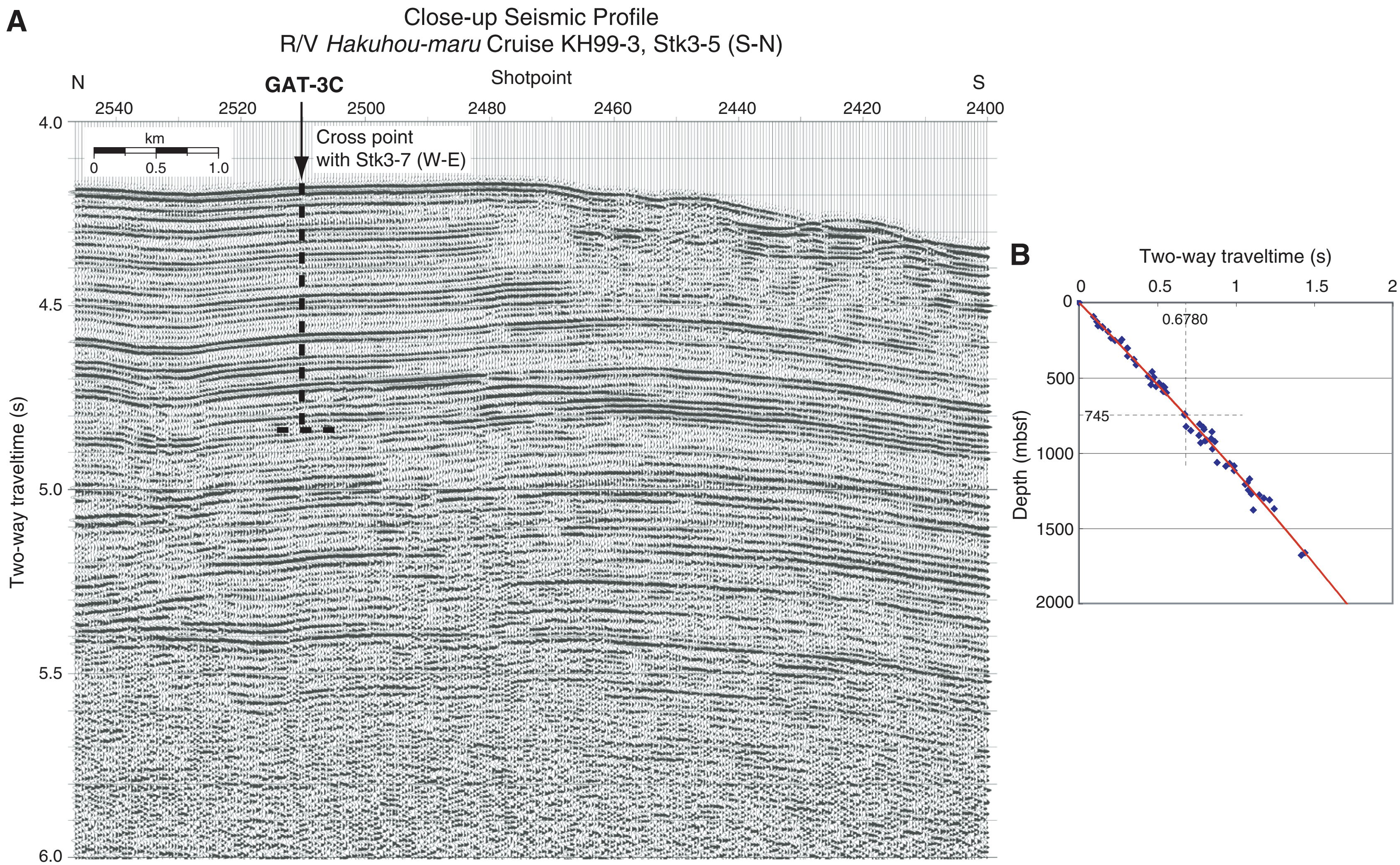

Figure AF40. 3.5 kHz subbottom profile survey from *Hakuhou-maru* Cruise KH99-3. **A.** Line Stk3-7 (W–E) across Site GAT-3C at 02:50:45. **B.** Line Stk3-5 (S–N) around Site GAT-3C, projected from the west on the cross point.

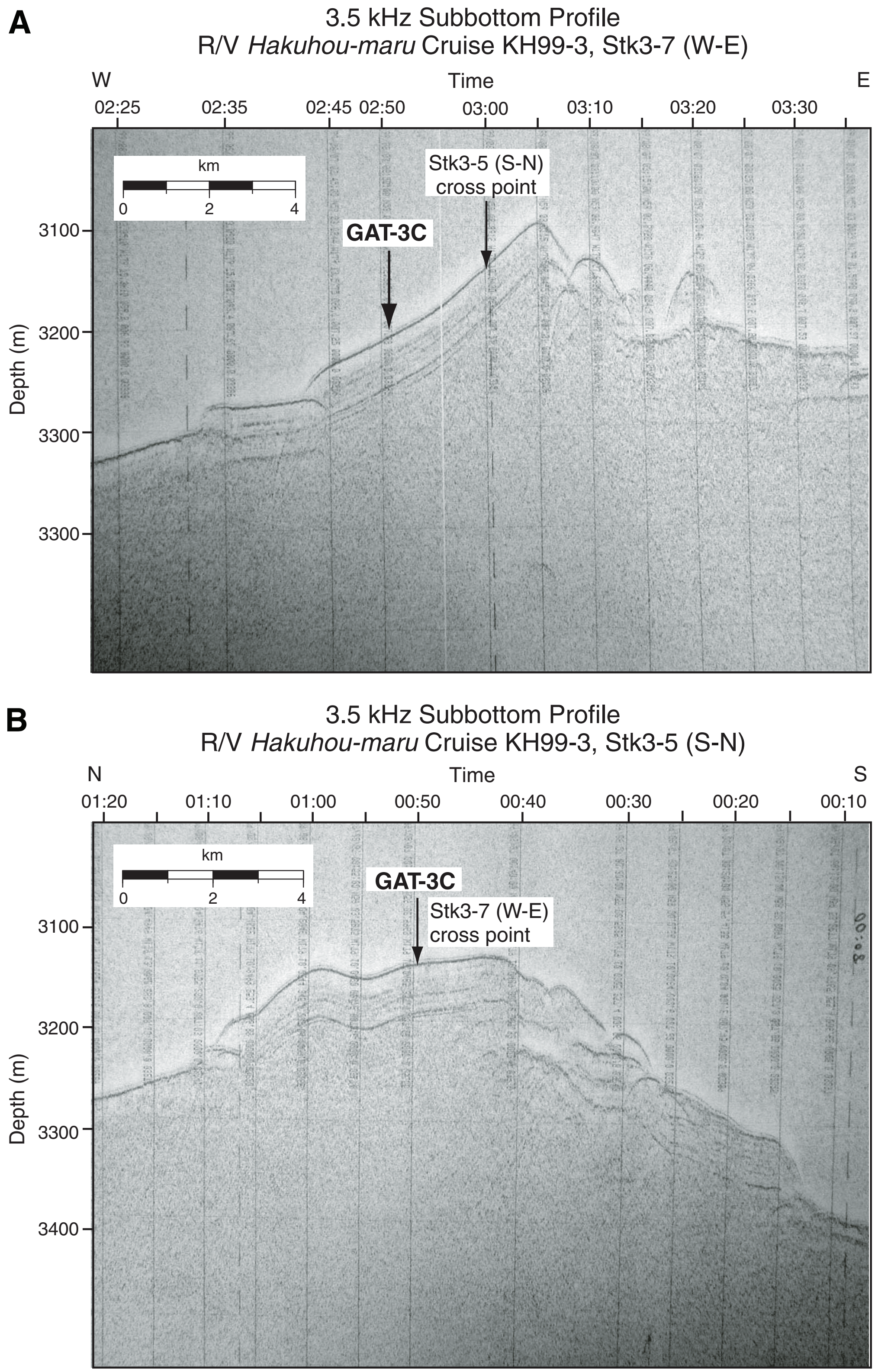

Figure AF41. Swath bathymetric map with track chart at time of *Hakuhou-maru* Cruise KH99-3 around Site GAT-3C. **A.** Plain image. **B.** Shaded relief image. Crossing of survey line is at 02:59:56, Shotpoint 2899, on Line Stk3-7 (W–E) and 00:49:55, Shotpoint 2510 on Line Stk3-5 (S–N). Site GAT-3C is at 02:50:45, Shotpoint 2860, on Line Stk3-7 (W–E).

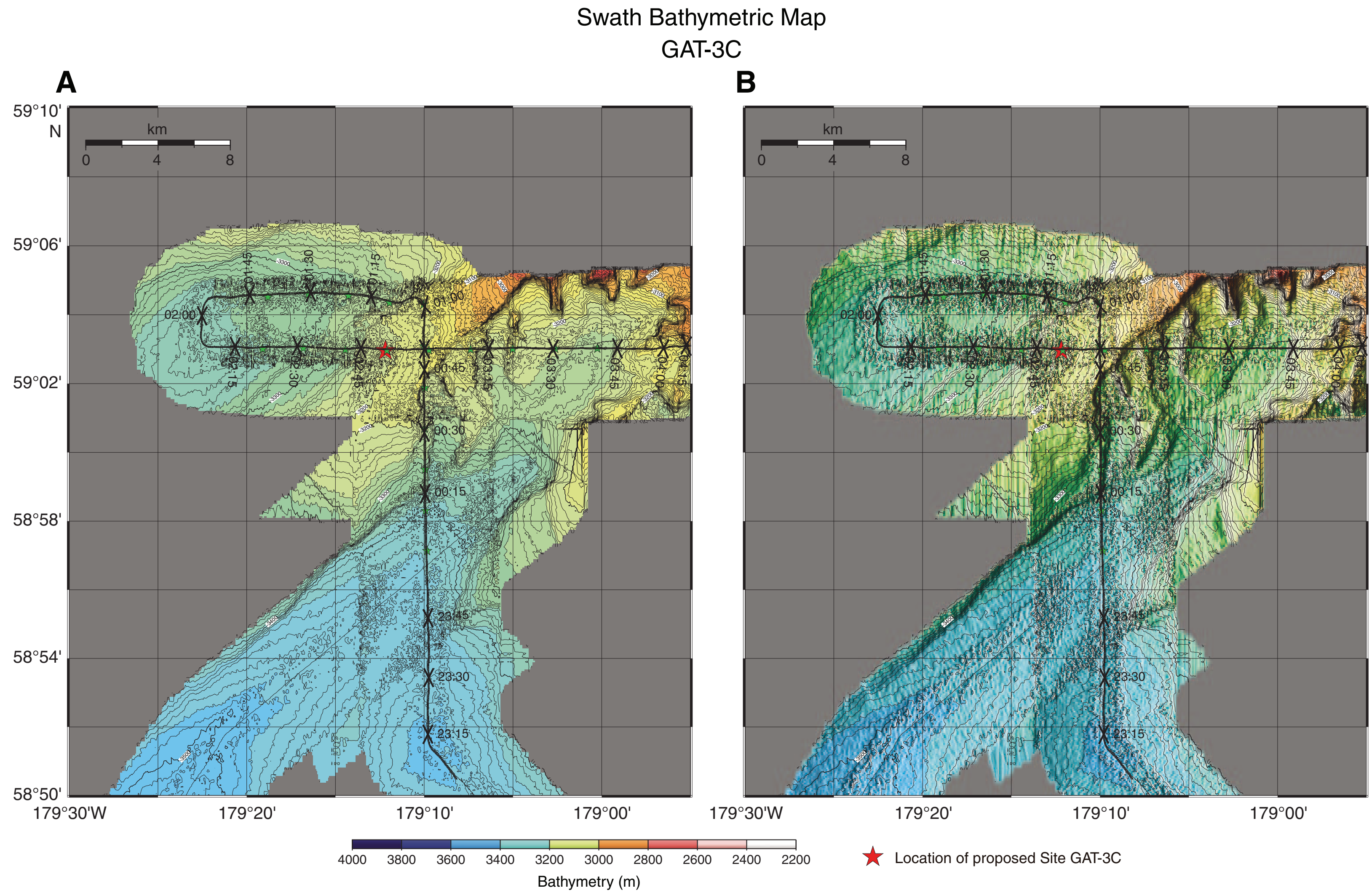

Figure AF42. Regional overview map around Site KST-1B (164°54.9′E, 55°55.6′N; water depth = 3435 m) with track-chart of USNS *Bartlett* Cruise 02, Leg 049, 232 Day, 1970, 22:14–17:32. Bathymetric image and contour line created by GMT (**gmt.soest.hawaii.edu**) using GINA Global Topo Data (**www.gina.alaska.edu**).

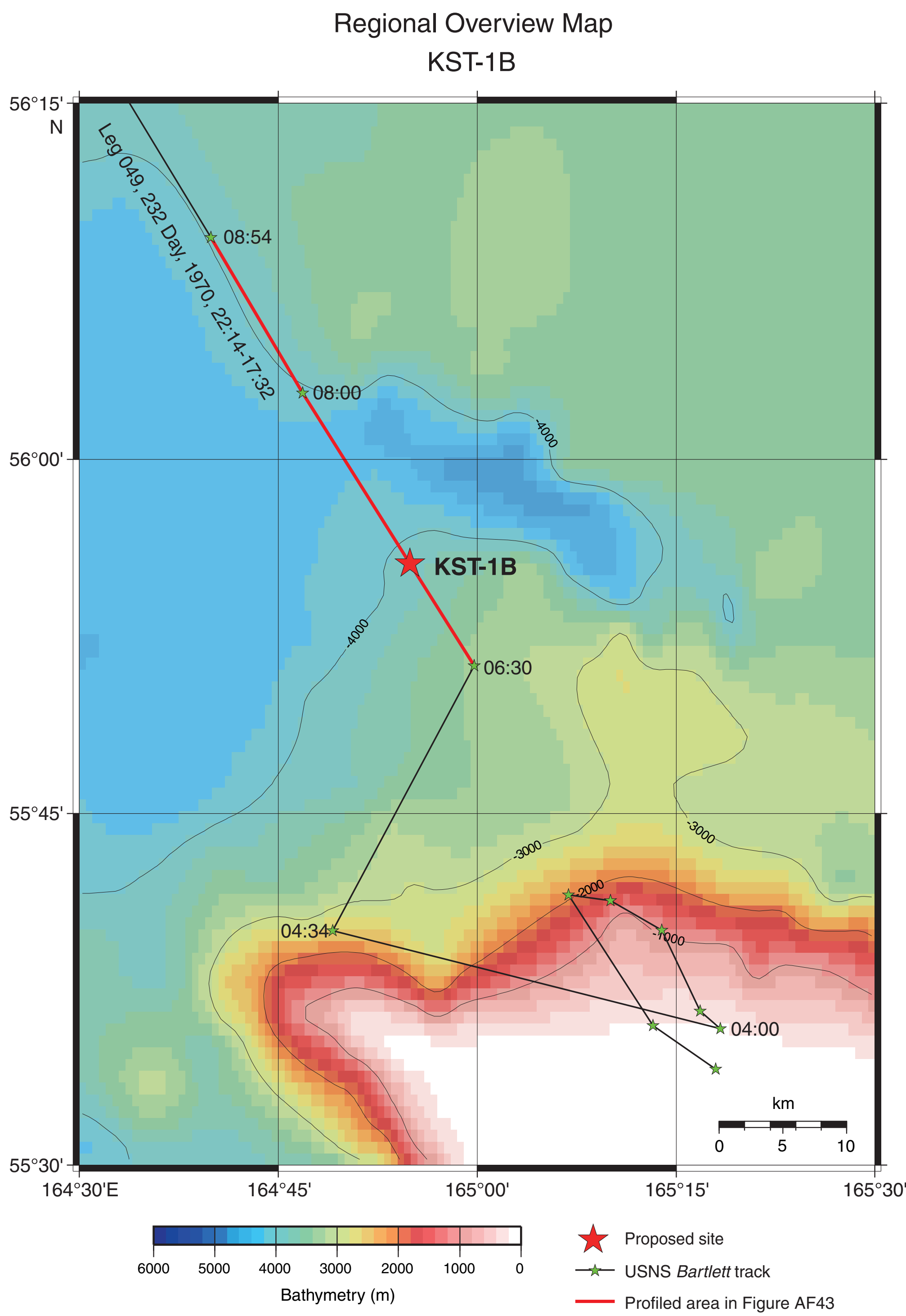

Figure AF43. Seismic profile of USNS *Bartlett* Cruise 02, Leg 049, 232 Day, 1970, 22:14–17:32 with location of Site KST-1B (164°54.9′E, 55°55.6′N; 7:03:46; water depth = 3435 m; penetration depth = 200 m).

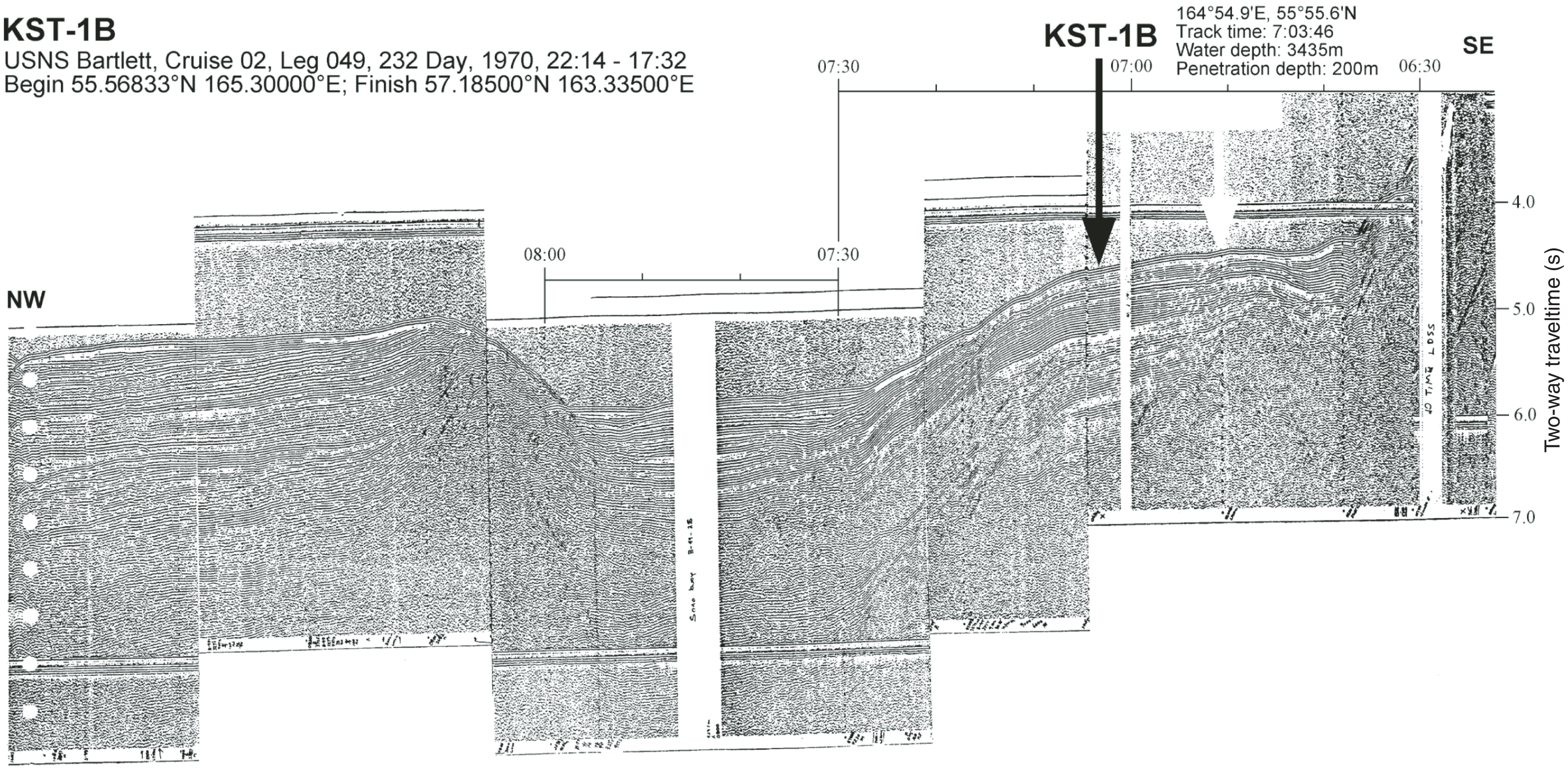

Figure AF44. Close-up seismic profile of USNS *Bartlett* Cruise 02, Leg 049, 232 Day, 1970, 22:14–17:32 with location of Site KST-1B (164°54.9′E, 55°55.6′N; 7:03:46; water depth = 3435 m; penetration depth = 200 m).

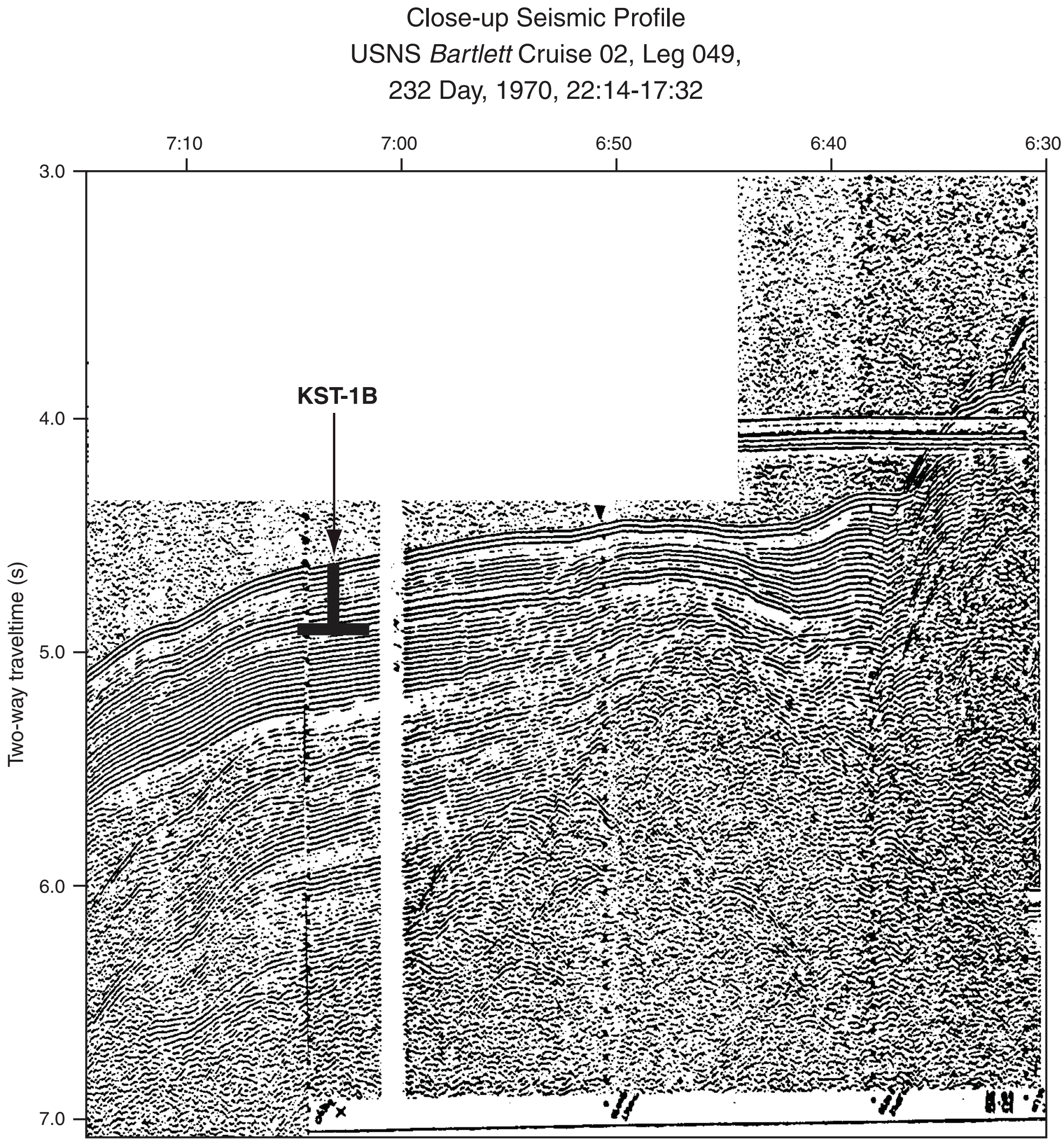

Figure AF45. Regional overview map with track chart of USNS *Bartlett* Cruise 02 (1970) across Sites SHR-3B and SHR-1B. Squares = study area of each site. Bathymetric image and contour line created by GMT (**gmt.soest.hawaii.edu**) using GINA Global Topo Data (**www.gina.alaska.edu**). See Figures **AF46** and **AF47** for detailed track information.

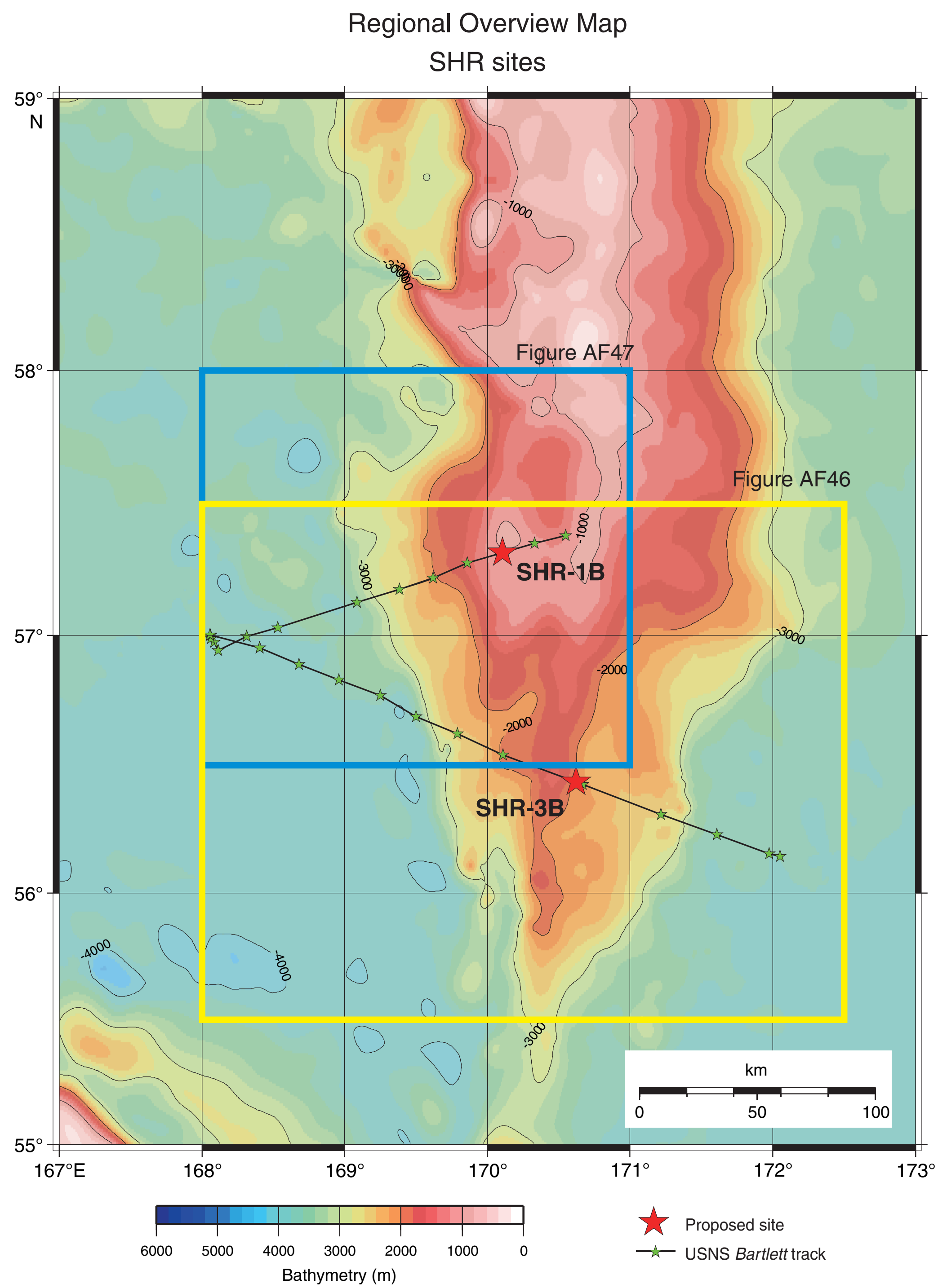

Figure AF46. Map of study area with track chart of USNS *Bartlett* Cruise 02, Leg 054, 235 Day, 1970, 23:14–14:00 across Site SHR-1B (170°06.4′E, 57°19.0′N; 0:30; water depth = 963 m). Bathymetric image and contour line created by GMT (**gmt.soest.hawaii.edu**) using GINA Global Topo Data (**www.gina.alaska.edu**).

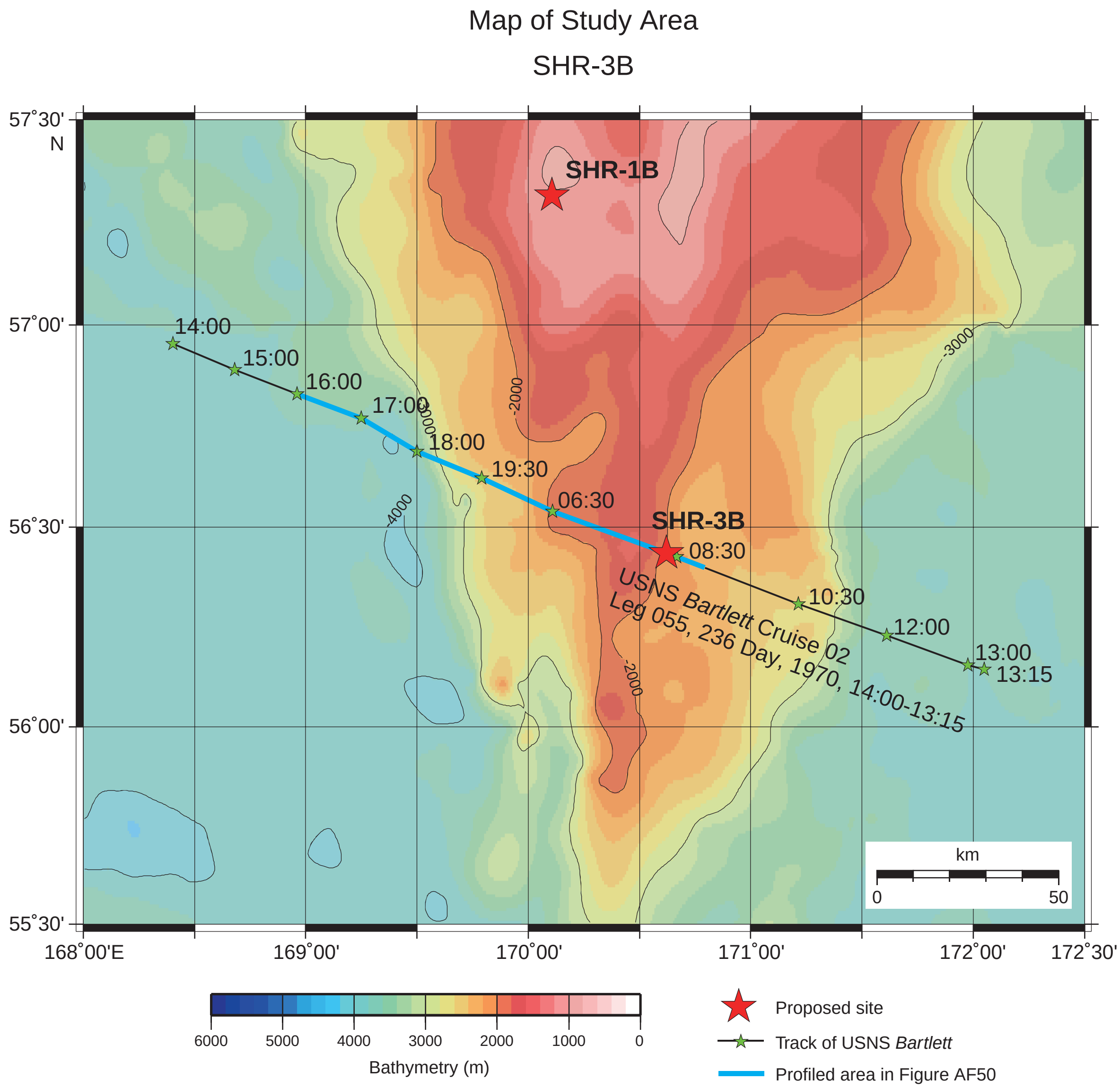

Figure AF47. Map of study area with track chart of USNS *Bartlett* Cruise 02, Leg 055, 236 Day, 1970, 14:00–13:15 across Site SHR-3B (170°37.2′E, 56°26.1′N; Shotpoint at 8:20; water depth = 2232 m). Bathymetric image and contour line created by GMT (**gmt.soest.hawaii.edu**) using GINA Global Topo Data (**www.gina.alaska.edu**).

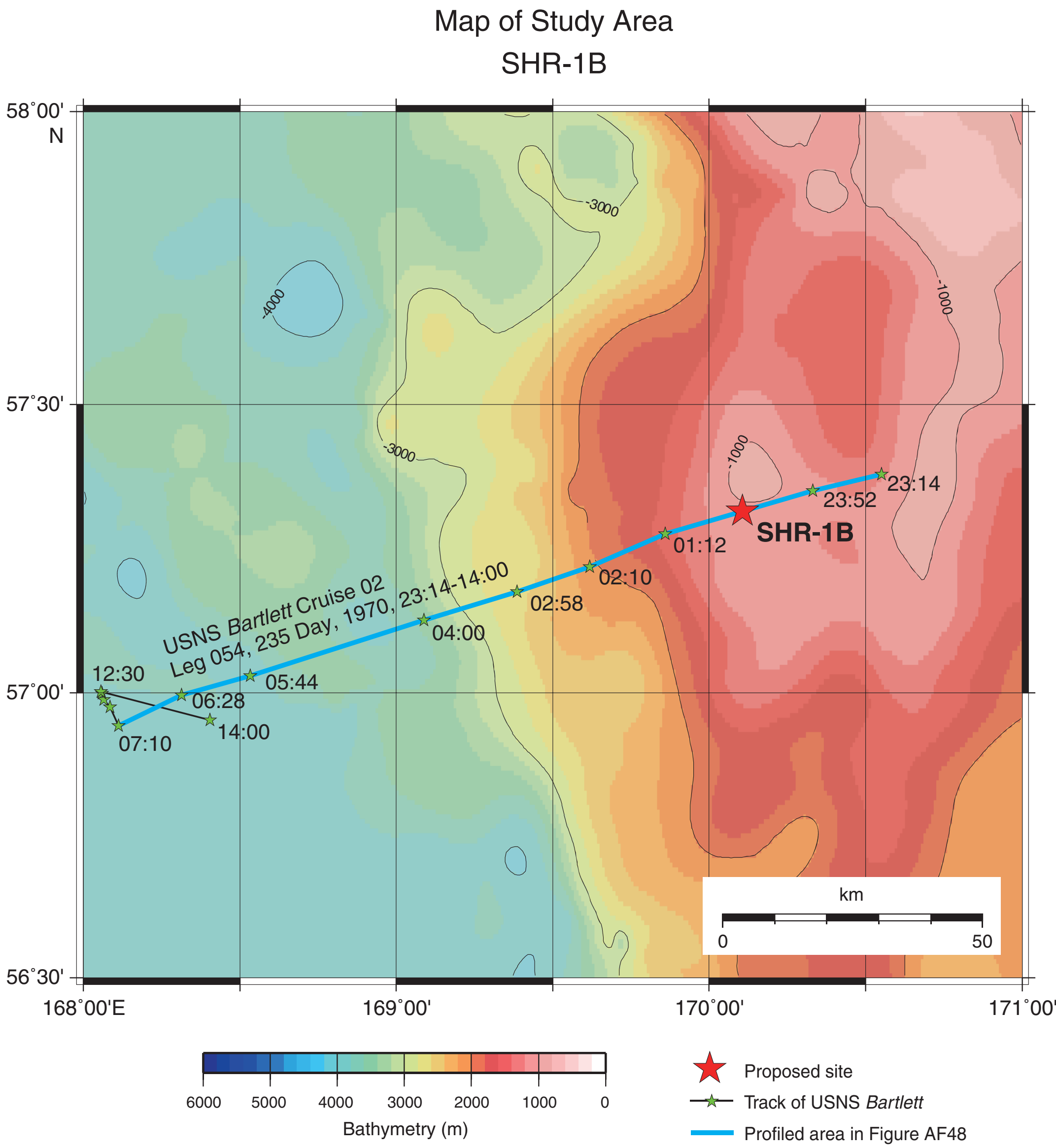

Figure AF48. Seismic profile of USNS *Bartlett* Cruise 02, Leg 055, 236 Day, 1970, 07:00–09:00 with location of Site SHR-3B (170°37.2′E, 56°26.1′N; 8:20; water depth = 2232 m, penetration depth = 200 m).

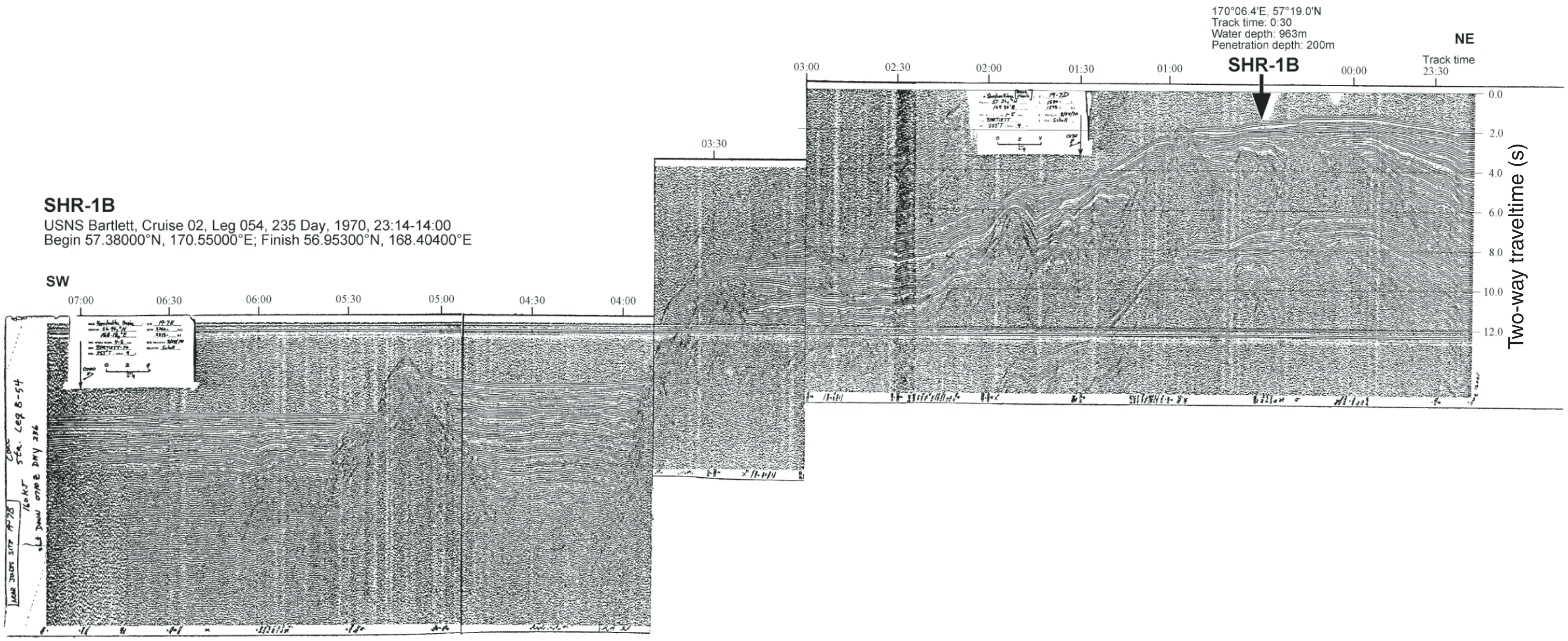

Figure AF49. A. Close-up seismic profile of USNS *Bartlett* Cruise 02, Leg 055, 236 Day, 1970, 07:00–09:00 with location of Site SHR-3B (170°37.2′E, 56°26.1′N; 8:20; water depth = 2232 m; penetration depth = 200 m). **B.** Time-depth conversion curve used for Site SHR-3B. Two-way traveltime and vRMS data collected from seismic profile of USGS *Lee* Cruise L6-80, Line 6, CDP 785. Water depth is deleted in this figure.

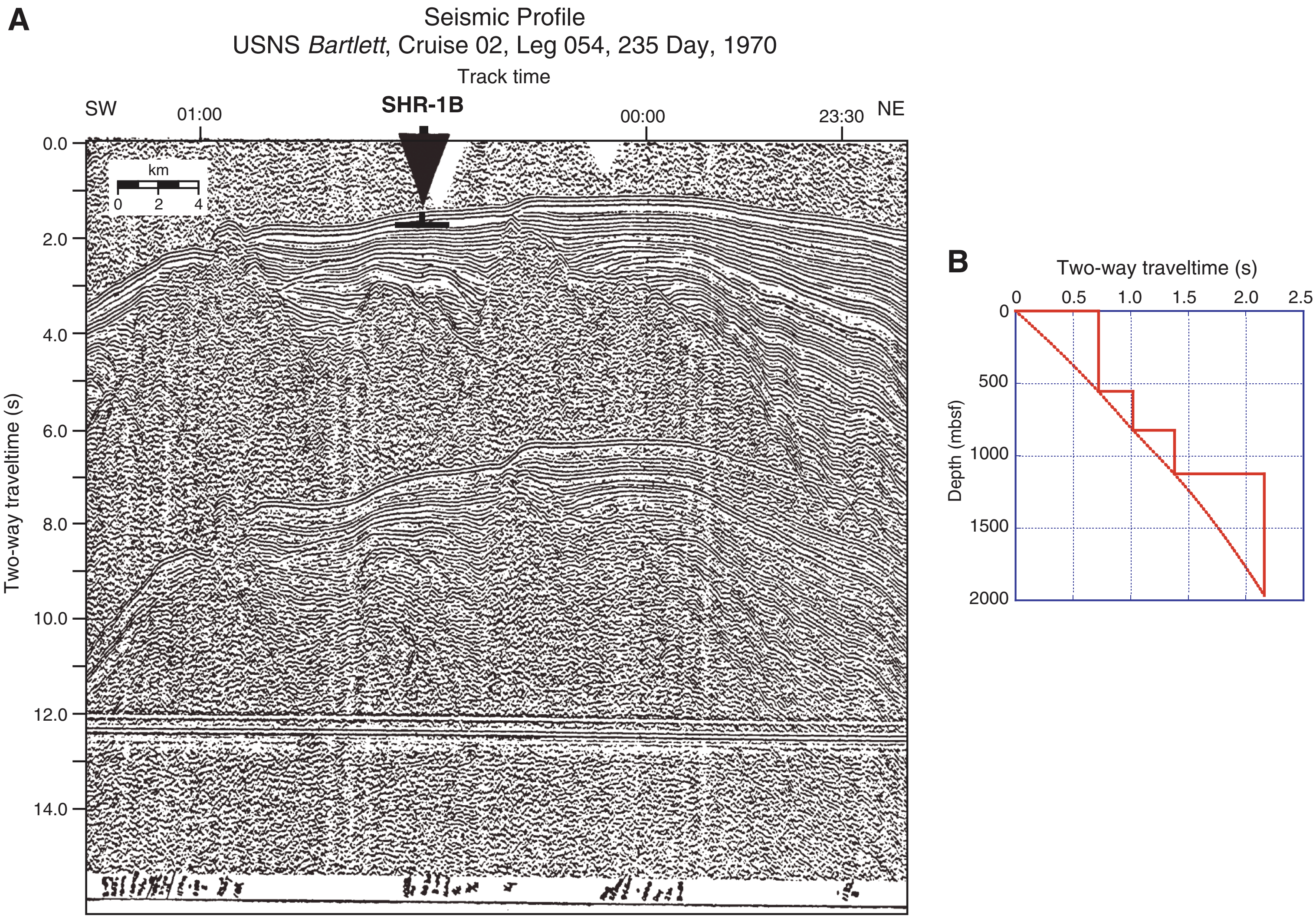

Figure AF50. Seismic profile of USNS *Bartlett* Cruise 02, Leg 054, 235 Day, 1970, 23:14–01:20 with location of Site SHR-1B (170°06.4′E, 57°19.0′N; 0:30; water depth = 963 m; penetration depth = 200 m).

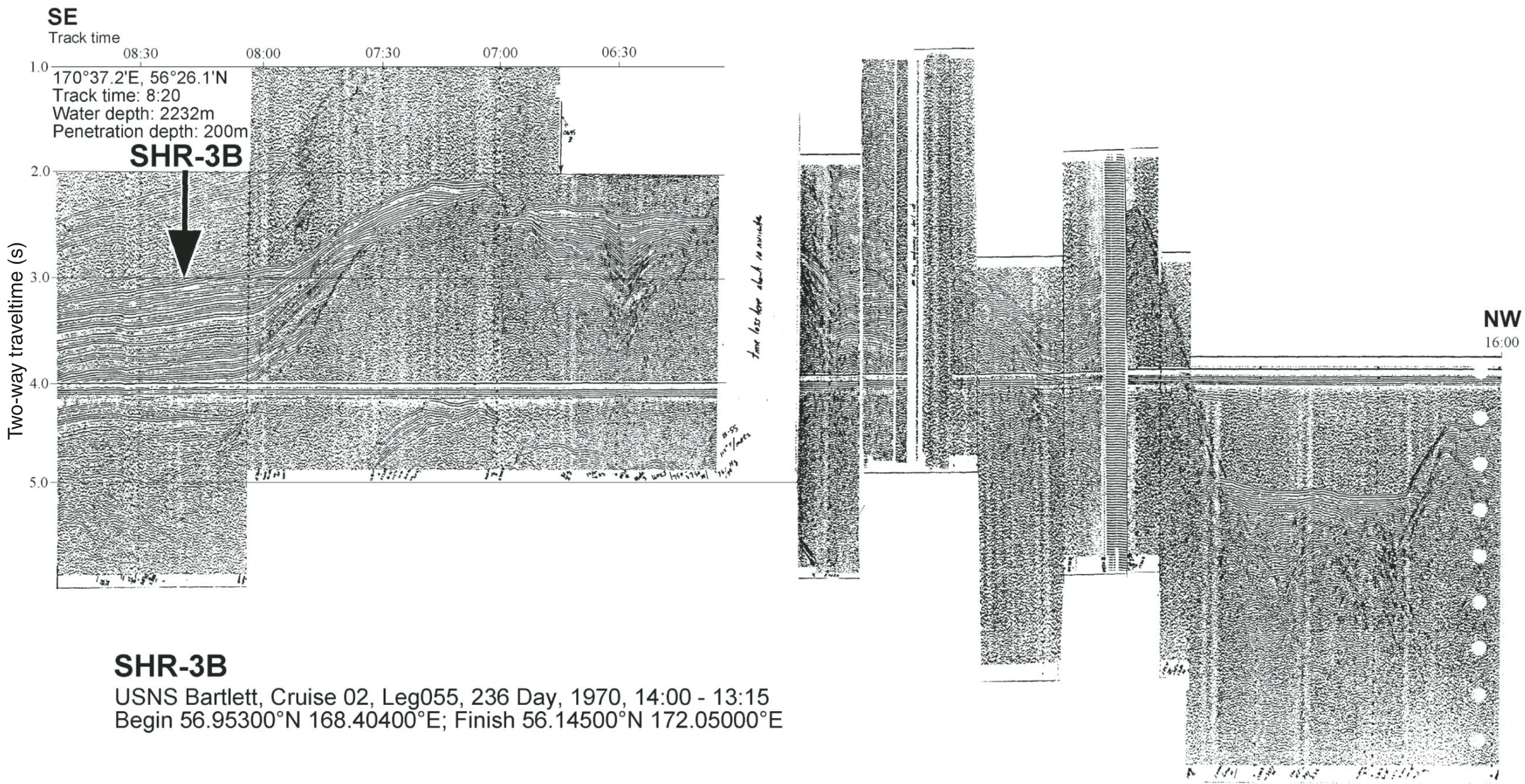

Figure AF51. A. Close-up seismic profile of USNS *Bartlett* Cruise 02, Leg 054, 235 Day, 1970, 23:14–01:20 with location of Site SHR-1B (170°06.4′E, 57°19.0′N; 0:30; water depth = 963 m; penetration depth = 200 m). **B.** Time-depth conversion curve used for Site SHR-1B. Two-way traveltime and vRMS data collected from seismic profile of USGS *Lee* Cruise L6-80, Line 6, CDP 785. Water depth is deleted in this figure.

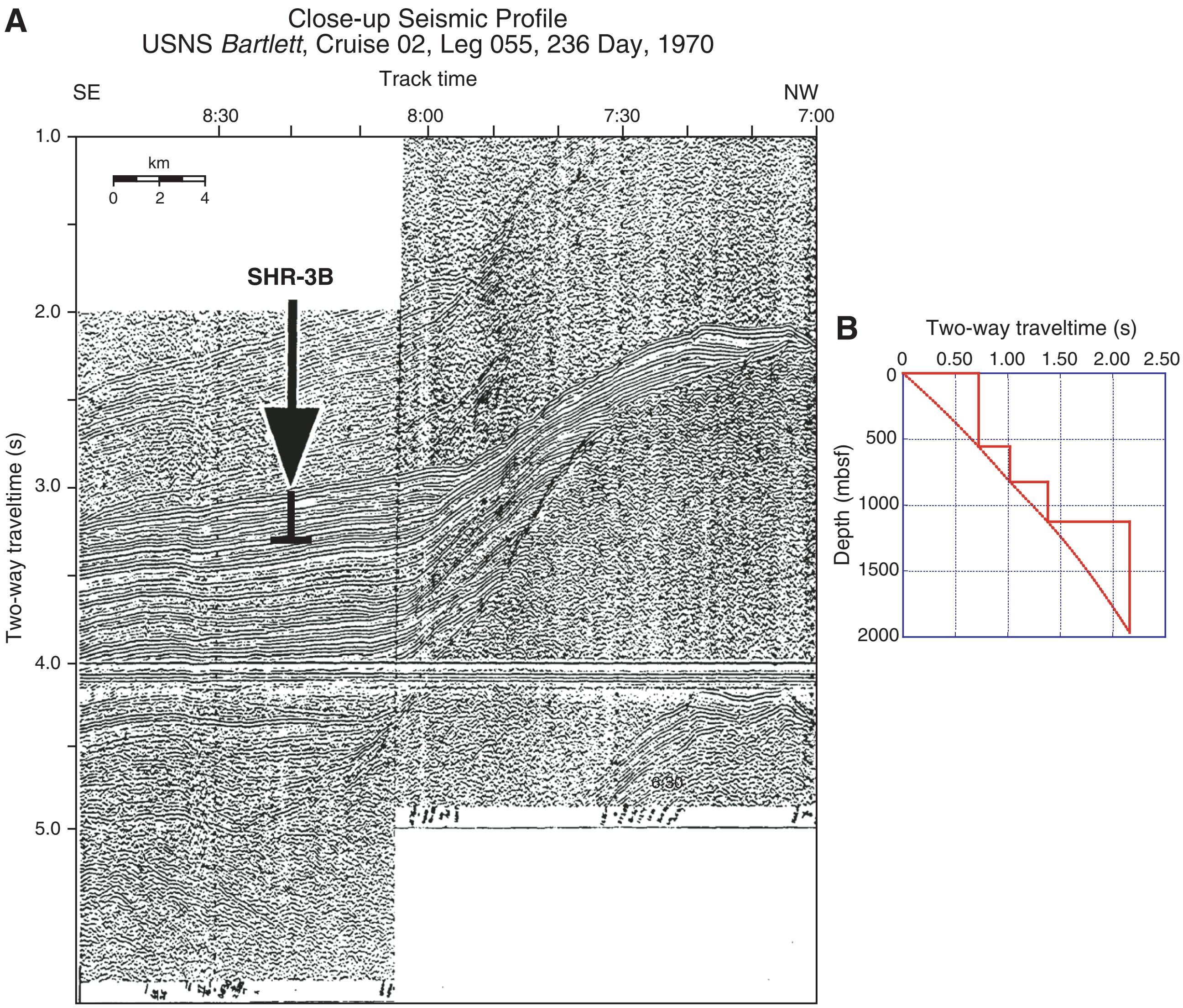

Figure AF52. Single-channel seismic profile of USGS *Lee* Cruise L6-80 Line 2 with locations of Sites UMK-3B and UMK-4D. CDP = common depth point.

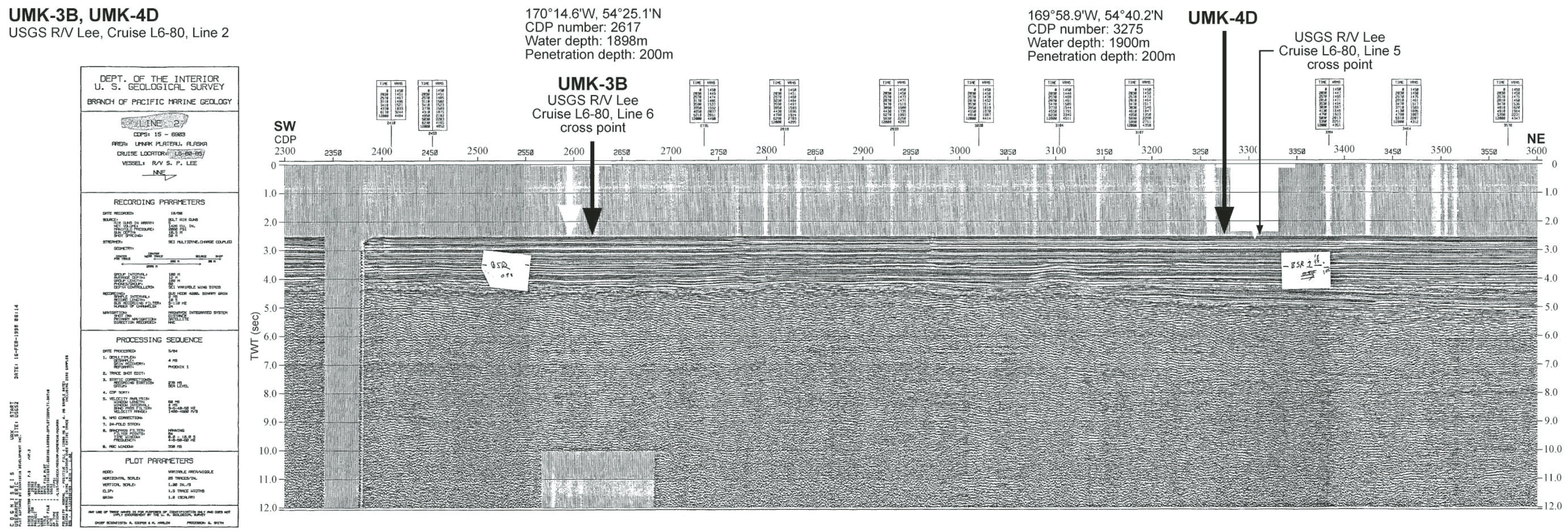

Figure AF53. **A.** Close-up seismic profile of USGS *Lee* Cruise L6-80 Line 2 across Site UMK-4D (169°58.9′W, 54°40.2′N; Shotpoint 3275; water depth = 1900 m; penetration depth = 200 m). **B.** Close-up seismic profile of USGS *Lee* Cruise L6-80 Line 5 near Site UMK-4D. Penetration depth is projected from the southwest on the cross point with Line 2 (Shot point 625; see Fig. **AF55**). Profiles are digitized from paper-form profiles at the SSDB. Stickied notation of the BSR was on the paper-form profile before digitization. CDP = common depth point.

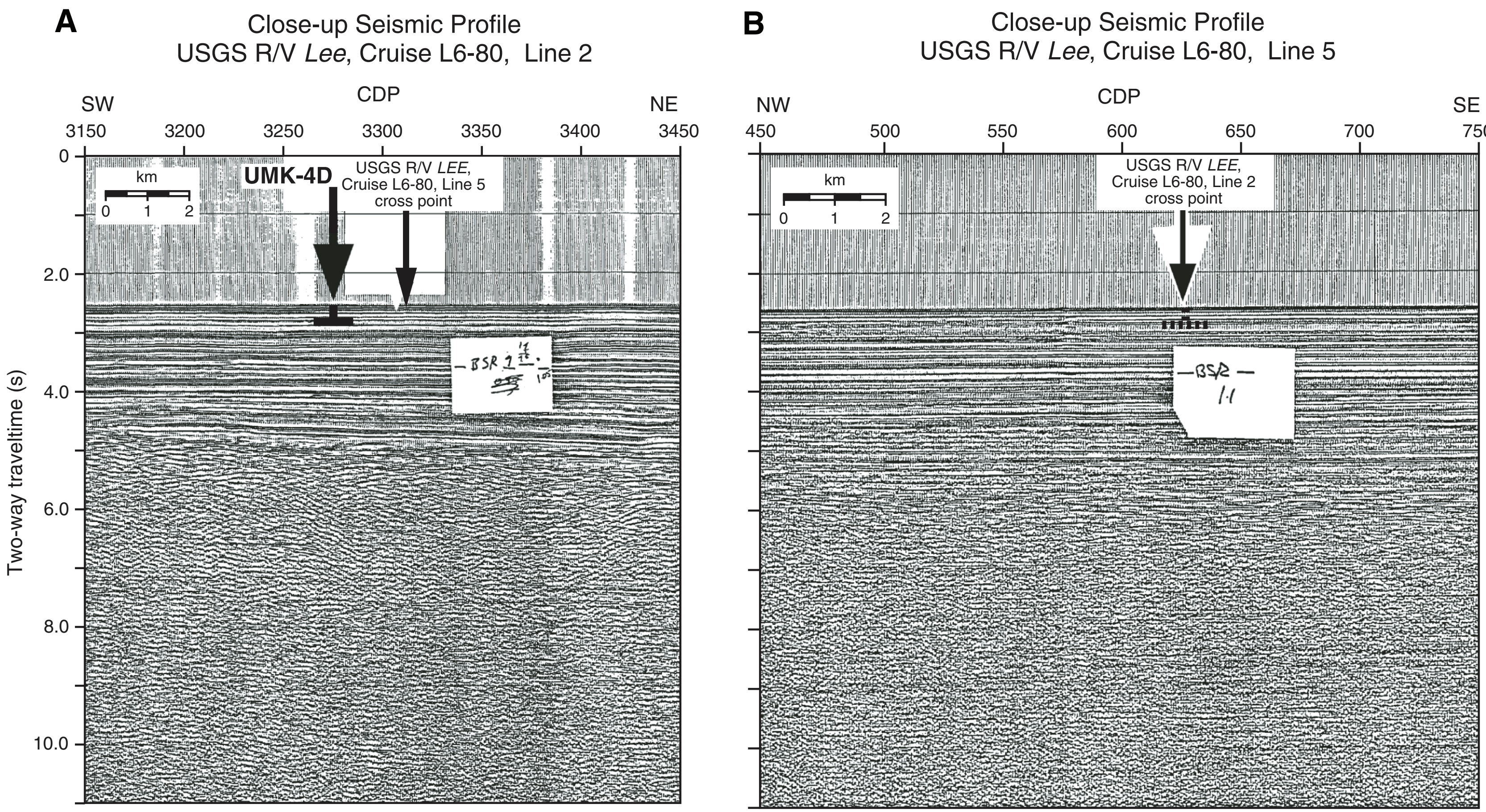

Figure AF54. Single-channel seismic profile of USGS *Lee* Cruise L6-80 Line 5 with location of Site UMK-4D.

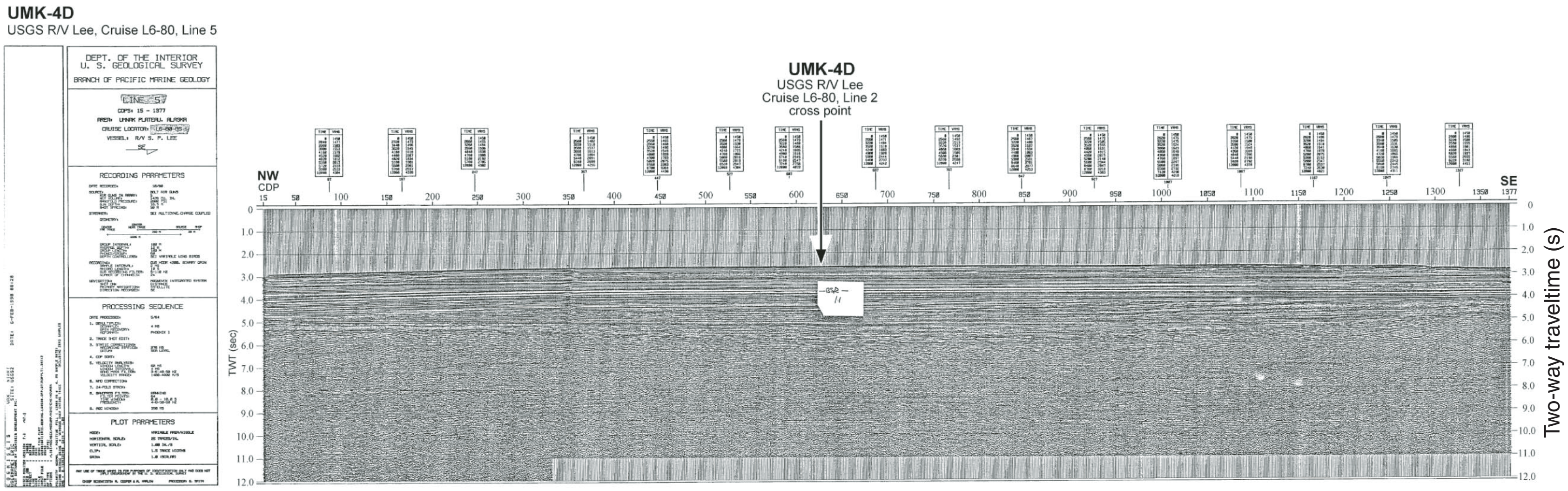

Figure AF55. Track chart of *Hakuhou-maru* Cruise KH99-3 Leg 3 around Sites UMK-4D (169°58.9′W, 54°40.2′N; water depth = 1900 m) and UMK-3B (170°14.6′W, 54°25.1′N; water depth = 1898 m), marked by red stars. Blue stars = sampling points of Cruise KH99-3 and are not same locations as sites. Square = area of swath bathymetry in Figure AF57. Bathymetric image and contour line created by GMT (gmt.soest.hawaii.edu) using GINA Global Topo Data (www.gina.alaska.edu).

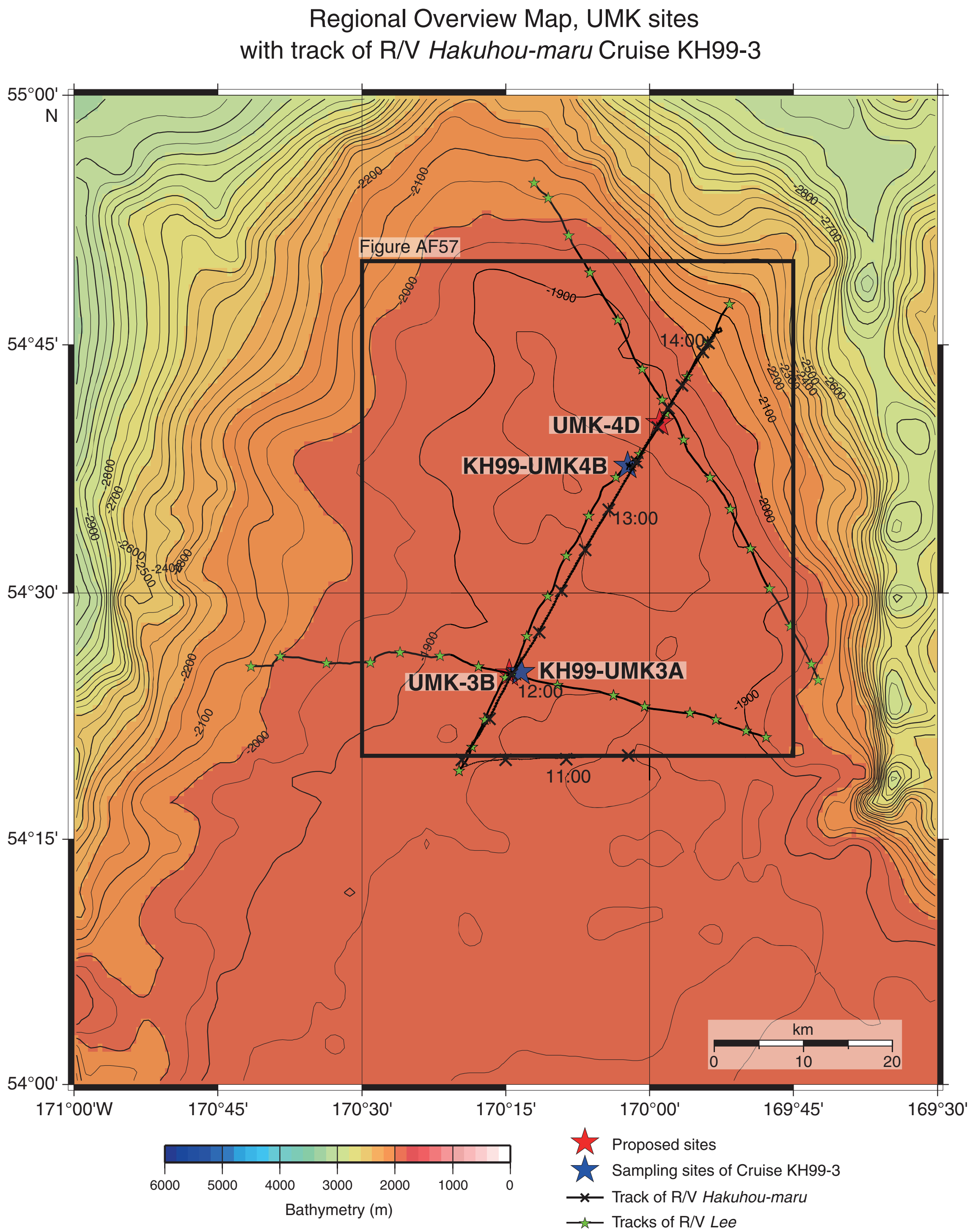

Figure AF56. 3.5 kHz subbottom profile survey from *Hakuhou-maru* Cruise KH99-3 around Sites UMK-4D (169°58.9′W, 54°40.2′N; water depth = 1900 m) and UMK-3B (170°14.6′W, 54°25.1′N; water depth = 1898 m). Sites (bold arrow) and sampling points in Cruise KH99-3 (thin arrow; KH99-UMK-4B and KH99-UMK-3A) are indicated. Horizontal axis of ship time corresponds to time annotation in swath bathymetric map.

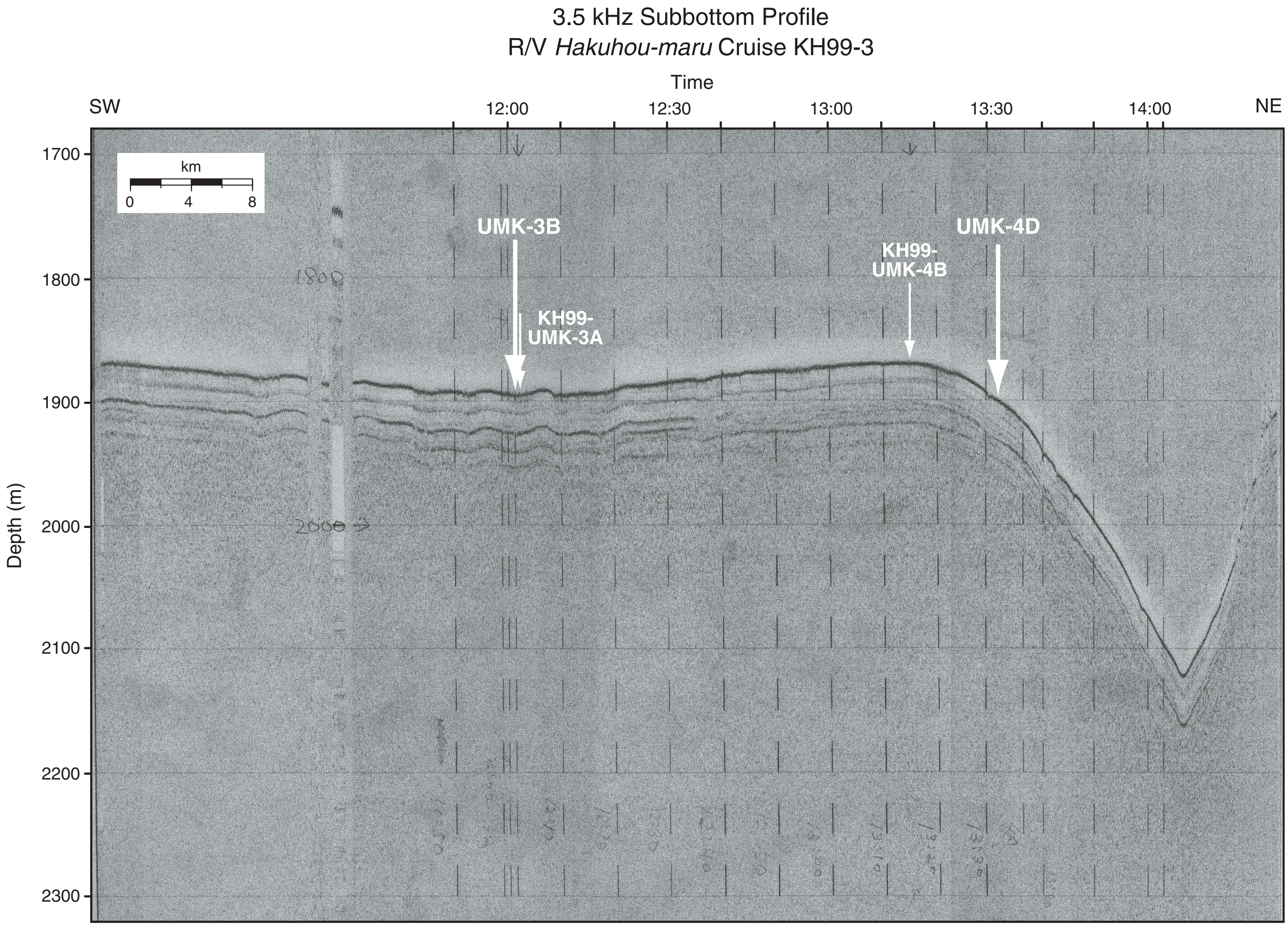

Figure AF57. Swath bathymetric map with track chart at time of *Hakuhou-maru* Cruise KH99-3 around Sites UMK-4D (169°58.9′W, 54°40.2′N; water depth = 1900 m) and UMK-3B (170°14.6′W, 54°25.1′N; water depth = 1898 m). **A.** Plain image. **B.** Shaded relief image.

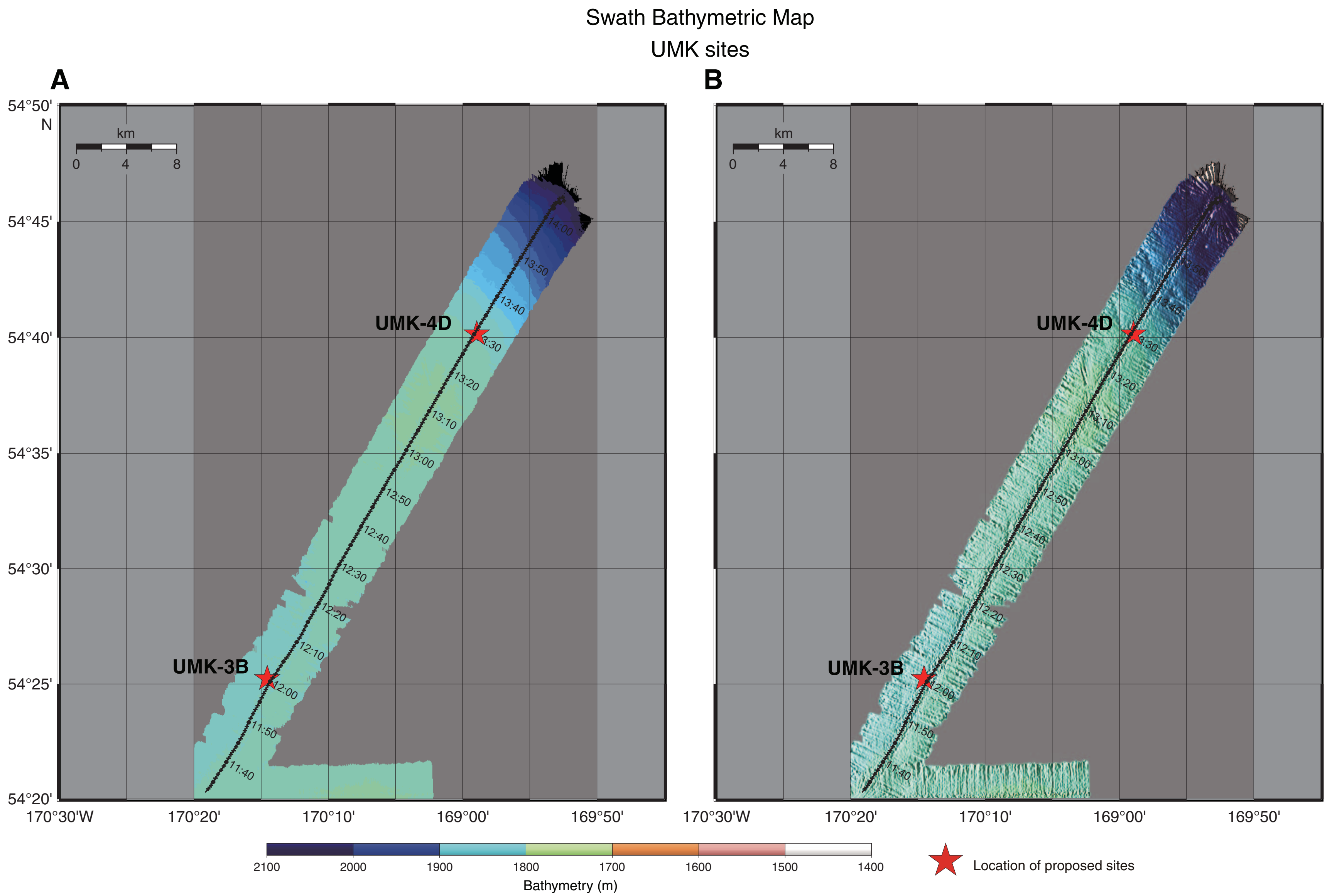

Figure AF58. Single-channel seismic profile of USGS *Lee* Cruise L6-80 Line 6 with location of Site UMK-3B. CDP = common depth point.

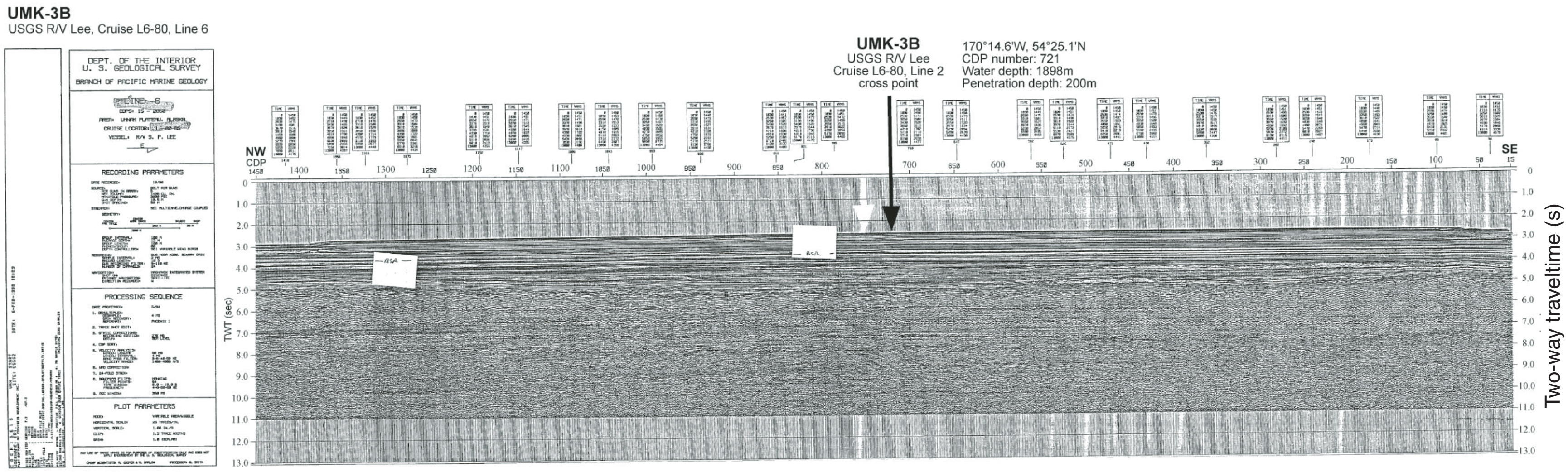

Figure AF59. A. Close-up seismic profile of USGS *Lee* Cruise L6-80 Line 2 with location of Site UMK-3B (170°14.6′W, 54°25.1′N; Shotpoint 2617; water depth = 1898 m) on cross point with Line 6. **B.** Close-up seismic profile of USGS *Lee* Cruise L6-80 Line 6 with location of Site UMK-3B (Shotpoint 721) on cross point with Line 2. Profiles are digitized from paper-form profiles at the SSDB. Stickied notation of the BSR was on the paper-form profile before digitization. CDP = common depth point.

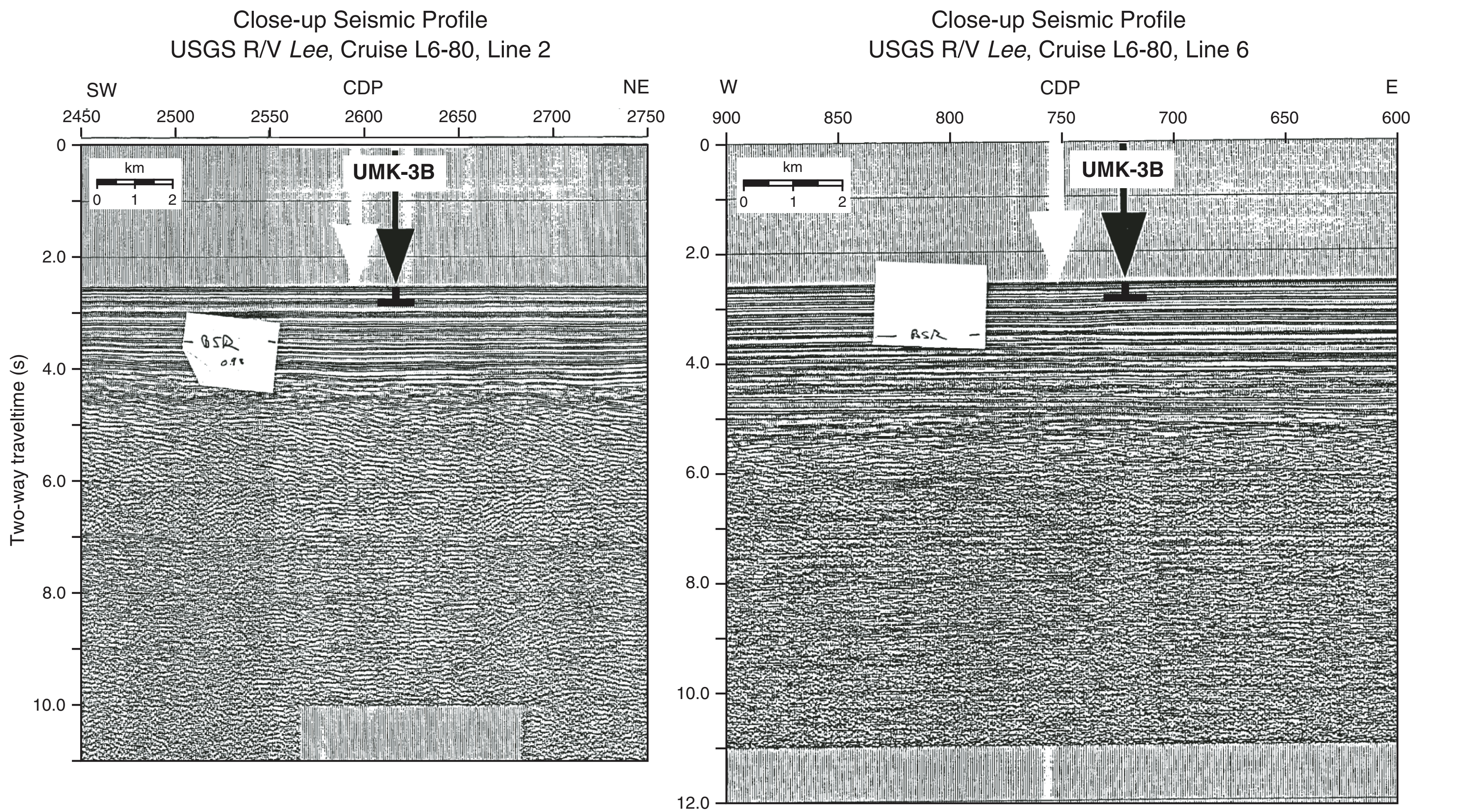

Figure AF60. Track chart of the area around Site NAV-1B.

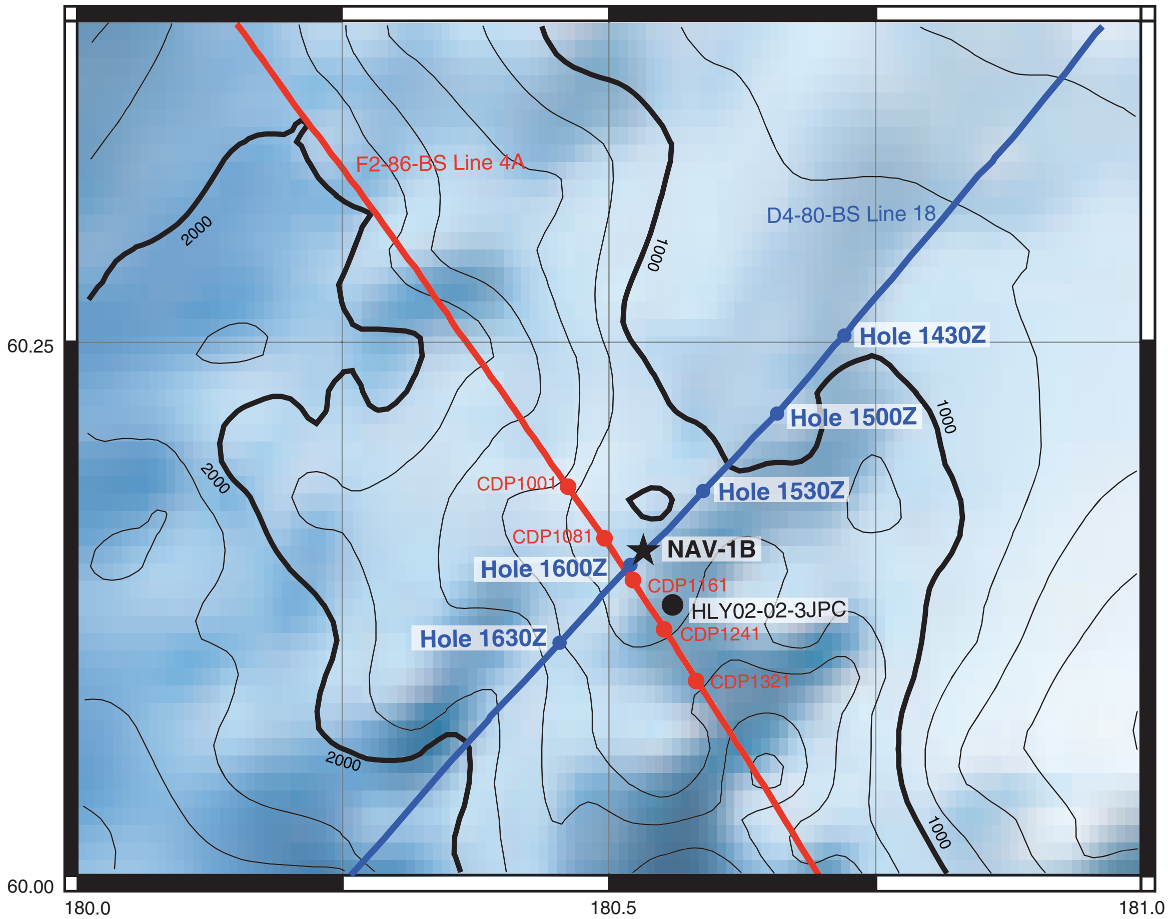

Figure AF61. Seismic profile of CDP1139 on *Farnella*-2-86 BS Line 4A.

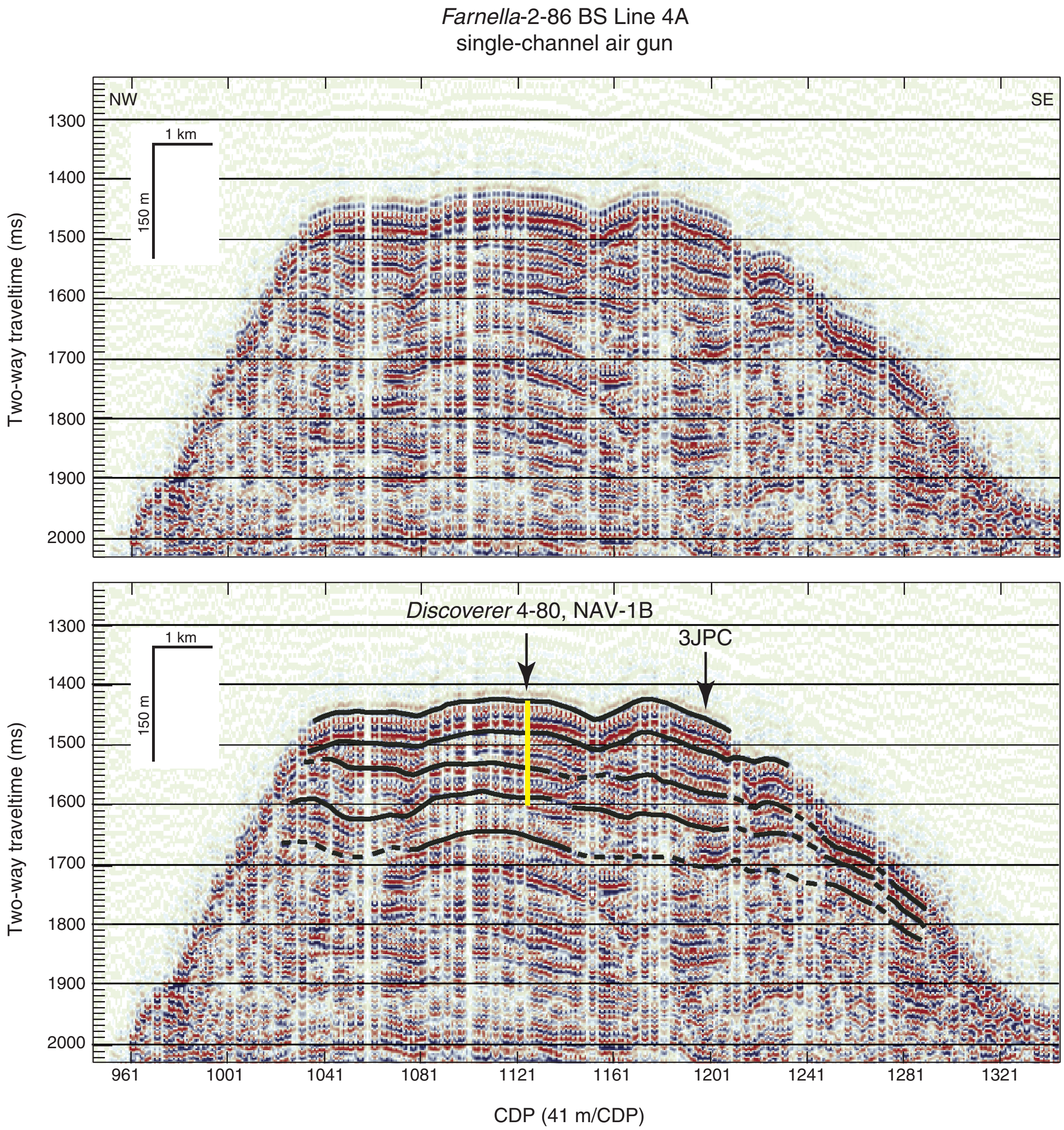

Figure AF62. Seismic profile of 1550Z on *Discoverer* 4-80 BS Line 18.

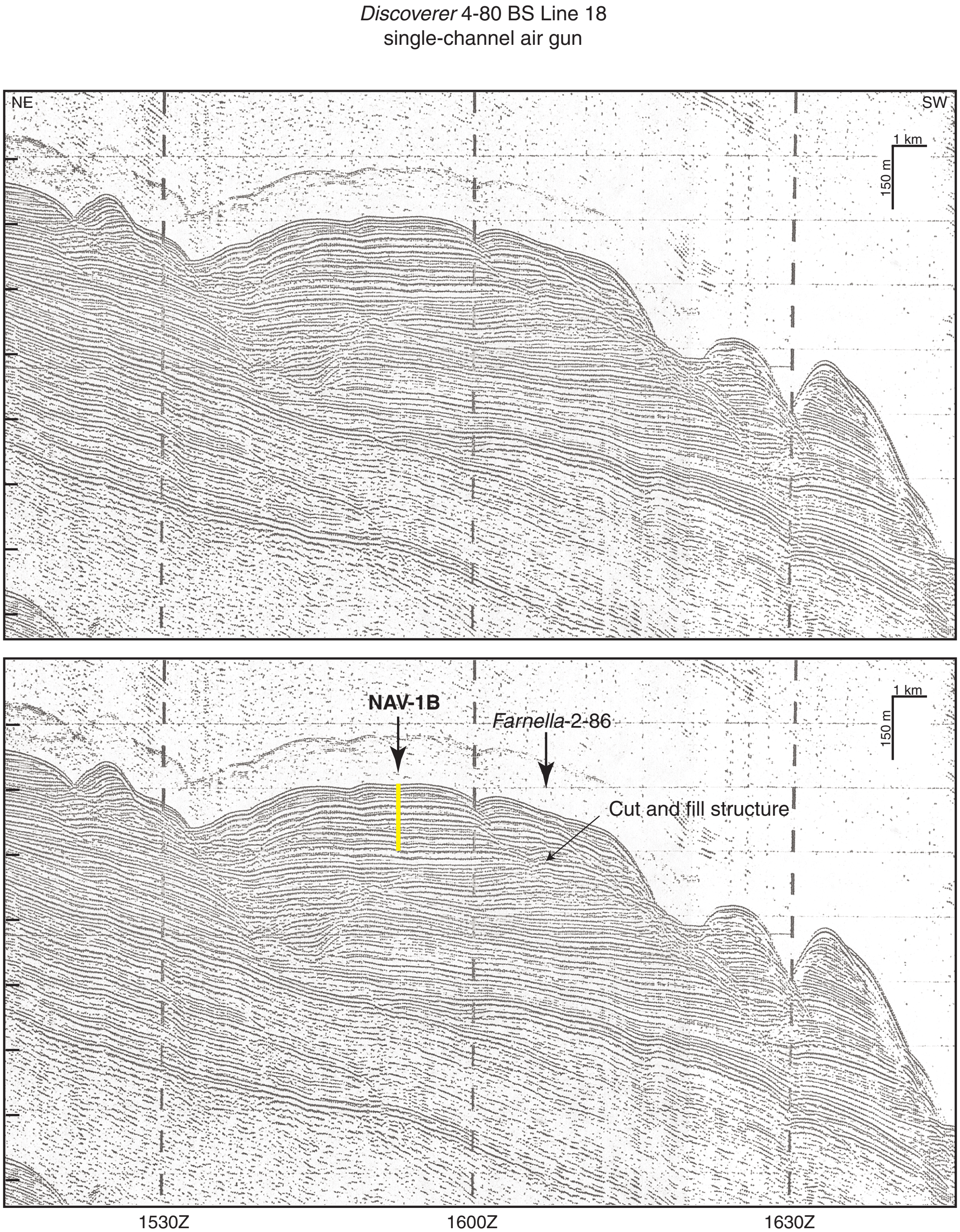

Figure AF63. Minisparker profile of Discoverer 4-80 BS Line 18.

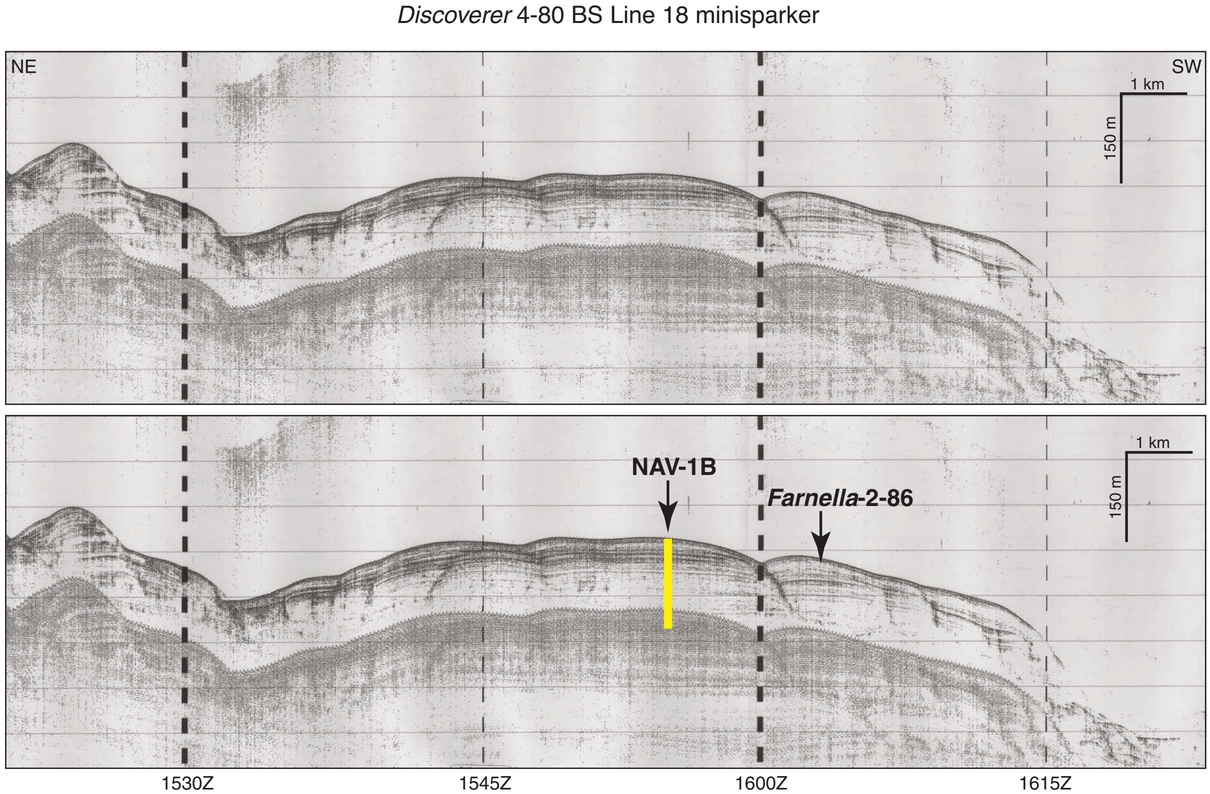

Expedition scientists and scientific participants

The current list of participants for Expedition 323 can be found at **iodp.tamu.edu/scienceops/precruise/beringsea/participants.html.**